CAPILLARY ELECTROPHORESIS AS A HIGH THROGHPUT SCREENING TOOL FOR PROTEIN PROTEIN INTERACTIONS

by

Jing Nie

A dissertation submitted in partial fulfillment
of the requirements for the degree of
Doctor of Philosophy
(Chemistry)
in the University of Michigan
2013

Doctoral Committee:

Professor Robert T. Kennedy, Chair
Professor Kristina I. Håkansson
Assistant Professor Brandon T. Ruotolo
Professor Euisik Yoon

To my family for their unconditional love and support

ACKNOWLEDGEMENT

I owe the deepest gratitude to my advisor, Professor Robert Kennedy, who introduced me to the world of separation and microfluidics and accepted me as his student. In particular, I want to thank him for always challenging me to achieve more and do better. I greatly appreciate his inputs on science and career development. Without his guidance and support over the years, none of the work in this thesis would have been possible.

Professor Kristina Håkansson is my role model as a female scientist. I had the fortune to work in her lab as a rotation student, learn Mass Spectrometry in her class, and work as a GSI under her supervision. I am very thankful for those overlaps I had with her, from which I learned a great deal about Mass Spectrometry and analytical chemistry.

I thank Professor Brandon Ruotolo for always being very encouraging and helpful to me. His insights and passion brought much inspiration and energy to our scientific discussions, which he is very kind to make time for.

I got to know Professor Euisik Yoon through his “Into to MEMS” class, which exposed me to the field of micro-fabrication. I thank him very much for joining my scientific committee and providing fresh perspective to my research.

I would like to give special thanks to the Kennedy Lab members, who are wonderful source of help and friendship. I would also like to express my appreciation to faculties and staff members from different departments and institutions of University of

Michigan, who made my study and life as a graduate student both smooth-going and enjoyable.

For the many friends that I had the privilege to have, I would like to thank them for the joyful memory we created together and being generous and forgiving to me.

Last but not least, I want to thank my family, for their selfless love and enduring faith in me. Especially, I would love to thank my husband Dr. Peng Song for taking me as I am and making me a better person through his love and support.

TABLE OF CONTENTS

LIST OF TABLES

Table

LIST OF FIGURES

LIST OF APPENDICES

LIST OF ABBREVIATIONS

ACE	Affinity Capillary Electrophoresis
AF 488	Alexafluor®488
APCE	Affinity Probe Capillary Electrophoresis
ATP	Adenosine 5'-triphasphate
Bag3	Bcl2-Associated Athanogene
BSA	Bovine Serum Albumin
CBQCA	3-(4-Carboxybenzoyl) quinoline-2-Carboxaldehyde
CE	Capillary Electrophoresis
CGE	Capillary Gel Electrophoresis
CIEF	Capillary Isoelectric Focusing
CITP	Capillary Isotachophoresis
cLC	capillary Liquid Chromatography
CZE	Capillary Zone Electrophoresis
EOF	Electroosmotic Flow
ESI	Electrospary Ioniztion
HEPES	4-(2-HydroxyEthyl)-1-PiperazineEthaneSulfonic Acid
IC_{50}	Half maximal inhibitory concentration
ITC	Isothermal Titration Calorimetry
Hsp70	Heat Shock Protein 70

FCPIA	Flow Cytometry Protein Interaction Assay
FRET	Fluorescence Resonance Energy Transfer
Kd	Dissociation Constant
LC	Liquid Chromatography
LIF	Laser Induced Fluorescence
LOD	Limit of Detection
HTS	High Throughput Screening
IC50	half maximal (50%) Inhibitory Concentration
MALDI	Matrix Assisted Laser Desorption Ionization
MEKC	Micellar Electrokinetic Capillary Chromatography
MS	Mass Spectrometry
NDA	naphthalene-2,3-dicarboxaldehyde
NMR	Nuclear Magnetic Resonance
OPA	o-phtalaldehyde
PAGE	Polyacrylamide Gel Electrophoresis
PEG	Poly Ethylene Glycol
PFOTCS	1H, 1H, 2H, 2H-perfluorooctyltrichlorosilane
PPI	Protein Protein Interaction
PVA	Polyvinyl Alcohol
RSD	Relative Standard Deviation
SDS	Sodium Dodecyl Sulfate
SPR	Surface Plasmon Resonance

ABSTRACT

CAPILLARY ELECTROPHORESIS AS A HIGH THROUGHPUT SCREENING TOOL FOR PROTEIN PROTEIN INTERACTIONS

by

Jing Nie

Chair: Robert T. Kennedy

Protein Protein Pnteractions (PPIs) are key players in all aspects of cellular functions. In depth understanding of PPIs and discovery of PPI targeted therapeutics requires facile and user-friendly PPI analysis. Capillary Electrophoresis (CE) is a valuable tool to study affinity bindings including PPIs. Fast separation speed and nanoliter sample consumption suggest great potential for CE based High Throughput Screening (HTS). To explore CE as a PPI analysis and HTS tool, we have developed a CE based assay for Heat Shock Protein70 (Hsp70) and its co-chaperone Bcl2-Associated Anathogene 3 (Bag3).

An Affinity Probe CE (APCE) method was developed for full length Hsp70 and Bag3 extracted from cell culture. In this assay, Hsp70 was labeled with Alexafluor® 488 and used as the affinity probe. With a surface modified capillary, the binding is detected

as Hsp70 and complex peaks resolved and detected using Laser Induced Fluorescence (LIF).

On a commercial instrument, the CE assay takes 6.5 min per run which allows a sample throughput of 220 tests per day. In a pilot screening, ~3300 small molecule library compounds were tested for novel inhibitor discovery. By comparing CE assay's performance to an existing high throughput screening platform Flow Cytometry Protein Binding Assay (FCPIA), CE showed much better specificity as evidenced by lower hitting rate and higher confirmation rates in confirmatory tests.

Fully realizing the low sample consumption benefit of CE based HTS requires low volume sample manipulation capability. Segmented flow microfluidics is an emerging technique that allows nanoliter to picoliter volume samples to be manipulated and coupled to CE analysis. In the second half of this thesis, unit operations of segmented flow microfluidics, namely splitting and reagent addition were developed to fulfill the need to aliquot and add reagent to nanoliter segmented flow samples. Based on these results, future work would be to integrate the CE separation with these sample manipulation techniques towards building a novel workflow for CE based HTS.

CHAPTER 1
INTRODUCTION

Overview

The objective of this thesis is to explore Capillary Electrophoresis (CE) as a High Throughput Screening (HTS) Tool for Protein Protein Interactions (PPIs).

Protein protein interactions control almost every aspect of cellular functions, and represent exciting opportunities for drug discovery. Targeting PPIs, nonetheless, is challenging[1]. And pursuing this "less paved road" entails facile and user-friendly assays that can be used to characterize validated targets as well as access drug candidates' capabilities in modulating these PPIs.

CE has great potential in fulfilling this need. Advantages of CE as compared to other PPI analysis include direct binding information, immobilization free, no limit on protein sizes, tolerance of impurities, low sample consumption, generic methodology development, multi-parameter readout, automation with commercial instrumentation, etc. These have been well demonstrated through antibody-antigen binding, DNA-protein binding and many other CE based affinity studies[2]. So far, these promises are yet to be fulfilled for protein-protein interactions. The technical bottlenecks such as protein adsorption and sensitive detection still need to be overcome.

In this work, we used a potential cancer target, Hsp70 (Heat Shock Protein 70) and Bag3 (Bcl2-Associated Athanogene 3) as our model system to demonstrate the

effectiveness of CE assay in PPI analysis. In developing a CE assay using full length recombinant proteins, we investigated the multiple facets of PPI assay development for a real world protein binding system. By doing so, we were able to address multiple challenges that were not previously addressed in CE based PPI studies.

High throughput screening is a key step in modern drug development pipeline. For PPI drug targets, HTS is very valuable since many traditional enzyme inhibitor development strategies are not directly applicable to PPI modulator discovery. HTS, on the other hand, offers a systematic way to discover active chemical entities from large chemical libraries. From the point view of assay development, HTS places most strict demands on data quality, system robustness, cost and analysis speed. CE features high separation efficiency, automation, minimum sample consumption, fast speed and parallelization, which provides a very attractive alternative for existing HTS platforms for PPI targets. To simply demonstrate, we worked on speeding up the CE assay for Hsp70 and Bag3 and adapted it to a HTS friendly format. In comparing to an existing PPI screening platform, Flow Cytometry Protein Interaction Assay (FCPIA), we attempt to answer a few key questions in pushing for CE based HTS: 1) what are the true benefits in using CE as opposed to available technologies; 2) are the benefits significant enough to justify the efforts involved in doing so; 3) what can be done to make CE more amendable for routine HTS analysis and what remains to be done.

μTAS (micro Total Analysis Systems) based on microfluidic principles is bound to revolutionize chemical analysis by miniaturizing, integrating and automating analytical instrumentation.[3] Capillary electrophoresis is the staple of "on-chip" analysis, as evidenced by the commercial success of chip based CE instruments. Taking full

advantages of both microfluidics and CE requires "unit operations" that allows robust nanoliter volume liquid handling and easy interface to other functionalities. In the second half of this thesis, segmented flow microfluidic unit operations, such as sampling and in drop chemical reactions are developed.

With the studies described in this thesis, we strive to pave the road towards facile CE PPI analysis and adapting it to HTS friendly format. With technological advancement and further demonstrations, we believe CE will be widely recognized as a powerful and yet practical tool for PPI analysis and make a significant addition to the toolbox of biological and medicinal researches.

Capillary Electrophoresis

Electrophoresis refers to the motion of charged particles or molecules relative to the fluid media under the influence of an external electric field. The velocity of the moving particle relative to the fluid the particle is suspended in is determined by the strength of the electric field and the electrophoretic mobility of the particle, which is defined in the following equation, where μ_e is the effective mobility, $v\ (cm/s)$ is the relative velocity and E represents the electric field (V/cm):

$$\mu_e = \frac{v}{E} \qquad \text{Eq. 1-1}$$

Electrophoretic mobility is characteristic of the property of the particle itself as well as the fluid environment as approximated from the Debye-Huckel-Henry theory:

$$\mu_e = \frac{q}{6\pi\eta r} \qquad \text{Eq. 1-2}$$

where q is the charge of the particle, η is the viscosity of the fluid media and r is the Stokes' radius of the particle.

Ever since Michaelis observed proteins migrate to their isoelectric points under an external electric field in 1909[4], the principle of electrophoresis has been widely applied in a myriad of electrophoresis separation techniques, among which are polyacrylamide gel electrophoresis (PAGE), sodium dodecyl sulfate (SDS)-PAGE and Isoelectric focusing (IEF). These electrophoretic separation techniques are not only ingenious in design and very powerful, but also inexpensive and user friendly. Decades after their first appearances, these techniques remain the staple of biochemistry and molecular biology laboratories.

Another milestone in the development of electrophoretic separation techniques is Capillary Electrophoresis (CE)[5]. What have been limiting the performance and analysis speeds of traditional electrophoresis separation are the convectional distortion of the analyte bands and excessive Joule heat in free solution and slab gel electrophoresis. Performing electrophoresis separation in a narrow bore fused silica capillary with inner diameter (i.d.) ranging from 5 to 200 μm greatly reduces convection and enhances heat dissipation. As a result, the separation efficiency and analysis speed of electrophoresis has reached an unprecedented level.

Following the pioneering research in late 1970's and 1980's, CE has evolved into a big collection of different separation modes. These include capillary zone electrophoresis (CZE) which is also known as free-solution CE (FSCE), micellar electrokinetic capillary chromatography (MEKC), capillary isoelectric focusing (CIEF), capillary gel electrophoresis (CGE), capillary electro-chromatography (CEC) and

capillary isotachophoresis (cITP). These various modes of capillary electrophoretic separation have been applied to almost every class of analytes, from inorganic ions, small organic molecules, to nucleic acids, peptides, proteins and higher order structures. Even organelles and viruses can be effective separated using CE.

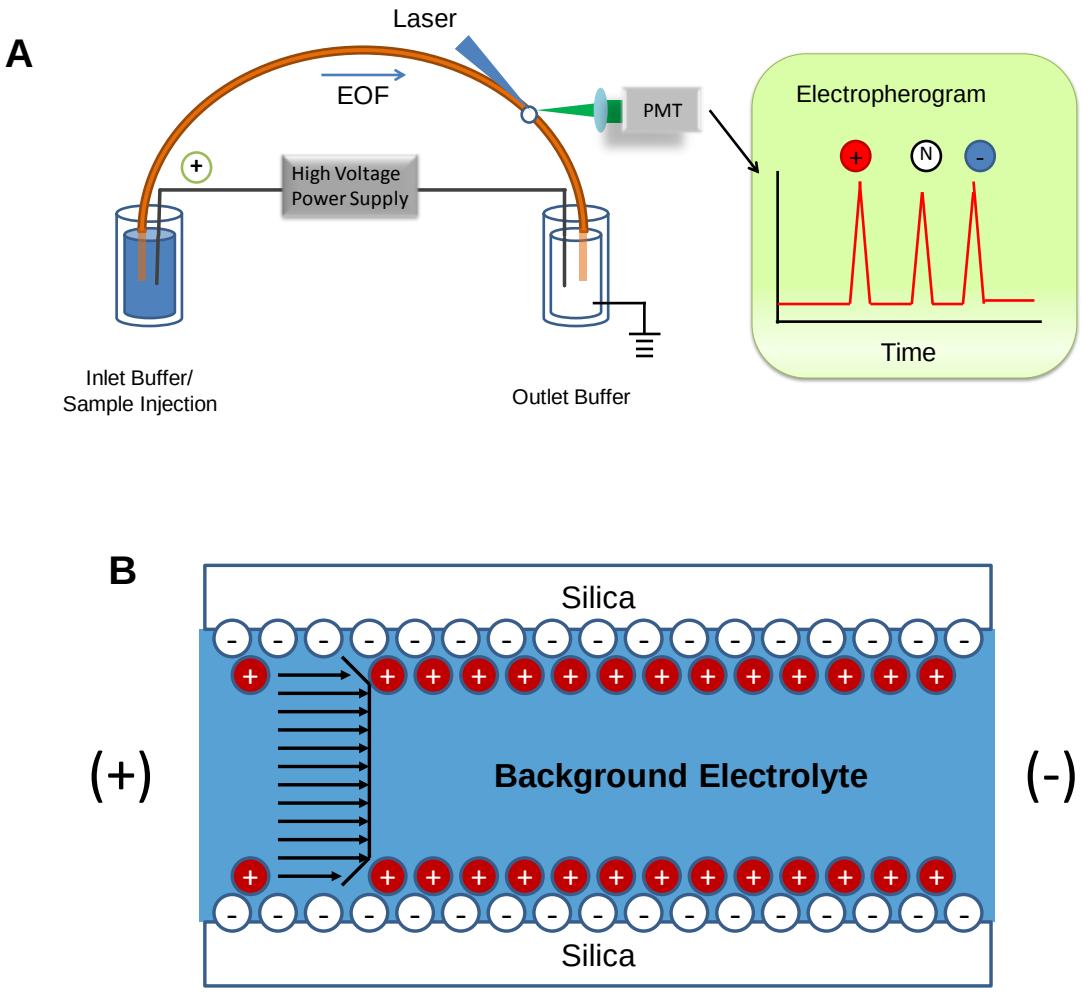

Figure 1-1. Schematic drawing of (A) CZE setup with Laser Induced Fluorescence (LIF) detection; (B) EOF.

Among different CE modes, Capillary Zone Electrophoresis (CZE) is the simplest and most commonly used one. In a CZE experiment, the separation capillary is firstly filled with buffer solution, which is also known as the background electrolyte (BGE). A sample plug is introduced from the capillary inlet and a high voltage is applied across the separation capillary. Different components in the sample zone are carried towards the detection point driven by Electroosmotic Flow (EOF) while being resolved into individual bands based on their differences in electrophoretic mobility (Figure 1-1A).

Electroosmotic flow is a key concept in CE and plays a very important role in CE method development. According to electrostatic double layer theory, when a surface is in contact with electrolyte solution, an electric double layer is formed at the solution/solid interface. Bare silica capillary is highly negatively charged due to very acidic silanol groups, which attract a layer of positively charged counterions that move when electric field is applied, dragging the bulk solution along, thus creating a net flow towards the cathode end of the capillary (Figure 1-1B), namely electroosmotic flow. The relation between electroosmotic flow velocity v_{eof} and external electric field E is given by:

$$v_{eof} = -\mu_{eof} E \qquad \text{Eq. 1-3}$$

and μ_{eof} is the electroosmotic mobility. In CZE, the apparent mobility μ_{app} that is measured for certain molecules are actually the sum of the electrophoretic mobility μ_e as described in Eq. 1-2 and the mobility due to electroosmotic flow (μ_{eof}):

$$v = \mu_{app} E = (\mu_e + \mu_{eof}) E \qquad \text{Eq. 1-4}$$

The significance of EOF in CE separation is three folds. Firstly, the direction and velocity of EOF determine the elution order and analysis speed. Bare silica capillary is

highly negatively charged under most pHs thus EOF is high (higher than the effective electrophoretic mobility of most charged molecules) and towards cathode so that neutral as well as negatively charged molecules that migrate against EOF can all be effectively separated and detected in the same run together with cationic species. However, more often than not, EOF is purposely suppressed or even reversed depending on the analyte and application. As an example, surface modification is commonly employed to reduce protein adsorption in CE based protein separations, and surface modification methods often reduces the EOF, sometimes to near zero. In the absence of the "electric-driven pump", both cationic and anionic analytes cannot be analyzed and detected in a single run and the separation speed is usually low.

Secondly, EOF has a plug shape flow profile. The implication of this is that comparing to chromatography separation where pressure driven flow with parabolic flow profile is the case, in CZE, diffusion is almost the single source of dispersion contributing to band broadening, provided factors such as Joule heating, injected sample plug width and adsorption are well controlled or inconsequential. So in ideal situations:

$$\sigma^2 = \frac{2D_i L_i}{(\mu_{eof}+\mu_e)E} \qquad \text{Eq. 1-5}$$

where σ^2 is the variance of the zonal peak of analyte i, D_i is the diffusion coefficient and L_i is the effective separation length. This also suggests that unlike in HPLC where increasing flow rate result in loss in efficiency primarily due to the mass transfer limit, increasing analysis speed in CE by increasing EOF does not pay the same price. Thus, the only limiting factors in separation speed become the capability in defining a sharp

injection band and the ability to apply high electric field without causing heat dissipation problem.

Finally, EOF phenomenon rises from surface charges, thus it is highly sensitive to surface property change. In CE practice, EOF is commonly used as an indicator of surface fouling when change in EOF is observed. Although EOF is not a must for successful CE separation, stable and reproducible EOF is indispensible for a method to be robust.

As mentioned above, sample injection for CZE is also of great importance because the size and shape of the injected sample plug determines both the separation efficiency and sensitivity. Both hydrodynamic (using pressure, vacuum or gravity) and electrokinetic (utilizing voltage and EOF) injection schemes are widely used and have their respective advantages and disadvantages. For example hydrodynamic injection does not cause injection bias against lower mobility molecules while electrokinetic injection does not require additional hydraulic system which eases system integration and automation.

Most commonly used CZE detection modes are UV, Laser Induced Fluorescence (LIF), electrochemical detection and Mass Spectrometry. By far, LIF is the most sensitive detection method for CE.[6] The sensitivity of LIF comes from the fact that fluorescence detection is not pathlength dependent. Tightly collimated and high intensity laser beams are excellent light source for exciting fluorophores inside a narrow bore capillary. The limit of detection (LOD) of LIF can reach as low as pM or even better. One limitation of LIF detection is that most analytes of interest are not natively fluorescent and fluorescent tagging is usually required. Fortunately, with a large variety of fluorescence labeling

reactions targeting specific functional groups being available through commercial sources, fluorescent tagging has becoming less of a limiting factor in CE-LIF method development. The majority of studies described in this thesis use LIF. Other detection schemes will be described in more detail when encountered.

Capillary Electrophoresis in Affinity Studies

The common themes of all separation techniques are purification, identification and quantification of individual analyte. In these areas, different separation methods, either chromatographic or electrophoretic has been very successful and widely used. It is less well known that separation techniques can also be used to study affinity interactions. And this potential is yet to be tapped with the advancement of biology and ever increasing need for techniques that characterize affinity interaction between bio-molecules.

Different molecules can be separated from each other through a broad spectrum of physical and chemical properties, such as size (size exclusion chromatography and gel electrophoresis), ionic character (ion exchange chromatography), hydrophobicity (reversed phase liquid chromatography), charged to size ratio (CZE), and so on. When interacting molecules co-exist in the sample, these properties often changes upon binding reversibly or irreversibly, which can be reflected as changes in their separation behaviors, such as peak shape change or retention/migration time shift.

Asymmetric peaks can be a nuisance if better identification and quantitation is the goal of analysis. In many separation techniques, such interactions are purposely

suppressed as exemplified by SDS-PAGE based protein separations. On the other hand, this phenomenon can be very useful in detecting affinity interactions. Specific to CZE based affinity studies, which separate molecules based on their differences in electrophoretic mobility, binding event can be detected as mobility shift. And this mechanism has been successfully applied in studying various ligand - receptor binding systems, such as metal ion - protein binding, small molecule - protein binding, antibody - antigen binding, peptide/protein - DNA binding, Aptamer - target binding, etc[7].

Despite the big variety of analytes and the existence of a large array of special separation modes, the majority of affinity analysis using CE falls into two general categories: equilibrium and non-equilibrium. In equilibrium modes, ligand molecules are added to the background electrolyte, which retard or speed up the migration of the receptor molecules relative to the BGE[8] (Figure 1-2A). During separation, the receptor is always in equilibrium with the ligand because the ligand concentration is constant across the full length of the capillary. The amount of mobility change due to binding is related to the concentration of binding partner present in the BGE as well as the binding strength, as described in Eq. 1-6.

$$\frac{\Delta\mu_R}{[L]} = K_b(\Delta\mu_R^{max} - \Delta\mu_R) \quad \text{Eq. 1-6}$$

$\Delta\mu_R$: mobility change of receptor, in $cm^2 \cdot V^{-1} \cdot S^{-1}$

[L]: Ligand concentration

K_b: Binding constant

$\Delta\mu_R^{max}$: mobility change of the receptor when it is saturated with the ligand

Non-equilibrium methods, as compared to equilibrium methods, operate under the conditions that equilibrium is not maintained during separation. Taking Affinity Probe Capillary Electrophoresis (APCE)[9, 10, 11, 12, 13] as an example, the ligand in this case is fluorescently tagged with a fluorophore and used as the affinity probe. A mixture of the affinity probe and its receptor is introduced as a sample plug as in normal CZE experiment. During separation, ligand, receptor and the affinity complex with different mobility are resolved into separate bands (Figure 1-2B). However, the separation buffer is free of either ligand or receptor, so during the separation process, as the sample zones of all three species are pulled apart, the local concentrations change, which breaks the equilibrium and result in the dissociation of the complex. As in equilibrium methods, for a single molecule at a specific time point, the mobility change due to binding is affected by the binding strength (relative time that this molecule spend as a free molecule and as a complex) and the local concentration of its binding partner. In contrast to equilibrium methods, the mobility difference between the complex and the free molecule also plays a significant role, which essentially requires sufficient separation power to resolve the complex from the free. In APCE, the binding event is eventually detected as part of the fluorescent signal of the affinity probe shifting away from its intrinsic migration time towards that of the complex.

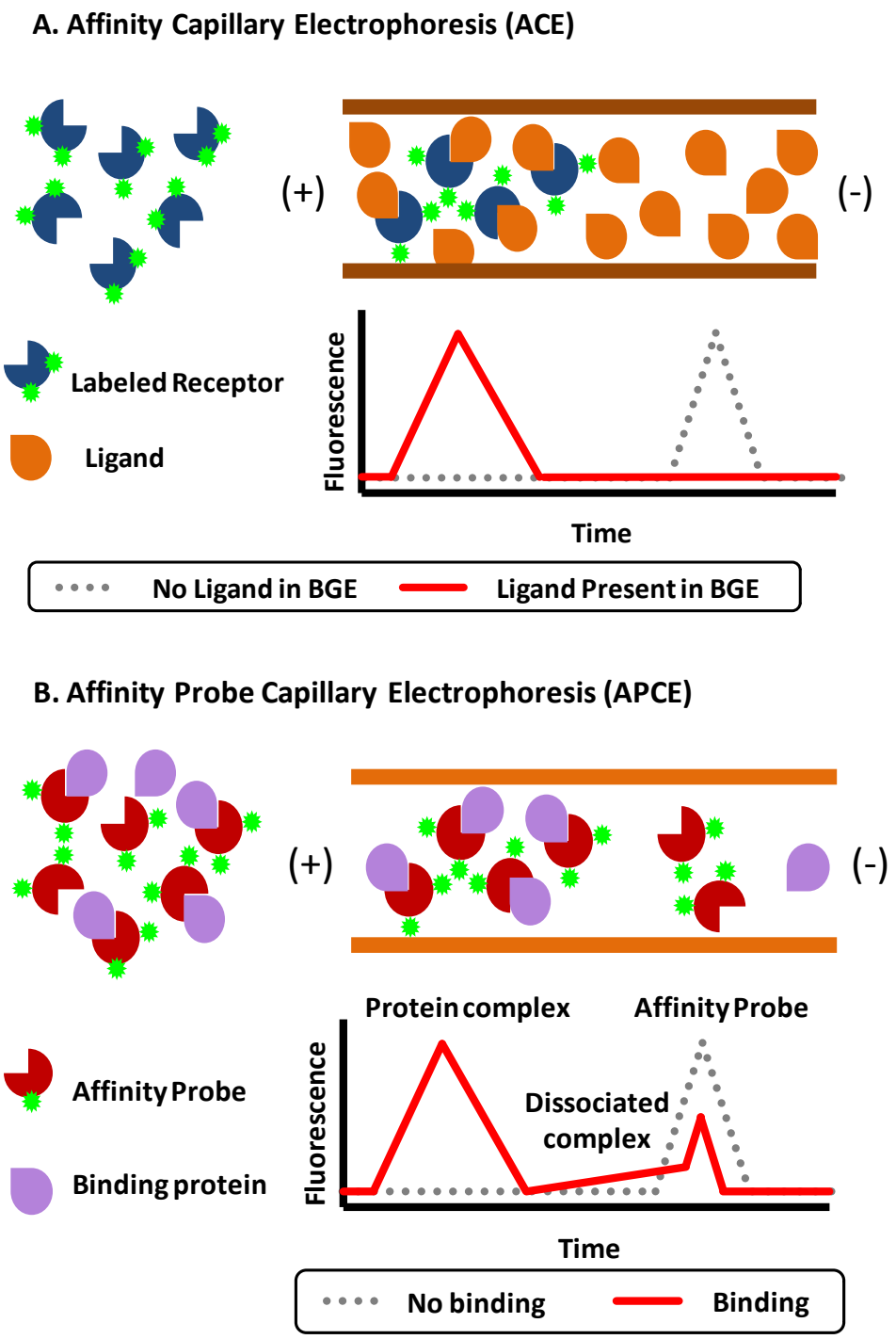

Figure 1-2. Illustration of (A) affinity CE. Receptor is labeled and ligand is added to the background electrolyte. Migration of labeled receptor is retarded when ligand is present in the BGE. (B) APCE. One binding partner is labeled as the affinity probe. CE separation of affinity probe and its binding partner results in a complex peak that is detected in the fluorescence detection mode.

Equilibrium methods and non-equilibrium methods have their respective advantages and limitations. Different separation modes can be chosen for specific applications. Equilibrium methods are more successfully applied in studying interactions between relatively small molecules (or metal ions) and bigger bio-molecules such as proteins. One practical consideration is that adding big molecules such as proteins in the separation buffer consumes a lot of material, which is not cost effective in many real world applications. Equilibrium methods heavily rely on accurate mobility measurement to determine binding parameters. However, often times, varying the ligand concentration in the separation buffer affects the magnitude of EOF. If both the electrophoretic mobility and the EOF mobility changes, and the contribution of EOF mobility change cannot be easily corrected for[14], the correlation between migration time shift and binding will be obscured and this approach will be out of favor.

On the other hand, non-equilibrium methods are easy to do and the sample consumption is kept at minimum. The limitation though, is that these methods require sufficient resolution in order to be effective, which is not always a trivial matter since binding does not guarantee large change in electrophoretic mobility. With transient binding systems, the separation process becomes a non-linear system where simple models fail to predict the exact separation outcomes and data interpretation is less straightforward[15]. This suggests the need for more theoretical works to elucidate the correlation between binding parameters and separation results.

Over the years, many different separation methods have been successfully developed for challenging binding measurements and novel applications. A few excellent

review articles covering this topic[2, 16, 17, 18] can be referred to if interested, and the details will not be repeated here. In this work, we exclusively use APCE due to low sample consumption and easiness of implementation.

Protein Protein Interaction

Protein protein interaction (PPI) is the non-covalent interaction between proteins and protein subunits. Multitudes of intermolecular forces, including electrostatic interaction, hydrogen bonding and hydrophobic interactions, are all key participants of the binding process. Compared to the deep enzyme substrate binding pockets, protein interfaces are much larger in size and more flat. PPI can be either stable or transient. Interactions between antibody and antigen, and the interactions that hold protein subunits together are good examples of stable PPIs. Many PPIs are transient, i.e. the binding is dependent upon conditions and the complex form cannot be isolated using immunoprecipitation or far-western blotting because complex formation is reversible.

Early protein research mostly focused on individual proteins. Recent advances have shown that most proteins do not act in solitude but interact with other proteins to form complexes. The tens of thousands of proteins encoded in the human genome interact with one another and form a vast network of "interactome"[19], which are responsible for the regulation of all aspects of cellular processes, including DNA replication, transcription, translation, signal transduction, cell cycle control and metabolism.

PPIs allow targeting of specific disease pathways and represent exciting opportunities for pharmacological intervention and drug discovery[1, 20, 21, 22]. This is

already evidenced by the success of therapeutic antibodies that target PPI involving disease pathways. Therapeutic antibodies have excellent properties: they are highly specific for their molecular targets and can be engineered to be stable in human serum. However, antibodies only target extracellular receptors and are lack of oral bioavailability. The large space of intracellular protein–protein systems has yet to be explored, which have been of great interest to small molecule drug development.

Despite these interests, PPIs were previously considered to be "undruggable". Recent successes, though, have clearly shown that potent and selective modulators can be identified. More than 50 inhibitors of PPIs have been reported in the literature and some have low nanomolar potency and are achieving clinical success. And with this growing appreciation comes an undeniable need for new and potent PPI modulators. As more PPIs come into focus, demand for fast and facile PPI analysis is growing.

Protein-Protein Interaction Analysis

Protein protein interaction has many measurable effects[23], such as change in allosteric properties, substrate channeling, formation of new binding site, size increase, etc. These changes can all be useful mechanism in developing PPI assays. However, PPIs are highly diversified and methodologies established for one specific PPI may not transfer smoothly to a different target. Developing a new assay for every emerging PPI target can be a daunting task for individual researchers and early drug discovery. In addition, these effects may not be specific to PPI and compounds that alter these properties may have no impact on PPI itself. In this light, approaches that offer generic methodology development and mechanisms that are PPI specific are preferred.

Method	Concept	Information
Analytical Ultracentrifugation[24, 25]	Protein binding results in mass and sedimentation rate change.	Binding/no binding, Kd.
Native gel electrophoresis[26]	Binding with another protein causes retardation in sieving through the gel matrix during electrophoresis separation.	Binding/no binding, semi-quantitative.
Size Exclusion Chromatography[27]	Resolving complexes and free proteins based on size difference.	Binding/no binding, quantitative and stoichiometry information possible.
Hydrogen–deuterium exchange[28, 29]	In deuterium labeled solution, the acidic groups that can be accessed by the solvent will have the hydrogen atoms exchanged to deuterium atoms. Low resolution structural information can be obtained from Nuclear Magnetic Resonance (NMR) or Mass Spectrometry (MS). Protein binding changes protein conformation and surface accessibility.	Binding/no binding, structural information regarding binding sites.
Chemical cross-linking coupled to LC-MS[30]	Similar to H/D exchange, cross linking happens to solvent accessible reactive sites and freeze the binding proteins in the bound state. Cross-linking site information can be identified taking proteomic analysis approaches.	Binding/no binding. Rough correlation to binding sites. Stoichiometry.
Mass Spectrometry	Using soft ionization techniques such as nano-ESI coupled to MS, protein complexes can be detected as mass to charge ratio changes.	Binding/no binding. Stoichiometry.
Ion-mobility Mass Spectrometry[31, 32]	Mobility (charge to cross section area ratio) is measured as gas phase ions fly through a drift tube filled with carrier buffer gas.	Binding/no binding. Stability of complex structures. Stoichiometry.

Nuclear Magnetic Resonance (NMR)[33]	NMR measures PPI's effect on the chemical shift of H and C atoms.	Binding/no binding, structural information.
Fluorescence Anisotropy[34]	Small and fluorescent molecule will acquire a much slower rotation rate in the solution and a greater retention of polarization in the emission light.	Binding/no binding, Kd and kinetic information
Fluorescence Resonance Energy Transfer (FRET)[35]	PPI induces protein conformation and FRET efficiency change	Binding/no binding, Kd and kinetic information
Amplified Luminescent Proximity Homogeneous Assay (AlphaScreen) [36]	Interacting protein pair are immobilized on two different beads, which when brought to proximity by binding, produces chemical luminescence signal.	Binding/no binding, Kd
Flow Cytometry Protein Interaction Assay (FCPIA)[37]	One protein immobilized on polymer bead. Binding protein is fluorescently labeled and the binding is detected by measuring bead associated fluorescence by flow cytometry (Figure 1-3 A).	Binding/no bindng, Kd.
Surface Plasmon Resonance (SPR)[38]	Refractive index change upon protein binding to the surface immobilized interacting protein.	Binding/no bindng, Kd, and kinetic information.
Isothermal Titration Calorimetry (ITC) [39]	Using thermodynamic parameters to determine interactions in solution. Most often used to study the binding of small molecules to larger macromolecules.	Enthalpy change, Kd, Stoichiometry.
X-ray crystallography[40]	Co-crystalization of binding proteins.	Detailed structural information and stoichiometry.
Scanning Electron Microscopy (SEM)[41]	SEM image of protein complexes.	Structural information.

Table 1-1. Commonly used methods for protein-protein interaction analysis.

Previously, many analytical methods have been developed to characterize PPIs. Most commonly used ones are listed in Table1.

Some of the listed methods are separation based. The method development is relatively straightforward, and data quality is considered to be high. Concerns with separation based methods are protein consumption and analysis speed.

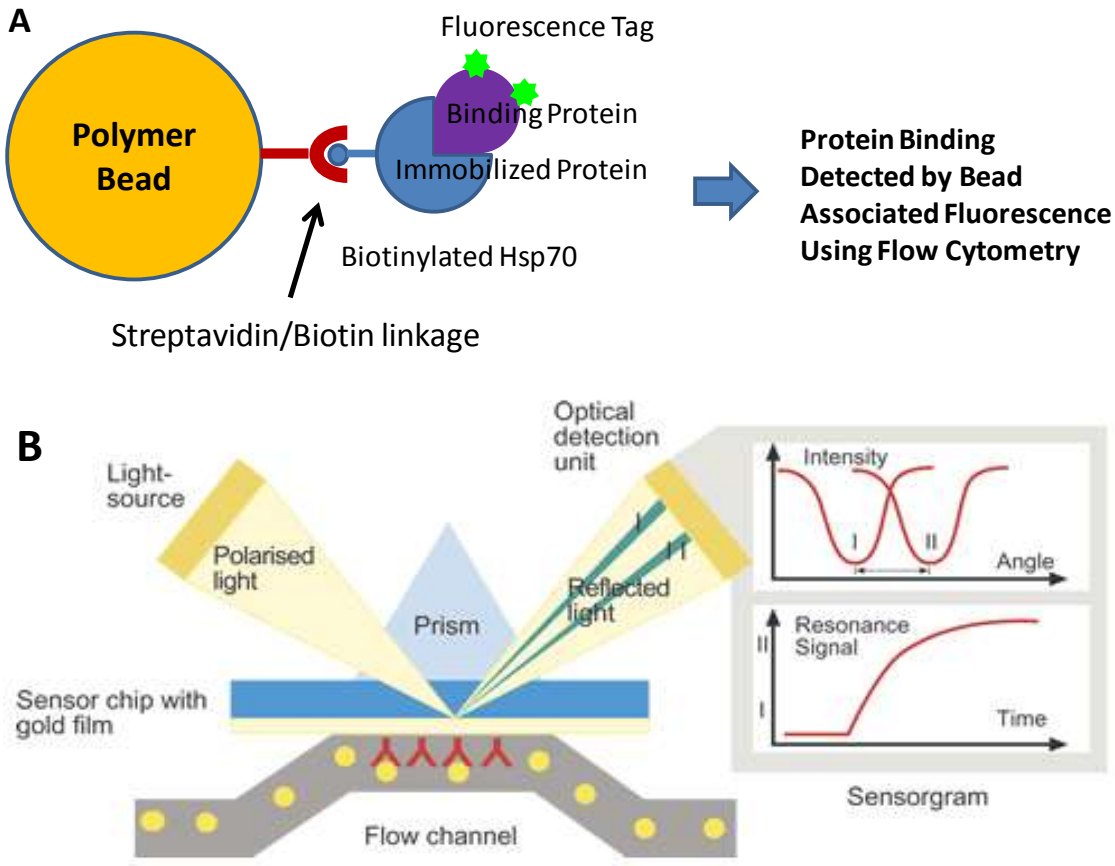

Figure 1-3. Schematics of how (A) FCPIA assay and (B) SPR works to detect PPI.

Fluorescence and chemiluminescence based methods are widely used for PPI analysis. The sensitivity is high and these platforms are compatible with micro-titer plates for rapid analysis of large sample sets. Limitations of these approaches, though is that both fluorescence and chemiluminescence are sensitive to the sample matrix.

Mechanisms other than binding can affect the signal intensity, and lead to false-positives and false-negatives. Labeling is another concern with fluorescence based methods. If labeling blocks the allosteric or binding site, affinity and response to inhibitors will change.

Surface Plasmon Resonance (SPR, Figure1-3B) is a very popular technique used to study protein protein interaction. It is label free and very useful in kinetic measurements. One drawback with SPR is that is involves immobilizing one of the binding proteins to a metal surface. Immobilization potentially blocks the binding sites of proteins and it is unrealistic to assume surface bound proteins behave the same as in free solution. Refractive index measurement cannot differentiate binding and non-specific adsorption. SPR is also costly compared to many alternative methods. Immobilization steps typically requires large amount of proteins to start with.

If structural information is desired, X-ray crystallography, Nuclear Magnetic Resonance (NMR), Scanning Electron Microscopy (SEM) and Mass Spectrometry based methods will be the methods of choice. Nonetheless, these methods require substantially more proteins and a lot of expertise, which may turn out to be overkill if only binding strength information is needed.

High Throughput Screening

High-throughput screening (HTS) is commonly used in drug discovery and relevant fields of biology and chemistry[42]. Using robotic liquid handling devices and fast speed analysis, HTS allows a researcher to quickly conduct millions of chemical, genetic

or pharmacological tests. Through this process one can rapidly identify active compounds, antibodies or genes which modulate a particular biomolecular pathway. The results of these experiments provide starting points for drug design and for understanding the interaction or role of a particular biochemical process in biology. Typically, 10,000 tests per day and above are called high throughput. Ultra high throughput refers to over 100,000 tests per day.

For protein-protein interaction studies, HTS is highly valuable and can be used for multiple purposes, such as identifying novel protein-protein interactions[19], drug screening against pathogenic PPI pathways, finding molecular mechanism and new use of existing drugs, and so on.

Currently, fluorescence based methods, such as fluorescence anisotropy, FRET, and FCPIA are the work horses for PPI targeted drug screening, primarily due to the superior sensitivity and easy interface to robotic sample handling and high-density miro-titer plate format. However, very few of the known PPI inhibitors were discovered through HTS. More specific assays that are less subjective to false-positives and false-negatives while still maintaining the HTS-friendliness are clearly in need to realize the true potential of HTS.

CE Based PPI Analysis and HTS

In principle, CE has many advantages as a PPI analysis tool. Firstly, it doesn't involve immobilization. Many immobilization related problems, such as non-specific adsorption can thus be avoided. Secondly, the mechanism of CE is specific to protein

binding events and interferences are less likely to occur. Thirdly, CE imposes no limitation the protein size. This gives CE an edge compared to the many methods that have to use smaller peptide fragments, which do not always represent the properties of full length proteins. Finally, CE is a free solution separation technique and in principle, there is no limit on sample matrix and separation buffer composition. This allows physiologically relevant separation conditions to be used that perturb the PPI to the least extent.

First CE based protein-protein interaction studies was in the early1990's where CE methods were developed to study the binding between Human Growth Hormone (HGH) and Anti-HGH antibody[43], Insulin and Insulin Antibody[10, 11], Protein A and IgG[44]. These early works focused on antibody-antigen binding measurement and CE based immunoassays, but the same concepts and techniques are applicable to protein protein interaction systems in a more general sense.

Following the pioneering works on antibody antigen binding analysis and CE based immunoassays, a few research works have been done exploring pharmacologically relevant PPIs. Using Fluorescence Anisotropy CE (FACE) and APCE, Yang and co-workers studied Src homology 2 (SH2) domain protein binding.[12] In this research, they showed that transient protein binding events between phosphorylated peptides and SH2 domain proteins can be quantitatively detected using either CE modes. They also showed that fast CE analysis allows rapid kinetic measurements. In another study[13], they showed that multiple peptide-protein complex can be detected in the same CE run, suggesting multiplexing capability of CE methods. This work also investigated the inhibitors' effect

on protein protein binding using fast CE assay, which further suggest that CE assay can be used in inhibitor and drug discovery applications.

These early works proved that CE can be used to study not only antibody-antigen binding, but can also be used to study transient interactions with fast dissociation rate. Many separation modes were experienced and APCE seemed to be both generic and reliable if full length proteins were to be used. Despite the previous efforts, the full potential of CE can has yet to be realized with full length proteins and demonstration with more PPI targets.

One of the unmet challenges is protein adsorption. Successful CE separation requires the capillary inner surface to be inert and analyte adsorption to be minimized, because adsorption consumes analyte and slows down EOF, which in turn compromised the reproducibility of the methods developed.

Protein adsorption process is initiated by electrostatic interaction between the positively charged groups on protein surfaces and the negatively charged silanol groups on bare silica capillary surface[45] (Figure 1-4). Through dehydration and enthalpy driven protein conformation change, protein adsorption process becomes irreversible.

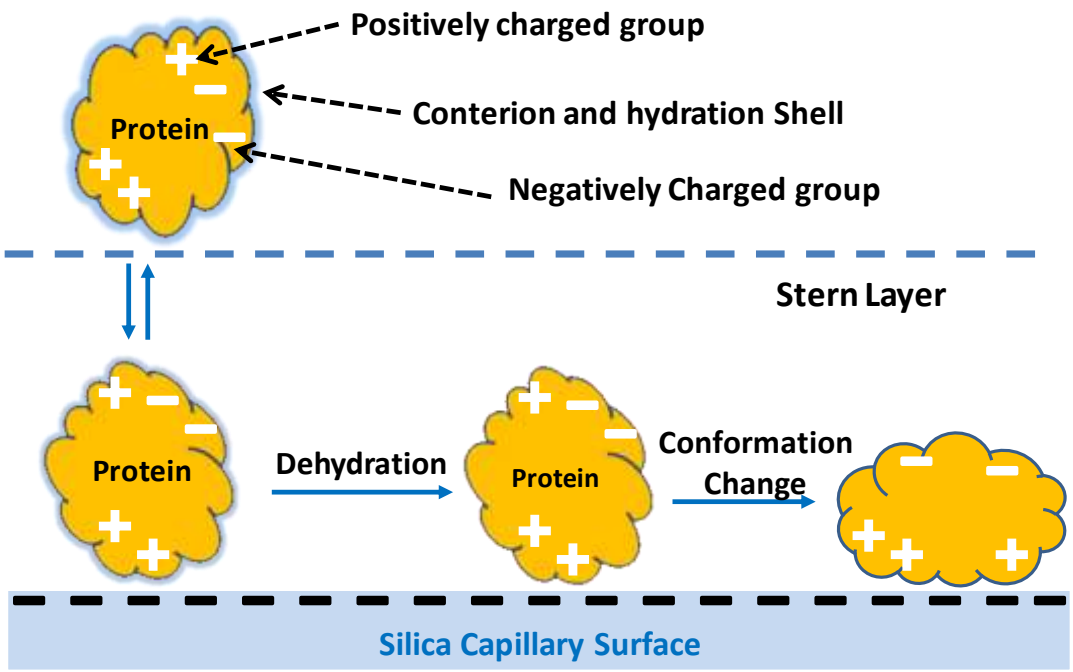

Fgiure 1-4. Illustrative drawing of protein adsorption onto bare silica surface.

Correspondingly, protein adsorption prevention strategies follow the guideline of minimizing electrostatic interactions, and specific approaches can be categorized into a few classes[7]: 1) extreme buffer pHs at which electrostatic repulsion dominates; 2) higher buffer ionic strength so the electrostatic attractions are weakened; 3) amine containing or zwitterion buffer molecules that compete with proteins for surface adsorption sites; 4) surface modified capillaries with surface charges neutralized or reversed. Excellent reviews can be found on specific approaches and applications[45, 46, 47, 48], and the details will not be elaborated here.

In PPI studies, it is inevitable that one or both binding proteins adsorb to the silica surface. In those cases, the strategies described above can be used. However, affinity studies places additional requirements for the separation conditions: the separation

conditions have to be gentle to the protein binding system and mimic the *in vivo* environment of these proteins as much as possible. Keeping these considerations in mind, extreme pHs, high concentration denaturing molecules and species that interfere with the protein binding have to be excluded from the toolbox of CE methodology development. In reality, surface modified capillary often turns out to be the most effective if not the only effective strategy.

Hsp 70 and co-chaperone Bag3

Hsp70 (~70 kDa) is a molecular chaperone that helps newly synthesized proteins to fold properly and is expressed in response to stress[49, 50]. In the latter role, Hsp70 binds to protein substrates and stabilize them against denaturation or aggregation until conditions improve. This chaperone broadly shapes protein homeostasis by protein quality control and turnover during both normal and stress conditions. Consistent with these diverse activities, genetic and biochemical studies have implicated it in a range of diseases, including cancer, neurodegeneration, allograft rejection and infection.

Specific function of Hsp70 is modulated by co-chaperones like Bcl2-associated athanogene 3 (Bag3). Bag3 binds the nucleotide domain of Hsp70 with high affinity. In cancer cells, the Bag3-Hsp70 complex stabilizes a number of key oncogenes by protecting Hsp70-bound substrates from degradation and suppresses apoptosis. Evidence has been found that silencing of Bag3 in multiple tumor lines sensitizes the cells to chemotherapy. For these reasons, Bag3-Hsp70 complex is a potential PPI drug target for cancer. Through this thesis, we use Heat shock protein 70 (Hsp70) and (Bag3) as the model protein binding system.

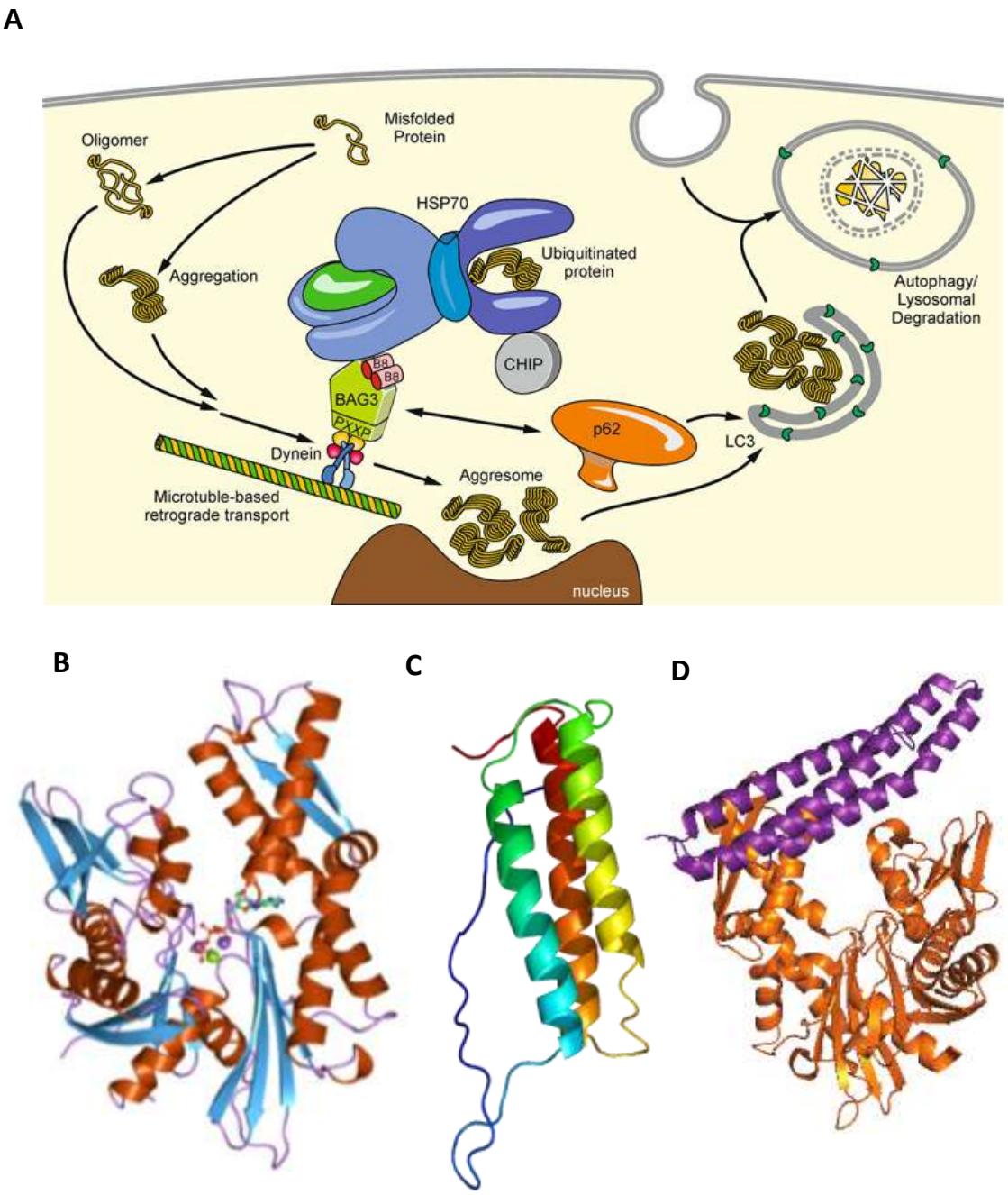

Figure 1-5. (A) Roles of Hsp70 and Bag3 in anti-apoptotic signaling[51]. Crystal structures of (A) nucleotide binding domain of Hsp70; (B) Bag3 and (C) Bag domain binding to the NBD domain of Hsp70[49].

Segmented Flow Microfluidics and Nanoliter Liquid Handling

Although CE injections take only nanoliter samples, at least 10 μL initial volume is needed in order for injection methods to work, which means over 99.9% of the samples are wasted. In high throughput screening, reagent consumption contributes to a big percentage of the total cost. While 10 μL is acceptable, in reducing sample consumption, CE's potential has yet to be unleashed.

The challenges in developing assays that work with nano-liter volume samples lie in the difficulty in handling these extremely small volumes. Commercially available CE instruments are compatible with 96- and 384-well plates with sample volume ranging from 10-100 μL. With fluorescence readout, 1524-well plates and as low as 1 μL sample can be achieved. However, further increase in array density and decrease in sample volume is almost impossible with the multi-well plate format limited by evaporation and reagent dispensing technologies.

Confining nanoliter sample plugs or segments by gas or immiscible liquid has recently emerged as a promising alternative to well plate-based screening[52]. As shown in Figure 1-6, the sample plugs or droplets immersed in the oil phase act as miniaturized reaction vessels and they can be manipulated automatically with the help of microfluidic droplet manipulation techniques and a combination of "unit operations". A full spectrum of sample manipulating techniques including sampling, dilution and reagent addition has been demonstrated. Many detection schemes, such as fluorescence, electrochemical, NMR, MS, enzyme assay and immunoassay have been demonstrated to be effective in coupling to segmented flow samples. Most noteworthy is the coupling of these

segmented samples to rapid and highly efficient CE separation[53, 54, 55], which is a significant addition to the toolbox of segmented flow.

A

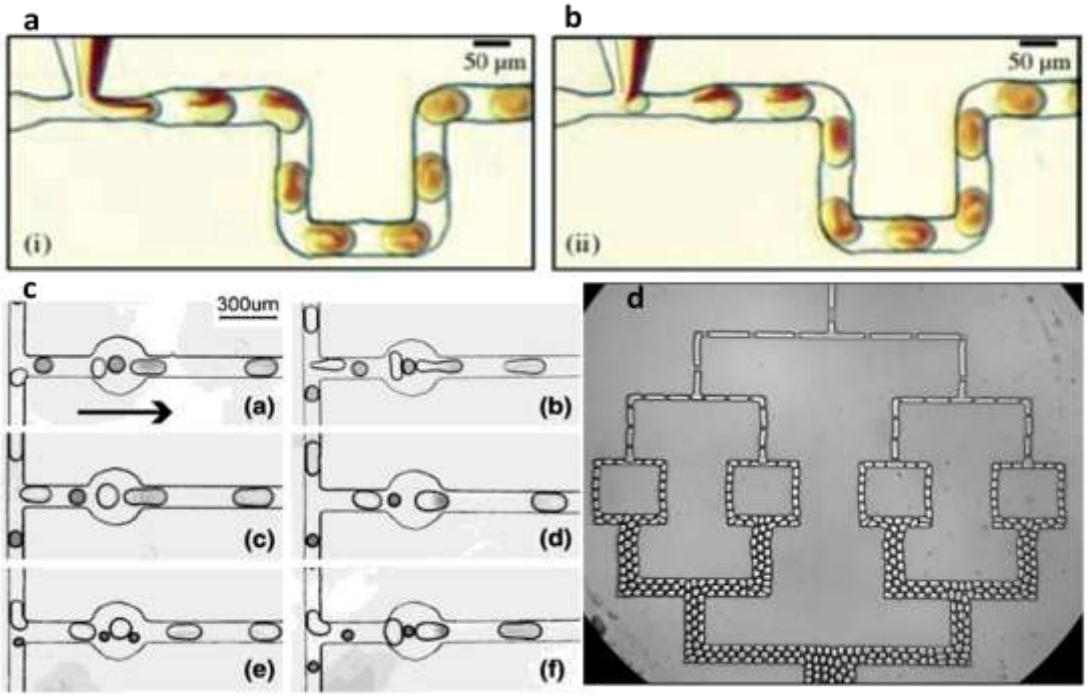

B

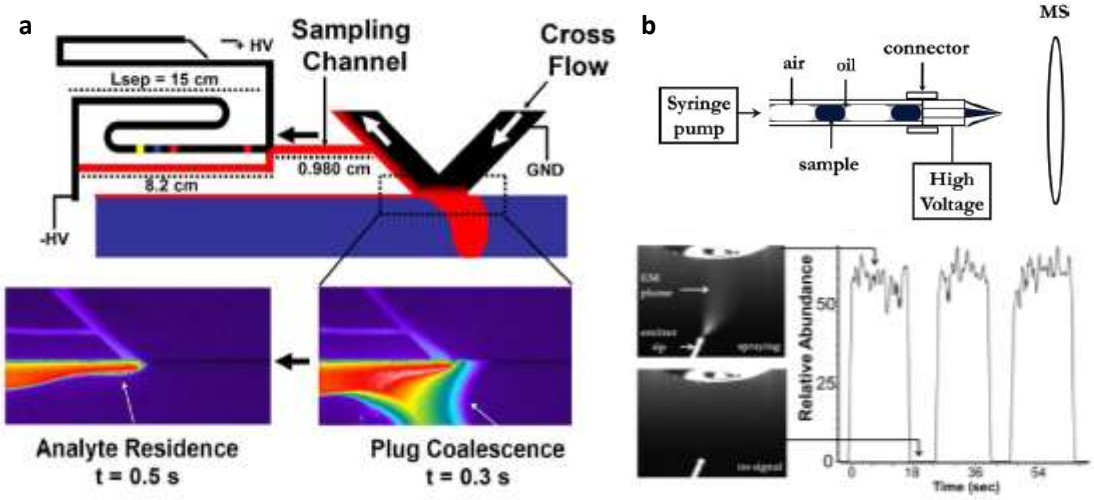

Figure 1-6. (A) Examples of droplet manipulations: a. droplet generation through a T-junction[56, 57]; b. mixing in droplets; c. controlled coalescence; d. droplet splitting. (B)

Interfacing droplet samples to CE separation[54] (a) and ESI-MS analysis[55] (b).

HTS experiment is comprised of multiple steps and a lot of sample handling and reagent addition steps are needed in addition to the final readout. We realized that robust and easy to interface "unit operation", such as sampling and reagent addition are needed in order to approach the goal of nanoliter HTS assay. Motivated by this thought, we developed a sampling device and a reagent injector for nanoliter size segmented flow samples, which will be covered in the second half of this thesis.

CHAPTER 2

CAPILLARY ELECTROPHORESIS BASED PROTEIN PROTEIN INTERACTION ASSAY FOR HSP70 AND BAG3

Introduction

Protein Protein Interactions (PPIs) controls virtually every aspect of cellular processes and are closely involved in many pathogenic pathways. Better understanding of PPIs and development of chemical probes and modulators of such interaction are not only actively pursued research topics, but also presents exciting opportunities for drug discovery[20, 21, 22]. Meeting these promises, however, requires facile analytical techniques that are capable of characterizing various PPIs and provide quantitative information regarding binding strength, kinetics, stoichiometry, and so on.

CE has long been shown to be successful in detecting non-covalent interactions and is principally sound for PPI analysis[2, 9, 12, 18]. Through various ligand-receptor binding studies, CE based methods have shown great potential in PPI analysis: 1) as a free solution technique, CE overcomes non-specific adsorption and potential blockage of active binding sites due to surface immobilization; 2) mechanism is binding specific and false responses from interfering mechanisms are minimized; 3) extremely low sample consumption and high tolerance to protein impurities, which makes CE amendable for challenging research and drug development tasks where protein availability and purity are both limited.

Previous efforts in CE based PPI analysis focused on answering two questions. Firstly, among the various modes of CE that can be used for affinity studies, which mode(s) is most favorable. Secondly, although CE has been demonstrated very useful in characterizing interactions between antibody and antigen and widely used as a strategy for developing fast and cost-effective immuno-assays[10, 11], is it feasible for other PPIs that are more transient in nature. Yang and co-workers were able to demonstrate with a peptide-protein binding model that both equilibrium methods and non-equilibrium methods can be used, and CE is highly effective in detecting peptide-protein complexes that have fast association and dissociation rates.[12, 13]

Despite these advancements, for CE to achieve widespread application in PPI analysis, more effort is needed in developing reliable labeling reactions that are friendly with intact proteins and yield stable protein conjugates if LIF detection were to be used, addressing protein adsorption that often compromises separation and assay robustness, and more successful examples that demonstrate generic methodology development for PPI analysis and applications with biologically relevant PPI targets.

In this work, we attempt to answer these challenges by developing a CE based PPI assay for Hsp70 and its co-chaperone Bag3. Heat shock protein70s (Hsp70s) are chaperone proteins that assist newly synthesized protein to fold and help to stabilize proteins as cells respond to stress[49]. Consistent with these cellular responsibilities, Hsp70 is implicated in many diseases such as Alzheimer's and cancer[58]. The specific function of Hsp70 is modulated by its co-chaperones, such as Bcl-2 associated Anathogene 3 (Bag3), which binds the nucleotide binding domain of Hsp70 with high affinity. Bag3 was found to have anti-apoptotic properties by divert a number of oncogenes from degradation

process and the mechanism is highly Hsp70 dependent.[59, 60, 61] Evidences suggest that Hsp70 and Bag3 binding is an interesting drug target for cancer.

With this PPI model system, we experienced ourselves with the key steps towards a successful CE assay. Full length Hsp70 extracted from cell culture was purified and labeled with Alexafluor® 488. By optimizing the surface modification, we were able to address the protein adsorption problem by using a covalently modified capillary. Using Affinity Probe CE (APCE), protein complex was detected with good sensitivity and reproducibility. The method is further validated by competitive binding and binding constant measurement experiments. This method has also been applied as a secondary confirmation assay for inhibitors identified from a flow cytometry based assay.

High Throughput Screening (HTS) is a very useful research tool and an important step in modern drug development pipeline. CE separation can be performed in seconds[62] consuming nanoliters of samples and less, suggesting great potential in HTS. In this work, we also explored the possibility of HTS. By applying pressure during separation, the analysis time was reduced to 6.5 min per assay, suggesting a moderate scale screening is possible with this approach. Further improvement on separation speed should be achievable by adapting the system to fast CE and micro-chip CE separations.

Experimental Section

Materials. Alexafluor488 SDP ester protein labeling kit was purchased from Life Technologies (Carlsbad, CA). Rhodamine 110 was from Invitrogen (Eugene, OR). 1H, 1H, 2H, 2H-perfluorooctyltrichlorosilane (PFOTCS) and all the other chemicals were

purchased from Sigma Aldrich (St. Louis, WO) otherwise noted. Fused silica capillary was purchased from Polymicro Technologies (Phoenix, AZ). Commercial surface modified CE capillaries, including polyacrylamide (eCAP neutral capillary) and polyamine modified ones were both purchased from Beckman Coulter Inc. (Fullerton, CA). Buffers were made in deionized water purified by E-Pure water systems (Barnstead International Co., Dubuque, IA).

Protein Purification and Labeling. Human Hsp70 (HSPA1) was purified as described in literature (reference) using a His column, TEV cleavage of the his tag, followed by an ATP agarose column. Human N-terminal his-tagged Bag3 was purified based on previous reports (reference). Briefly, Bag3 was precipitated by ammonium sulfate (0-30% of saturation) followed by a His column and TEV cleavage of the his tag. Bag3 was dialyzed overnight into buffer (25mM HEPES, 10mM NaCl, 15mM β-mercaptoethanol, 0.1mM EDTA, pH 7.6) and subjected to ion-exchange chromatography on a Mono-Q HR 16/10 column (GE Healthcare). Finally, Bag3 was purified by size exclusion chromatography on a Superdex 200 gel filtration column (GE Healthcare). Hsp70 was labeled with AlexaFluor® 488 5-SDP ester according to the supplier's instructions. After labeling, the reaction products were cleaned up gel filtration to remove any residual labeling reagents. Protein concentrations are determined by BCA assay. These proteins were stored under -80 °C as small aliquots and thawed upon analysis.

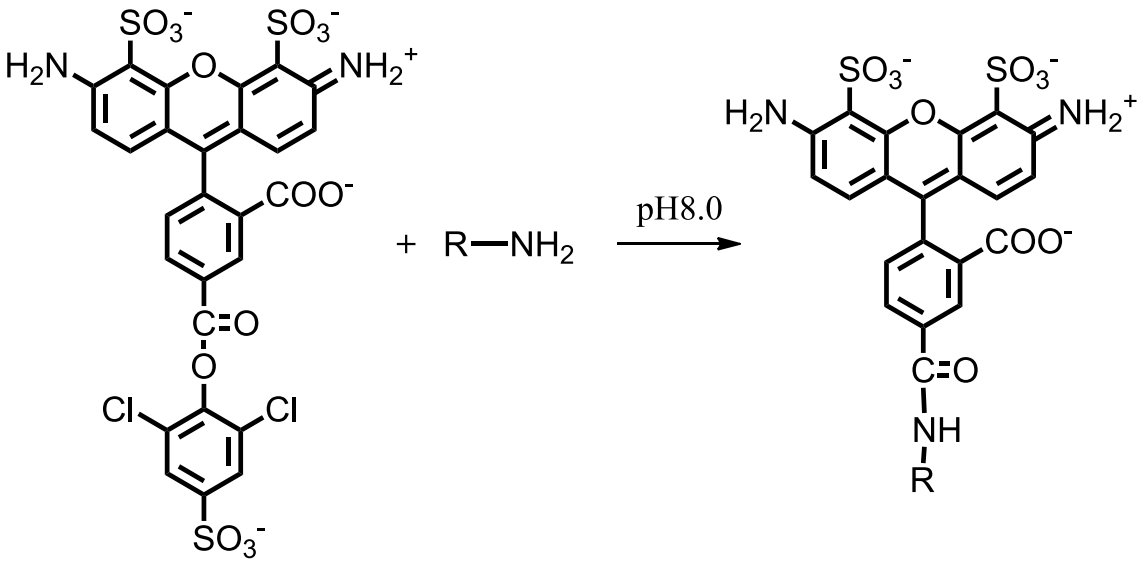

Alaxafluor 488 SDP ester

Figure 2-1. Alexafluor® 488 SDP ester react with amines to form fluorescent conjugates.

PFOTCS derivatized capillaries. 50 mm inner diameter 360 mm outer diameter polyimide coated fused silica capillaries were derivatized using a home built setup consisting of a pressure bomb and oil bath that controls temperature (Figure 2-1A). The acidic silanol groups on the silica surface are modified covalently with a silanization reagent PFOTCS (Figure 2-1B). The derivatization reaction is carried out by pressurizing the liquid solvent placed in a stainless steel pressure bomb through the capillary tubing. Tank nitrogen (Cryogenic Gases, Detroit, MI) at 30 p.s.i. is used as the pressure source for all the steps described in below. Three steps of rinsing and activation: 1) MeOH rinse at room temperature; 2) RCA solution (NH_4OH:H_2O_2:H_2O v:v:v = 1:1:5) rinse at 120 °C; 3) 0.1 M HCl rinse at 90°C. Every activation step takes 1 hour. After activation, the residual liquid is purged out of the capillary and the capillary inner surface is dried under

dry nitrogen flow at 165 °C overnight. 10% (volume percent) PFOTCS dissolved in toluene was continuously infused for 3 hours at 120 °C. After reaction, the derivatized capillary was rinsed with toluene and methanol to rinse off residual reactive species. The capillary is emptied and further dried in oven at 80 °C overnight. Detection window is burned by hot sulfuric acid and the capillary ends were sealed with capillary wax until being used.

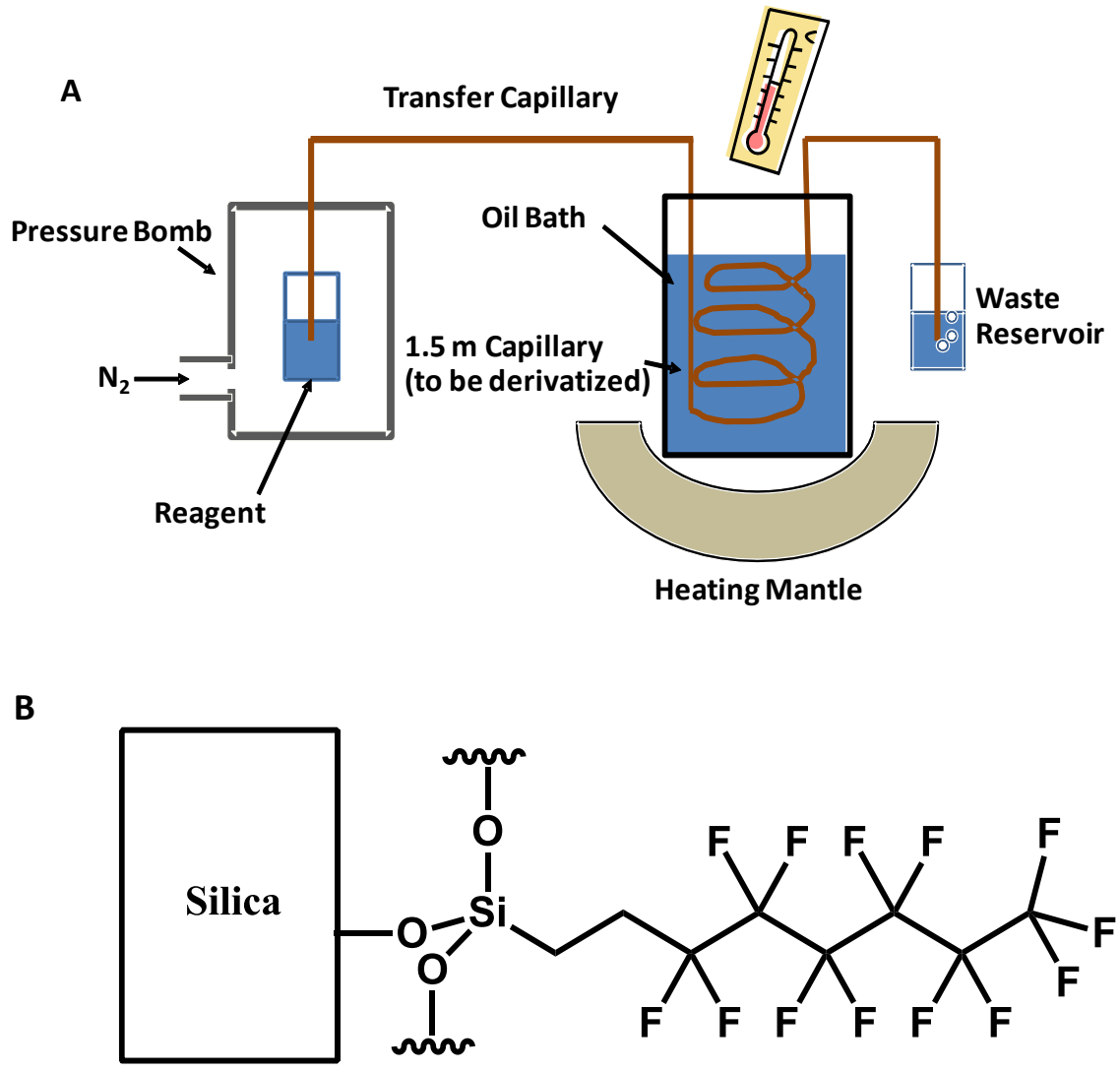

Figure 2-2. A. Home-built setup for capillary derivatization. B. Illustration of silica

surface after PFOTCS derivatization.

Capillary electrophoresis. Beckman Coulter MDQ/PACE capillary electrophoresis system (Beckman Coulter Inc., Fullerton, CA) was used in most of the experiments described herein unless otherwise noted. Separation cartridge and sample storage temperatures were both maintained at 25°C. LIF detection used 488-nm light from a 20 mW optically pumped semiconductor Sapphire laser (Coherent, Santa Clara, CA) that is coupled to the LIF detection module through fiber optics. Emission was filtered by a 520 ± 10 nm band-pass filter. The CE instrument was controlled by P/ACE 32 Karat Software Version 5.0 installed on a computer. In all CE experiments, the short end of 30 cm long capillaries was used corresponding to a 10 cm effective separation length.

Screening of four surface modified capillaries. To determine what surface chemistry works the best to prevent protein adsorption, four different surface modified capillaries were tried with the same protein samples containing Hsp70 and Bag3 under different separation conditions as summarized in the table in below.

Bonding	Separation Buffer	Buffer Additive
None	50 mM Tris 192 mM glycine pH 8.3	None
Polyacrylamide	40 mM Tris pH8.0	None
Polyvinyl alcohol	10 mM Phosphate pH7.5	None
Polyamine	40 mM MES-Citrate pH6.0	None
PFOTCS	10 mM Phosphate pH7.5	0.01% Tween20

Table 2-1. Separation conditions for four different surface modified capillaries

For all the separation experiments, separation buffers were made fresh daily and filtered by 0.2 μm membrane filter (GE Healthcare, Piscataway, NJ) to remove particulates. Protein samples used were 1 μM labeled Hsp70 dissolved in sample buffer (25 mM HEPES pH7.5, 5 mM $MgCl_2$, 10 mM KCl, 1mM ATP and 0.2% (w/v) Tween20) to test if expected change in peak heights and peak shape could be detected after Bag3 was added. In all these experiments, pressure injection at 0.3 p.s.i. for 5 second was used. Electric filed was kept at 500 V/cm for all CE experiments. For polyarylamide and polyamine modified capillaries, reversed polarity was used. Normal polarity was used for all the other capillaries.

Titration and competitive binding experiments. After optimizing the surface modification, the CE method was submitted to a series of tests to evaluate the validity and quantitative performance of the CE assay. To determine the quantitative response of adding unlabeled Bag3 to Alexafluor 488-Hsp70 (abbreviated as Hsp70-488 from now on), a titration experiment was performed using CE-LIF as readout. In the titration experiment, the concentration of Hsp70-488 was fixed at 1 μM and unlabeled Bag3 was added for multiple times to create increasing Bag3 concentrations. Bag3 concentration ranged from 0 to 2.5 μM at different increments. 3 electropherograms were obtained for each Bag3 concentration. In the competitive binding experiment, 2 μM unlabeled Hsp70 was added to the mixture of 1 μM Hsp70-488 and 1 μM Bag3. In both experiments, protein samples were dissolved prepared in 25 mM HEPES pH7.5 buffer with 5 mM MgCl2, mM KCl, 1 mM ATP and 0.2% (w:v) Tween20.

Inhibitor screening and dose response studies. 18 compounds were identified as inhibitors for Hsp70-Bag3 binding by Flow Cytometry Protein Interaction Assay (FCPIA). The developed assay was used as a secondary confirmatory assay for these 18 compounds. DMSO was used to make 10 mM stock solutions except #18 was dissolved in water at 3 mM concentration due to poor solubility in DMSO. In the CE screen, all 18 compounds were tested at 100 uM final concentration with 1 uM Hsp70 and 1 uM Bag3. Free to complex peak area ratio were taken and used as a criteria for inhibitor screen. Dose response studies were carried out for CE confirmed inhibitors #9, #14, #16 and #17. Analogues of #9 were also studies by dose response studies using the CE assay.

Data analysis. CE data was analyzed with Cutter 7, which is home-written software[63]. Curve fitting and dissociation constant Kd determination was carried out using Origin 6.0 (OriginLab, Northampton, MA) which was also used for Dose-Response Curves (DRCs) and IC50 determination. Error was reported as ± standard error from the average. Origin 6.0 was also used for graphing the data.

Results and Discussion

Reducing protein adsorption by capillary surface modification. Initial method development with bare silica capillary achieved limited success due to protein adsorption problem. Two samples, one containing Alexafluor® 488 labeled Hsp70 (Hsp70-488) and another with equal concentration of unlabeled Bag3 added, were tested using bare silica capillaries and standard separation conditions. In the APCE mode, it is expected that upon addition of a unlabeled binding partner, the peak of the affinity probe, i.e. Hsp70-

488, should decrease and a new peak that correspond to the affinity complex should appear. However, as is shown in Figure 2-3A, the Hsp70 peak decreased, but the complex peak was not observed. We hypothesized that the missing of complex peak is due to protein adsorption, and this hypothesis was confirmed by total fluorescence signal measurement and fluorescent microscopy studies (data not shown) that suggests no quenching in fluorescence upon adding Bag3 and strong retention of fluorescence species on capillary inner surface after Hsp70 and Bag3 mixture was applied.

Protein adsorption was widely observed with CE based separations and one of the consensuses is that surface modified capillaries can be used to effectively counteract the tendency of protein sticking to capillary surface. Among the various surface modifications that have been reported successful, we chose four different surface modifications that are popular in their own categories: polyacrylamide and PVA are representatives of neutral and hydrophilic surface polymer coatings, polyamine that reversed surface charge, and PFOTCS that is neutral and hydrophobic and used in combination with a surfactant Tween20[64] to generate a dynamic and continuously refreshed neutral and hydrophilic surface coating.

Among the four columns tested, both polyarylamide and PFOTCS were successful in detecting expected appearance of complex peak as shown in Figure 2-3B and 2-3E. With PVA and polyamine coating, the reduction of Hsp70 peak was also was observed with addition of Bag3, but the results were not any superior than bare-silica capillary and separation took much longer time. Between polyacrylamide and PFOTCS, PFOTCS clearly offers better resolution. Although Tween20 has to be used as a buffer modifier, tests from the collaboration lab found the existence of this surfactant does not

intervene with the Hsp70 and Bag3 binding. Eventually, we settled down with the PFOTCS column which will be used throughout the rest of this research.

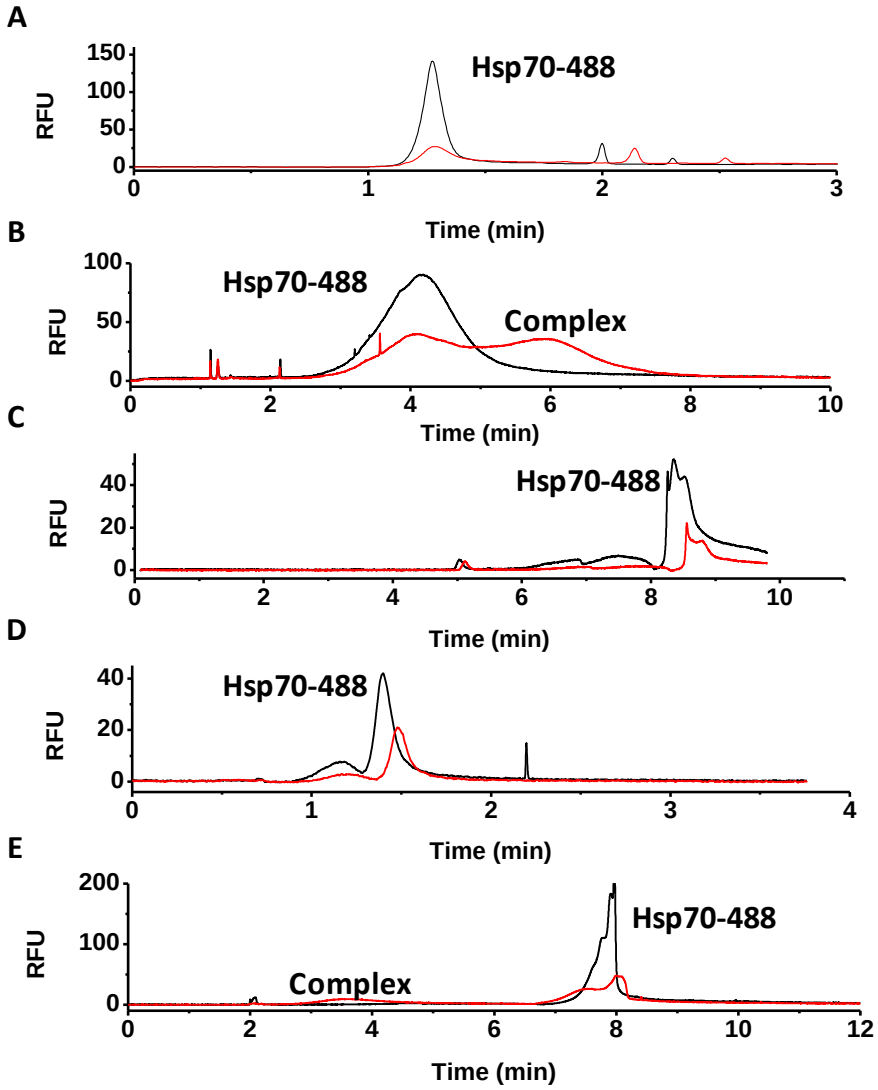

Figure 2-3. Electropherograms' response to adding Bag3 to Hsp70-488. Comparison is made between A. bare silica capillary, B. polyacrylamide capillary, C. polyamine coated capillary, D. PVA coated capillary and E. PFOTCS capillary that is dynamically coated with Tween20. Black traces represent without Bag3 added, and red traces are with Bag3 added. 3 second pressure injection at 0.5 p.s.i. and 500V/cm electric field was used for all the separations. Except for polyacrylamide and polyamine columns, normal polarity was used with 10 cm effective separation length.

Method validation. After addressing the protein adsorption problem, we subjected our method to competitive binding experiment to validate. In this experiment, unlabeled 2 μM Hsp70 was added to the mixture of 1 μM Hsp70-488 and 1 μM Bag3. Unlabeled Hsp70 will compete with Hsp70-488 for available Bag3 in the sample. Because Bag3 is at lower concentration compared the concentration that is needed for all Hsp70, competition frees some Bag3 bound labeled Hsp70. As a result, the amount of fluorescent complex decreases and the free Hsp70-488 increases, which is reflected as the decrease in complex peak and increase in Hsp70-488 peak. As shown in Figure 2-4, this is exactly what we observed empirically. The complex peak with migration time of 3.3 minute was reduced and free Hsp70 peak became taller. These results further confirmed the identity of the two major peaks.

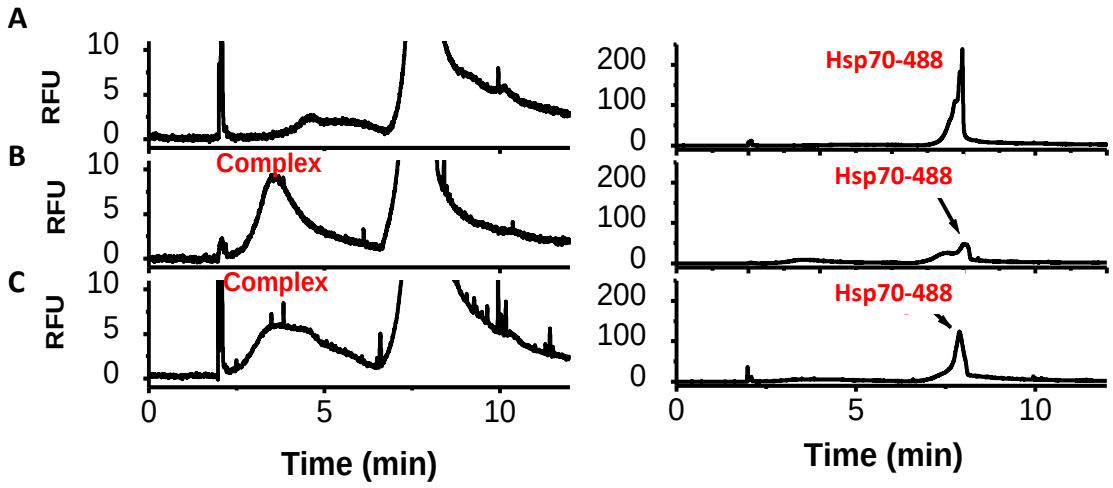

Figure 2-4. Electropherograms of (A) 1 μM Hsp70-488; (B) 1 μM Bag3 added and (C) 1 μM unlabeled Hsp70 added. Electropherograms in the same row are the same except being drawn to different scales.

Next, we tested the quantitative performance of this method by a titration experiment and dissociation constant Kd determination. Previously, the effectiveness of this assay was confirmed by qualitative measurements showing the relative peak heights and peak areas respond to Bag3 concentration changes as predicted by theory. In principle, with LIF detection that responds linearly to concentration change, CE method is capable of quantitative measurements as well. To demonstrate, we obtained electropherograms with at constant Hsp70 concentration and increasing concentration of Bag3. As shown in Figure 2-5, the complex peak increased with Bag3 concentration, and the peak area of the complex peak correlates with the Bag3 concentration added conforming to a saturation binding model.

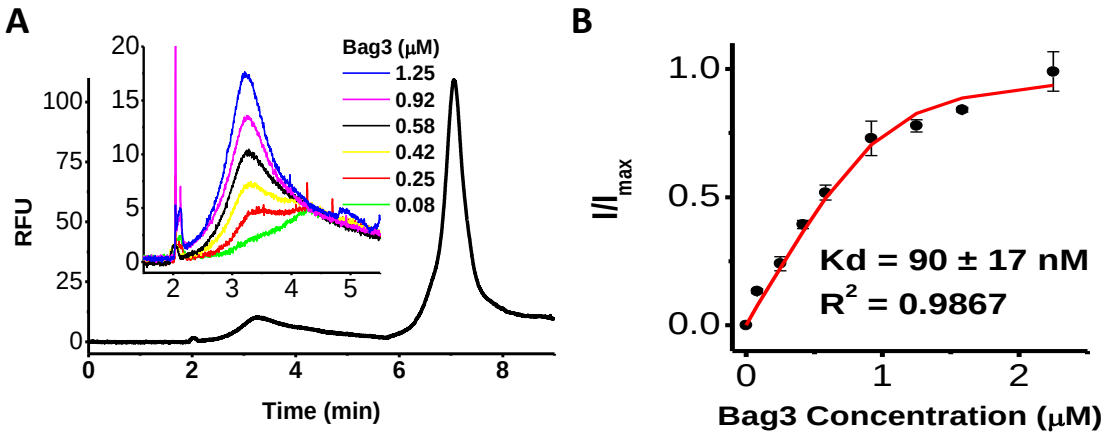

Figure 2-5. (A) Titrating Bag3 to Hsp70 cause complex peak to increase and (B) the response can be used to quantitatively determine the Kd of Hsp70-488 and Bag3 to be 90 ±17 nM.

By applying non-linear regression according to equations Eq. 2-1, assuming the peak area of complex peak is proportional to the concentration of complex in the sample

solution at equilibrium, dissociation constant Kd of Hsp70 and Bag3 is determined to be 90 ±17 nM. With the same proteins and flow cytometry assay, the Kd was determined to be 30 nM. The two values are within the same magnitude. The three fold decrease in affinity may be attributed to the fact in the CE assay, Hsp70 is labled, whereas in the flow cytometry assay, Bag3 is labeled. Another contributing factor is could be that Hsp70 has self-association property. Immobilized Hsp70 is less affected by the self-association of Hsp70 causing a decrease of apparent Kd being measured as compared to CE.

$[A] \cdot [B] = K_d \cdot [AB]$

$[A] = [A]_t - [AB]$

$[B] = [B]_t^x - [AB]$

$[AB] = k \cdot I_{AB}^y$

$kI_{AB}^{max} = [A]_t$

$([A]_t - \frac{I_{AB}^y}{I_{AB}^{max}} \cdot [A]_t)([B]_t^x - \frac{I_{AB}^y}{I_{AB}^{max}} \cdot [A]_t) = K_d \cdot \frac{I_{AB}^y}{I_{AB}^{max}} \cdot [A]_t$ (**Eq.** 2-1)

[A]: Concentration of protein A at equilibrium

[B]: Concentration of protein B at equilibrium

[AB]: Concentration of protein complex AB at equilibrium

K_d: Dissociation constant

$[A]_t$: Total concentration of protein A. Here the fixed concentration of Hsp70-488 is used

$[B]_t^x$: Total concentration of protein B, which is the x on the saturation curve

I_{AB}^y: Signal intensity of protein complex. Here we use the combined peak area of complex peak and dissociation bridge, which is the y on the saturation curve.

k: Constant that is the ratio of peak area and protein complex concentration at equilibrium.

I_{AB}^{max} : Signal intensity at saturation point of the titration experiment.

Small molecule inhibitor confirmation and IC_{50}s. With the method validated, we used the CE assay as a secondary confirmatory assay for inhibitors indentified in a by the flow cytometry assay. 18 compounds were tested (compound information can be found in Appendix A) at 100 μM. By taking free to bound peak area ratio, a single selection criterion can be established to compare the inhibitory effect of different compounds to the control. Since the presence of inhibitor cause complex to dissociate, the complex peak will decrease and the free peak will increase if a compound has inhibitory effects on Hsp70 and Bag3 binding, resulting in a net increase in free/complex peak area ratio. Although either decrease in complex or increase in free can be used as selection criterion, taking ratio is more advantageous because it corrects for variations in injection volume and long term light source fluctuation. Also, it obviates the need for internal standards.

From Figure 2-6A, compound #9, #14, #17 and #18 were confirmed as inhibitors as the free to bound ratios exceeded average + 2.5 SD (standard deviation). As an example of confirmed inhibitors, the electropherograms of samples with and without 100 mM #14 are compared in Figure 2-6B. In this case, addition of #14 lowered the complex peak and heightened the free peak. #14 is epigallocatechin gallate, abbreviated as EGCG, which is a type of catechin that is most abundant in green tea extracts. EGCG has been shown to have multiple theraputic benefits against cancer and neurodegeneration. The molecular mechanism is found to be related to the binding and inhibition of Bcl-xl proteins and the Hsp90 family. It is not surprising that EGCG also shows efficacy in inhibiting Hsp70-Bag3 binding. The IC_{50} of EGCG is determined to be 14 ± 4 μM through a dose response study (Figure 2-6C).

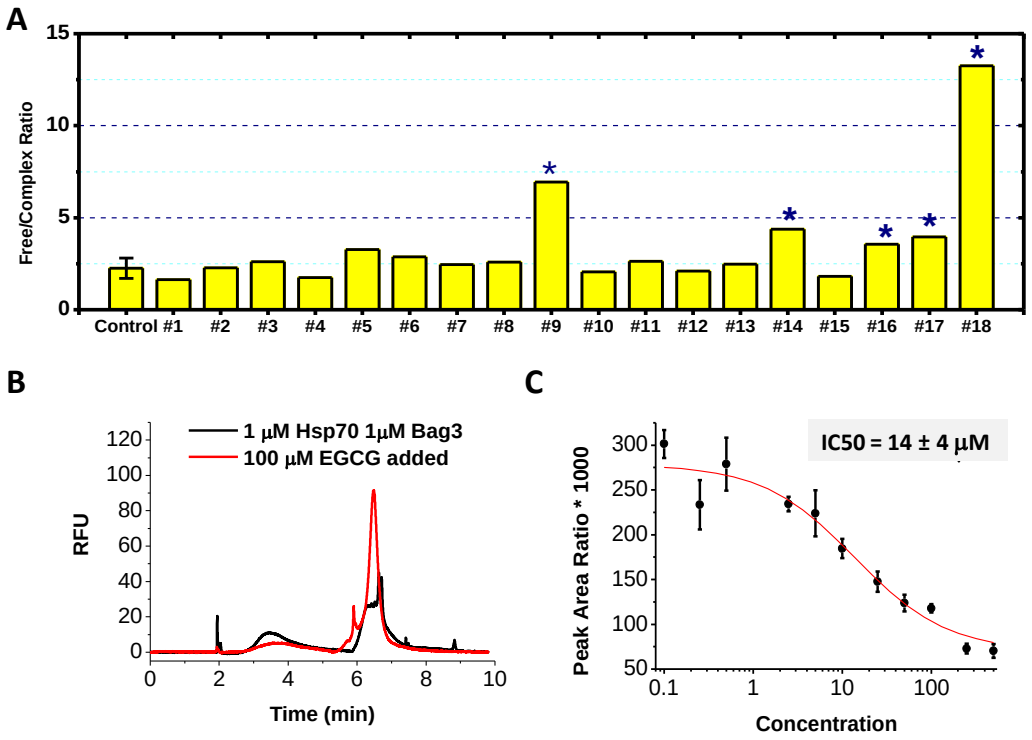

Figure 2-6. A. Free/bound peak area ratios measured by APCE for 18 potential inhibitors of Hsp70 and Bag3 binding. Control value is shown with error bars representing 2.5 times standard deviation from the average of 3 replicates. Asterisk labeled compounds were considered to be significant. B. electropherograms of 1 μM Hsp70 and Bag3 with and without 100 μM EGCG. C Dose response curve of EGCG using CE.

#9 analogue studies. Later on, we used the CE assay for another pharmacological study where the structure efficacy relationship was studied for inhibitor #9 (Figure 2-7A) using compounds with similar structures. DRC curves of 8 structural analogues (#9A –H, identities are specified in Appendix B) were obtained with the CE method as shown in Figure 2-7B. Among the 8 compounds, #9C and #9G showed similar efficacy as #9 itself. #9A, #9B and #9H showed inhibitory effects only at much higher concentrations. Structural analysis indicates that both the core structure, which is the anthraquinone

structure and the carboxylic acid group are responsible for the inhibition of Hsp70 and Bag3 binding. Agreement was achieved between CE study and flow cytometry data, which also confirmed that #9C, G, A B and H are inhibitors and #9C and #9G has best efficacy.

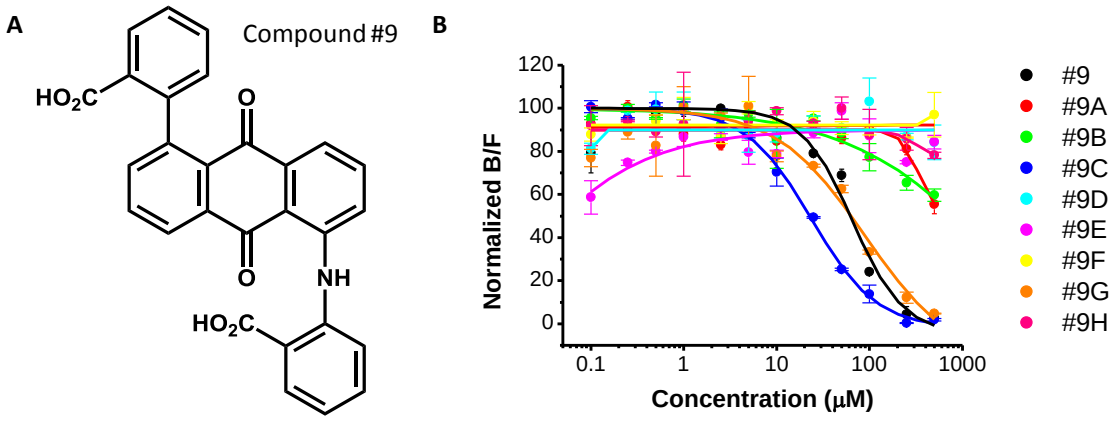

Figure 2-7. A. Chemical structure of compound #9. B. DRCs of #9 and its structural analogues.

Speed up separation by using pressure. With adequate resolution, the CE separation can be sped up by simply apply hydrodynamic pressure across the capillary to push the injection plug towards the detection point and force the separation to complete in shorter time. Previously, the CE separation was only driven by the electric field. By applying 0.5 p.s.i. pressure across the separation capillary, the linear flow rate was increased by 6.0 cm·min^{-1}. Combined with EOF, which is 3.6 cm·min^{-1} at 500V/cm, the increased flow rate allowed the separation to be completed in 3 minutes (Figure 2-8), suggesting a moderate scale screening with a few thousand tests should be feasible.

Hydrodynamic flow with parabolic flow profile inevitably reduced resolution and efficiency. Higher pressure and faster separation with the current system is impossible because we found 0.5 p.s.i. was the highest pressure that can be applied before the complex peak and the free peak begin to merge, in which case binding information will be lost.

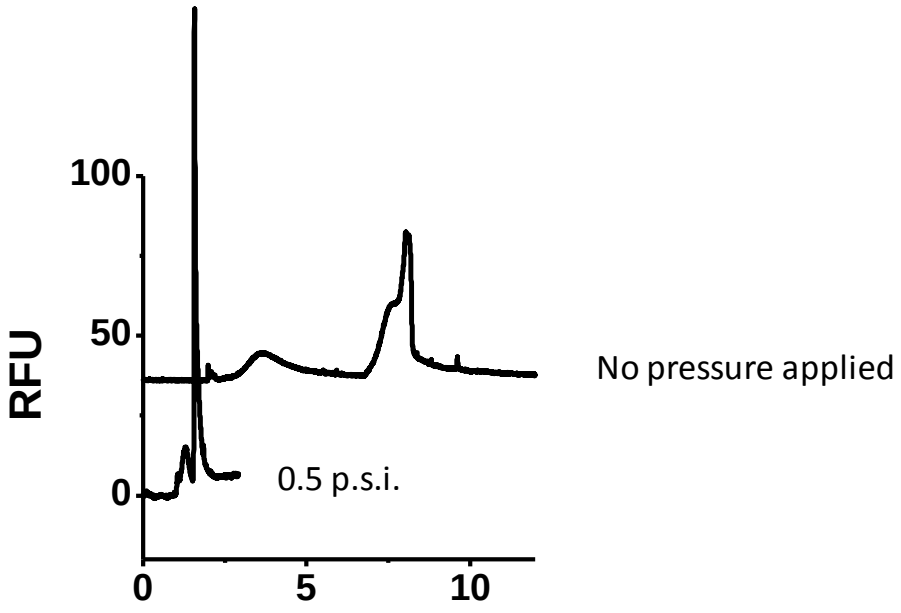

Figure 2-8. Comparison of electropherograms of identical sample and similar separation conditions except in the experiment shown by the front signal trace, 0.5 p.s.i. pressure was applied with the same direction as EOF across 30 cm long 50 mm inner diameter capillary.

Conclusions

In this study, we developed a capillary electrophoresis assay that can be used to detect protein protein interaction between Hsp70 and Bag3. Full length recombinant proteins were used confirming CE based methods places no limitations on protein size

and are friendly to proteins purified from cell cultures. The CE assay was verified by competitive binding experiment. In Kd determination and IC50 measurements, CE exhibited good quantitative performance and great potential in pharmacological studies such as inhibitor efficacy assessment. By applying pressure during separation, the separation time was reduced to 3 minutes on a commercial CE instrument.

CHAPTER 3
MODERATE SCALE DRUG SCREENING TARGETING HSP70 AND BAG3 INTERACTION USING CAPILLARY ELECTROPHORESIS

Introduction

Protein-protein interactions (PPIs) are involved in nearly every aspect of cellular life[65, 66, 67] and have gained attention as potential drug targets for various human diseases[68, 69], and with this growing appreciation comes an undeniable need for new and potent PPI inhibitors. Historically however, PPIs have been relatively difficult to target due to various factors including large surface areas, relatively flat interfaces, lack of natural ligand binding sites, as well as the transient nature of protein complexes[70, 71, 72, 73]. High throughput screening (HTS)[22] is highly valuable for challenging PPI modulators discovery, but among over 100 PPI inhibitors been identified, very few of them were discovered by HTS, and facile and HTS friendly assays are clearly in need to unleash the full power and many benefits of HTS.

Currently, several methods are employed to screen for PPI inhibitors. These platforms can be divided into two general classes: platforms that measure small molecule binding to one protein partner, and platforms that measure direct disruption of a PPI. The first class includes techniques such as NMR, surface plasmon resonance (SPR), differential scanning fluorimetry, and various *in silico* methods. While these techniques have been successful in producing PPI inhibitors[71], they are explicitly designed to find molecules that bind to one protein partner and may not affect the desired PPI. Therefore,

platforms that measure direct PPI disruption are a more straightforward approach, and this includes techniques such as FRET, fluorescence polarization (FP), flow cytometry protein interaction assay (FCPIA) and others. These methods can have significant limitations when it comes to protein size and buffer conditions. Other limitations of these methods exist in that they can require large amounts of protein/peptide material in the case of FP or immobilization of one partner in the case of FCPIA. Due to these limitations, we have sought to develop a novel PPI screening platform using capillary electrophoresis.

Capillary electrophoresis (CE) methods have long been shown to be successful in probing non-covalent interactions *in vitro*[8, 16, 18, 74]. Similar to Electrophoretic Mobility Shift Assay (EMSA), capillary electrophoresis directly detects binding events by resolving charged species from their affinity complex form based on the difference in electrophoretic mobility. Unlike EMSA, free solution is often used as the separation matrix. In principal, CE is highly feasible for PPI analysis[13]. Compared to many platforms that are available, CE does not impose any limitation on protein size nor does it require immobilization. High separation efficiency, low sample consumption, fast separation, high degree of automation utilizing commercial instrumentation and straight forward quantification all make CE attractive for high throughput screening of PPIs[62, 75, 76, 77]. Realizing this potential, however, requires: 1) Addressing challenges such as protein adsorption, labeling of proteins and adequate resolution under non-denaturing conditions; and 2) Demonstration of assays for biologically relevant targets.

In Chapter 2, a CE assay was developed to analyze the binding between heat shock protein 70 (Hsp70) and Bcl2-associated anthanogene 3 (Bag3). Previous results

have also shown that this assay can be used as a moderate throughput assay for inhibitor discovery and confirmation. In this chapter, we report the first use of capillary electrophoresis as a protein-protein interaction screening platform using Hsp70-Bag3 as a model PPI. After developing validating the CE based protein-protein interaction assay, we screened a pilot collection of ~3300 small molecules. Another using an existing PPI HTS technology, Flow Cytometry Protein Interaction Assay (FCPIA) was performed and the results were compared head to head with the CE screening to reveal the advantages of using CE as opposed to available method.

Experimental Section

Protein Purification and Labeling. Human Hsp70 (HSPA1) was purified as previously described[78, 79] using a His column, TEV cleavage of the his tag, followed by an ATP agarose column. Human N-terminal his-tagged Bag3 was purified based on previous reports[80]. Briefly, Bag3 was fractioned by ammonium sulfate (0-30% of saturation) followed by a His column and TEV cleavage of the his tag. Bag3 was dialyzed overnight into Buffer A (25mM HEPES, 10mM NaCl, 15mM β-mercaptoethanol, 0.1mM EDTA, pH 7.6) and subjected to ion-exchange chromatography on a Mono-Q HR 16/10 column (GE Healthcare). Finally, Bag3 was subjected to size exclusion chromatography on a Superdex 200 gel filtration column (GE Healthcare). Hsp70 and Bag3 were labeled with Alexa Fluor® 488 5-SDP ester (Life technologies) according to the suppliers instructions on amine reactive probes. Hsp70 was biotinylated using EZ-link NHS-Biotin (Thermo Scientific) according to the suppliers instructions. After labeling, the proteins were subjected to gel filtration to remove any unreacted label.

Capillary Surface Modification. Bare fused silica capillary with inner diameter of 50 μm and outer diameter of 360 μm is purchased from Polymicro Technologies (Phoenix, AZ). The acidic silanol groups on the silica surface are modified covalently to reduce protein adsorption. The derivatization reaction is carried out by infusing liquid solvent and solutions through the capillary using a home built setup consisting of a stainless steel pressure bomb made in house and oil bath for reaction temperature control . Tank nitrogen (Cryogenic Gases, Detroit, MI) at 30 p.s.i. is used as the pressure source for all the steps described in below. Three steps of rinsing and activation: 1) MeOH rinse at room temperature; 2) RCA solution (NH_4OH:H_2O_2:H_2O v:v:v = 1:1:5) rinse at 120 °C; 3) 0.1 M HCl rinse at 90°C. Every activation step takes 1 hour. After activation, the residual liquid is purged out of the capillary and the capillary inner surface is dried under dry nitrogen flow at 165 °C overnight. 10% (volume percent) 1H, 1H, 2H, 2H-perfluorooctyltrichlorosilane (sigma, St. Louise, MO) in toluene is continuously infused for 3 hours at 120 °C. After reaction, the derivatized capillary is infused with toluene and methanol to rinse off residual reactive species. The capillary is emptied and further dried in oven at 80 °C overnight. Detection window is burned by hot sulfuric acid and the capillary openings are sealed with capillary wax until being used.

Capillary Electrophoresis. Beckman Coulter MDQ/PACE was used in most of the CE experiments unless otherwise noted. 30 cm of the derivatized capillary was used with effective separation length of 10 cm. Capillary temperature was kept at 25 °C for all experiments. Separation buffer was 10 mM sodium phosphate pH7.5 with 0.01% Tween 20 (w:v) as the buffer modifier. All separation buffers were made fresh every day by from 5X stock solution. All buffer solutions are made using water purified and deionized

to 18 MΩ resistivity using a Series 1090 E-pure system (Barnstead Thermolyne Cooperation, Dubuque, IA) and filtered by membrane filter (0.2 uM pore size, Watman, GE) to remove particulates.

Separation method consisted of three steps: 1) 1 min rinsing using with separation buffer; 2) Pressure/vacuum injection at 0.3 p.s.i. for 5 s; 3) 500 V/cm electric field with normal polarity was used resulting in current of 14.0 uA. 0.5 p.s.i. pressure is applied during separation to generating a pressure driven flow at the same direction of EOF to force separation to complete in 3 min. LIF detection was accomplished using a 20 mW optically pumped semiconductor Sapphire laser (Coherent, Santa Clara, CA) as a light source coupled to the Beckman Coulter MDQ/PACE LIF detection module through an optical fiber. 488 nm line was used and emission light was detected at 520 nm. All data was collected by 32 Karat software and exported as ASCII files, which is further processed using software written in house[63].

Small Molecule Libraries. The MicroSource MS2000 library contains 2000 bioactive compounds with a minimum of 95% purity. The collection contains 958 known therapeutic drugs, 629 natural products and natural product derivatives, 343 compounds with reported experimental biological activities and 70 compounds approved for agricultural use. The University of Michigan Center for Chemical Genomics (CCG) Focused collection library includes ~1000 small molecules with target specific activities (Wnt Pathway, Kinases, etc.) as well as natural products. The CCG Biofocus NCC library is an NIH Clinical collection that contains ~450 small molecules that have a history of use in human clinical trials including some FDA approved drugs. The activity of promising compounds was confirmed with repurchased samples from commercial

sources including Sigma-Aldrich, Enzo Life Sciences, Cayman Chemical, Acros Organics, Alfa Aesar, and MP Biomedicals.

Screening with Capillary Electrophoresis. Experiments were performed in 96-well conical bottom PCR plates (ISC BIoexpress). A stock solution of Alexa Fluor® 488 labeled Hsp70 and unlabeled Bag3 was prepared fresh daily in assay buffer (25mM HEPES, 10mM KCl, 5mM $MgCl_2$, 0.3% Tween-20 pH 7.5) so that the final concentration of both proteins was 500nM in the assay. Compounds and DMSO were dry spotted in plates prior to protein addition using a Moquito liquid handler (TTP Labtech). Assay buffer (5µL) was added to each well except for positive control wells that received 5µL of unlabeled Hsp70. Hsp70-Bag3 solution (10µL) was then added to each well. All additions were added using a Matrix Electronic Multichannel pipette (Thermo Scientific). Plates were incubated for at least 15 minutes and then analyzed on the capillary electrophoresis system.

High-throughput Flow Cytometry Protein Interaction Assay. The assay procedure was adopted from previous reports[81]. In brief, biotinylated Hsp70 was incubated with streptavidin coated polystyrene beads (Spherotech) for one hour prior to assay for immobilization. A stock solution of Alexa Fluor® 488 labeled Bag3 was prepared in assay buffer (25mM HEPES, 10mM KCl, 5mM $MgCl_2$, 0.3% Tween-20 pH 7.5) so that the final concentration of Bag3 was 30nM in the assay. Assay buffer (5µL) was added to each well of a black 384 well plate (Thermo Scientific), followed by compound or DMSO addition (0.2µL) using a Biomek HDR (Beckman). Positive control wells received 5µL unlabeled Hsp70 instead of assay buffer. Bag3 solution (10µL) was then added to each well, followed by Hsp70-bead addition (5µL). All components other

than compounds were added using a Multidrop dispenser (Thermo Fisher Scientific). Plates were incubated for 15 minutes then analyzed using a Hypercyt liquid sampling unit in line with an Accuri® C6 Flow Cytometer. Median bead associated fluorescence was calculated using Hyperview software for each well and data was uploaded to the Mscreen database.

Results and Discussion

Development of CE based PPI assay for Hsp70 and Bag3. The CE method used here are slight modified from the method described in Chapter 1. Again, Affinity Probe Capillary Electrophoresis (APCE) is used (Figure 3-1A) where one of the binding partners is labeled with a fluorescent tag and used as the affinity probe. The binding event is detected by resolving the affinity probe and protein complex from the affinity probe itself based on the difference in electrophoretic mobility and detecting both peaks by laser-induced fluorescence. Because separation breaks the equilibrium, dissociation of the complex may occur during the separation, resulting in a "bridge" connecting the complex and the free peak. In our experiment, Alexafluor-488 labeled Hsp70 is used as the affinity probe and will be referred to as Hsp70-488 from now on.

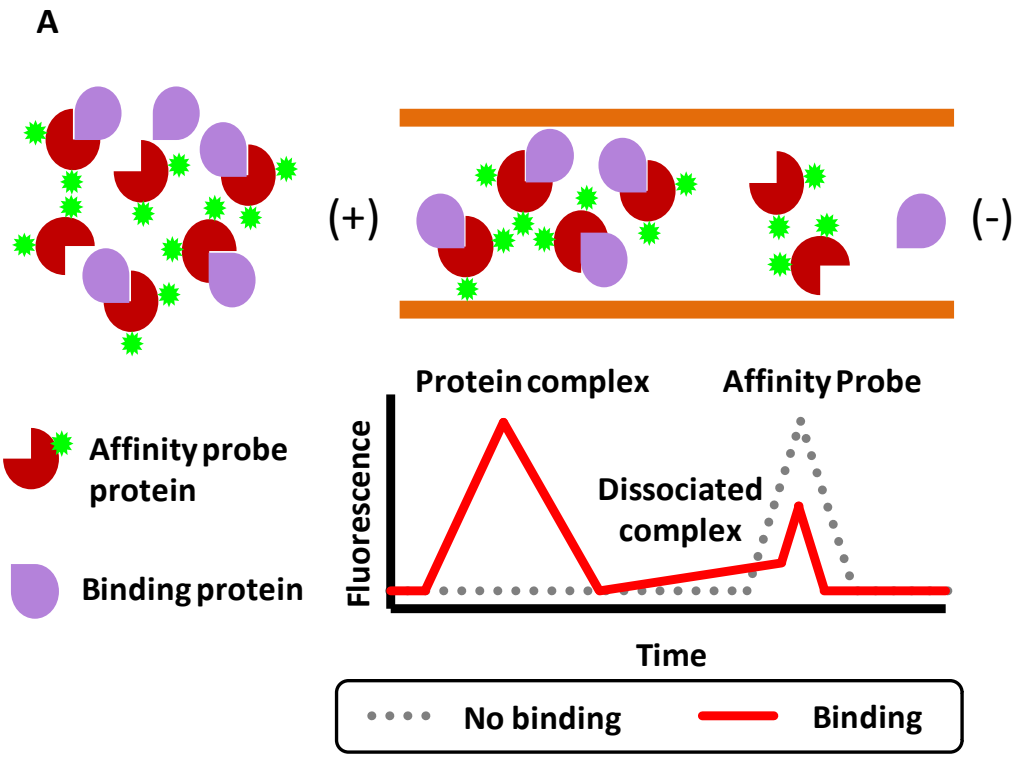

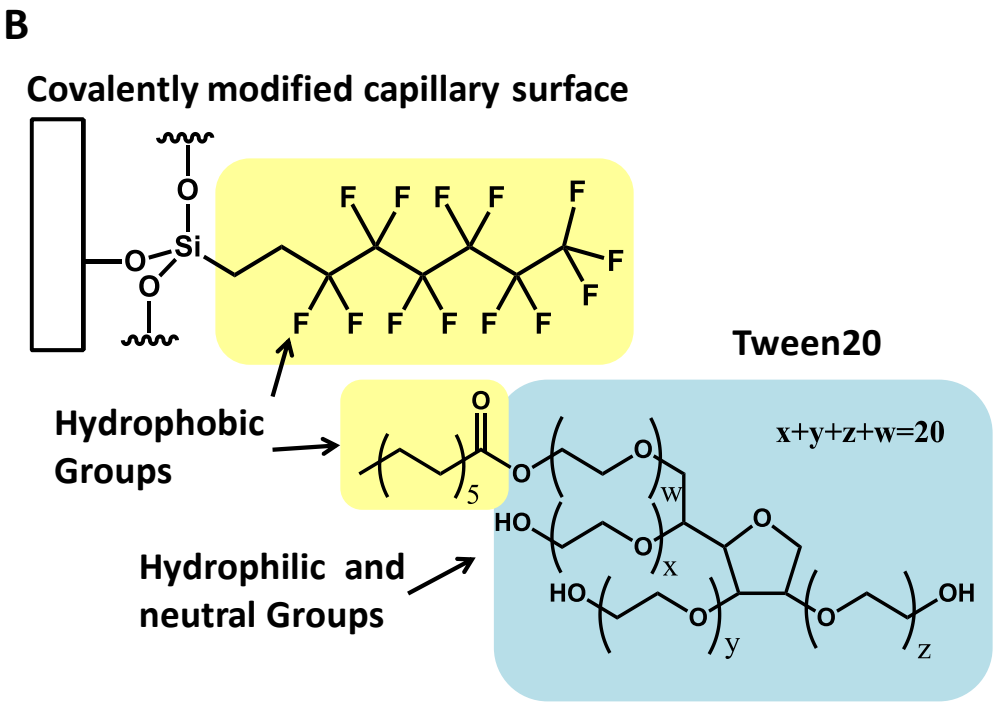

Figure 3-1. A. Illustration of how APCE works to detect protein binding events. B. Capillary surface modification that were used to prevent protein adsorption.

Using covalently modified the capillary surface and Tween 20 (0.01% w/v) as a buffer modifier, a dynamic and hydrophilic capillary wall coating that can be refreshed during separation and rinsing steps,[64] effectively preventing protein adsorption and providing adequate resolution under gentle separation conditions. With 500 V/cm, 10 cm effective separation length and 0.5 p.s.i. pressure during separation, the mixture of Hsp70-488 and unlabeled Bag3 results in two individual bands (migration time of 96 and 122 seconds), which correspond to the complex and the free Hsp70 respectively.

The CE separation method was submitted to a series of experiments to test its validity and quantitative performance. The dissociation constant of Alexafluor-488 labeled Hsp70 and Bag3 was determined by titrating 0.5 μM labeled Hsp70 with unlabeled Bag3. The peak area of the complex peak as well as the dissociation bridge both increase as a function of Bag3 concentration (Figure 3-2A). Plotting the peak area against the Bag3 concentration and non-linear regression according to Eq. 2-1 a binding constant of 23±8 nM, which is in good agreement with the 15 nM Kd obtained from the FCPIA platform using the same proteins and fluorescent tag.

Competition binding experiments with unlabeled Hsp70 were also performed. The IC_{50} of unlabeled Hsp70 was determined to be 0.24 μM (Figure 3-2B), which agrees very well with the protein concentrations used and the labeling efficiency of Hsp70.

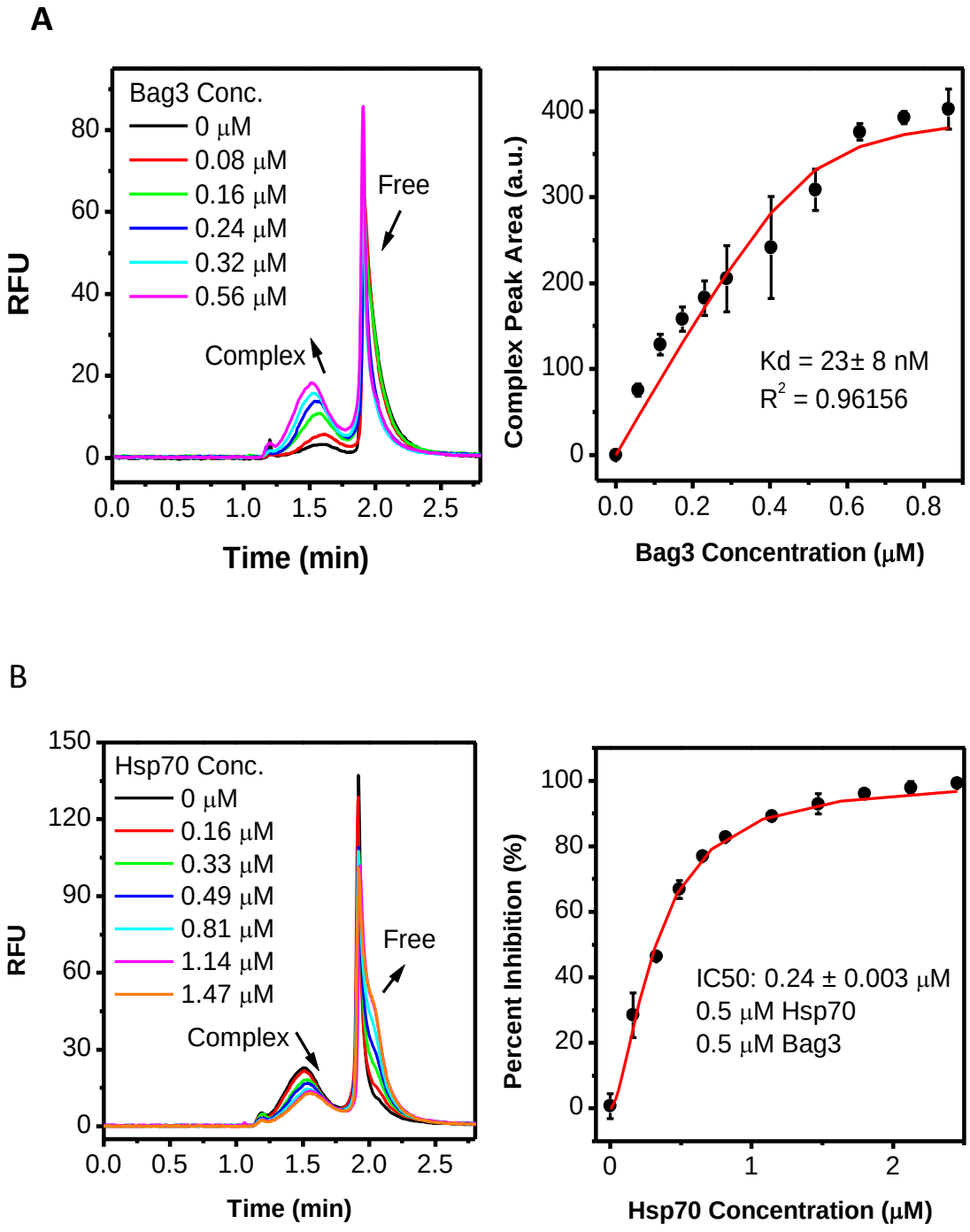

Figure 3-2. A. Titration experiments and curve fitting for Kd determination. B. Electropherograms showing the inhibitory effect of unlabeled Hsp70 on Alexafluor 488-Hsp70 and Bag3 binding. IC50 of unlabeled Hsp70 was determined by dose response study.

Adapting CE for Screening. After validating capillary electrophoresis as an effective platform for detecting Hsp70-Bag3 interactions, we sought to test the method in repetitive analysis to determine its suitability for a screen. The Beckman/Coulter MDQ system is capable of analyzing samples from 96 well PCR plates in series. With our finalized method, every CE assay takes about 6.5 min including 1 min rinsing, 5 s injection and 3 min separation, which gives an overall throughput of 220 samples per day.

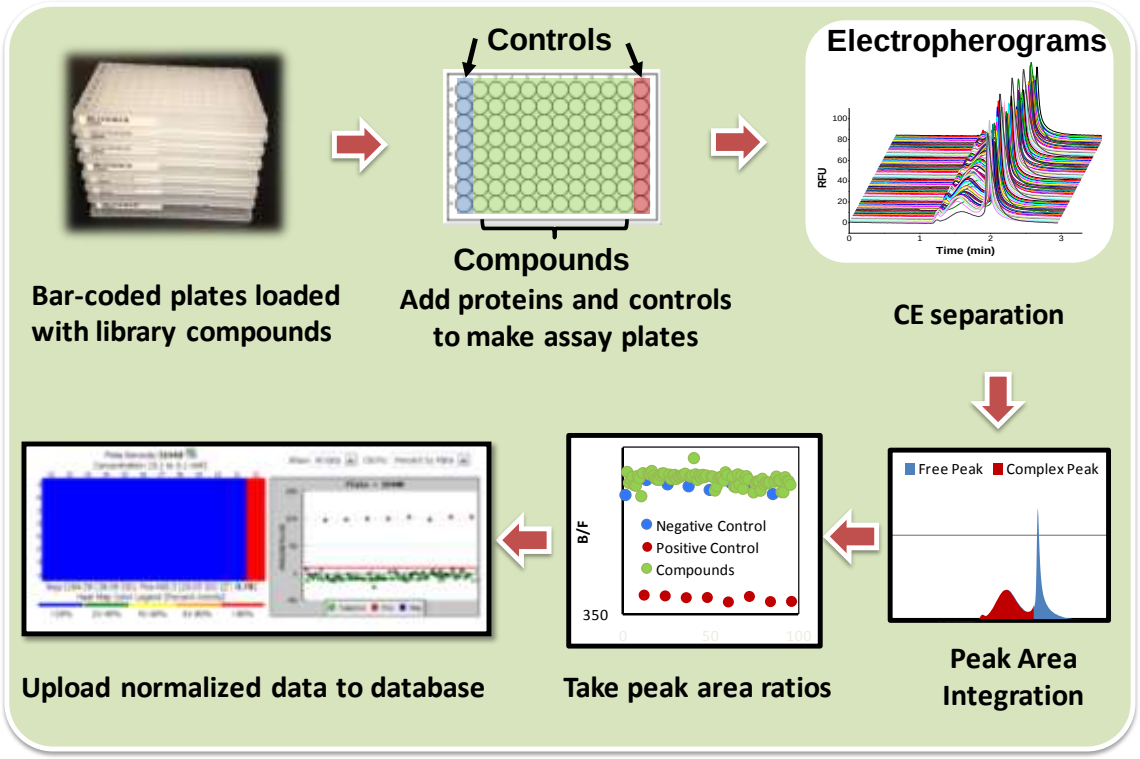

Figure 3-3. CE screen workflow.

The workflow of a screening experiment is shown in figure 3-3. Briefly, library compounds were deposited in barcoded 96 well PCR plates by robotic sample handlers. Proteins and buffer were added so each final assay contains 500 nM Alexafluor 488-

Hsp70, 500 nM Bag3 and 20 mM library compounds. Each plate contains 16 control samples. 8 negative controls contains DMSO without any compound added. Positive controls contains 2 μM unlabeled Hsp70. The plates were run by the CE instrument and an electropherogram was obtained for each sample. The Electropherograms from each plate were further analyzed and peak integration was performed. Instead of uploading all the Electropherograms, in the CE screen, peak area ratios (complex/free) are taken and used as for inhibitor selection criteria[82] which are further normalized to control samples and uploaded to database. To determine the feasibility of CE as a screening platform we determined a Z factor for the assay. For calculation of Z scores, we analyzed one 96 well plate with half of them being negative controls and the rest the positive controls. The calculated Z factor was 0.78, which is well above a value of 0.5 which indicates an assay is acceptable for screening[83].

Screening of a small-molecule pilot collection and comparison with FCPIA screen. Using these conditions, we screened a small pilot library (~3300 compounds) in the CE platform (Figure 3-4A). As a comparison, the same collection was screened using another PPI assay, FCPIA (Figure 3-4B). In FCPIA, one protein partner (Hsp70) is biotinylated and immobilized on streptavidin coated polystyrene beads, while the other PPI partner (Bag3) is fluorescently labeled. The two are then incubated together and analyzed using a flow cytometer to measure bead-associated fluorescence[37].

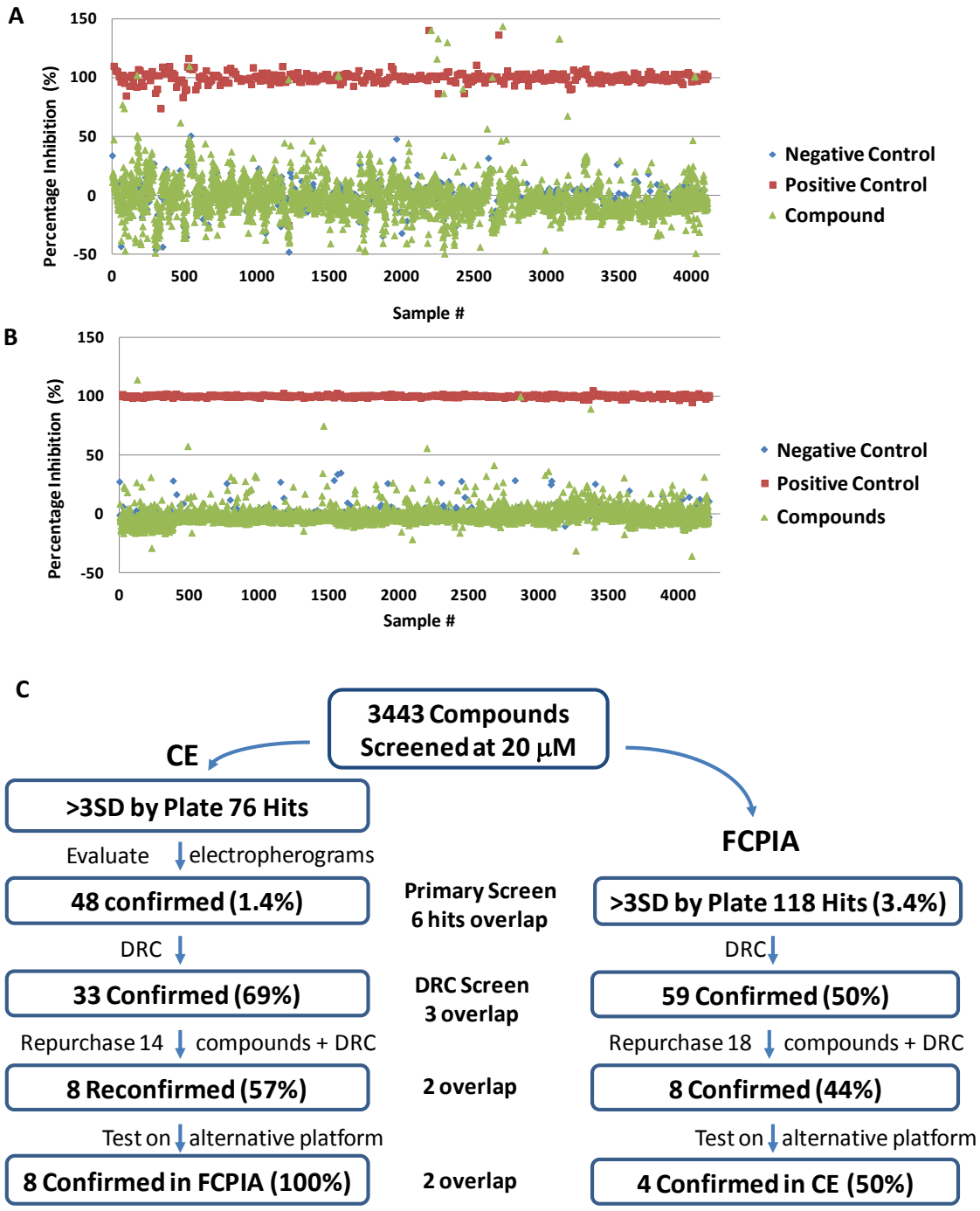

Figure 3-4. Overview of the primary screening results of A. CE platform and B. FCPIA platform. C. Triage breakdown of two screen platforms.

Samples were screened at a single concentration (20 μM) in both platforms. Compounds that exhibited inhibition ≥ 3 SD from the controls were considered "hits". CE identified 79 primary hits using this cutoff (2.3%), while FCPIA identified 117 (3.4%) with only 6 primary hits identified by both platforms (Figure 4C). Because the same nominal proteins and same libraries were used, the low overlap for hits was unexpected. This may be due to higher sensitivity of the FCPIA assay, which used a lower Bag3 concentration. This view is supported by the finding that the CE assay did not detect some low efficacy inhibitors such as compound 9 and 17. Another likely factor is that protein modification and immobilization play a role in the assay. CE used labeled Hsp70 and no protein immobilization. FCPIA used labeled Bag3 and immobilized Hsp70. Immobilization and labeling may affect the interaction, accessibility of allosteric binding sites, and accessibility of protein-protein binding interface.

To further evaluate the screen results, hits found by CE were then triaged based on activity and raw electropherograms to reduce the number of "real" hits to 48. Specifically, Electropherograms of all 79 initial hits were retrieved and inspected. "False positives" that were caused by injection failure or abnormal peak shapes were manually rejected before further dose-response studies. In this step, electropherograms of 79 primary hits were retrieved and inspected for abnormal peak shapes. In this step, 31 compounds were removed from the inhibitor list reducing the number of "real" hits to 48. Figure 3-5B and 3-5C are examples electropherograms that were considered abnormal. In the case of 3-5B, the signal was very low probably due to injection failure or protein aggregation. Whereas in 3-5C, the B/F ratio was low simply because the compound was fluorescent at the same excitation and emission wavelengths as Alexafluor488. The

compound peak overlaps with the free hsp70 peak, but it can still be told from the normal behaving compound (Figure 3-6A) and be teased out from the list of potential inhibitors.

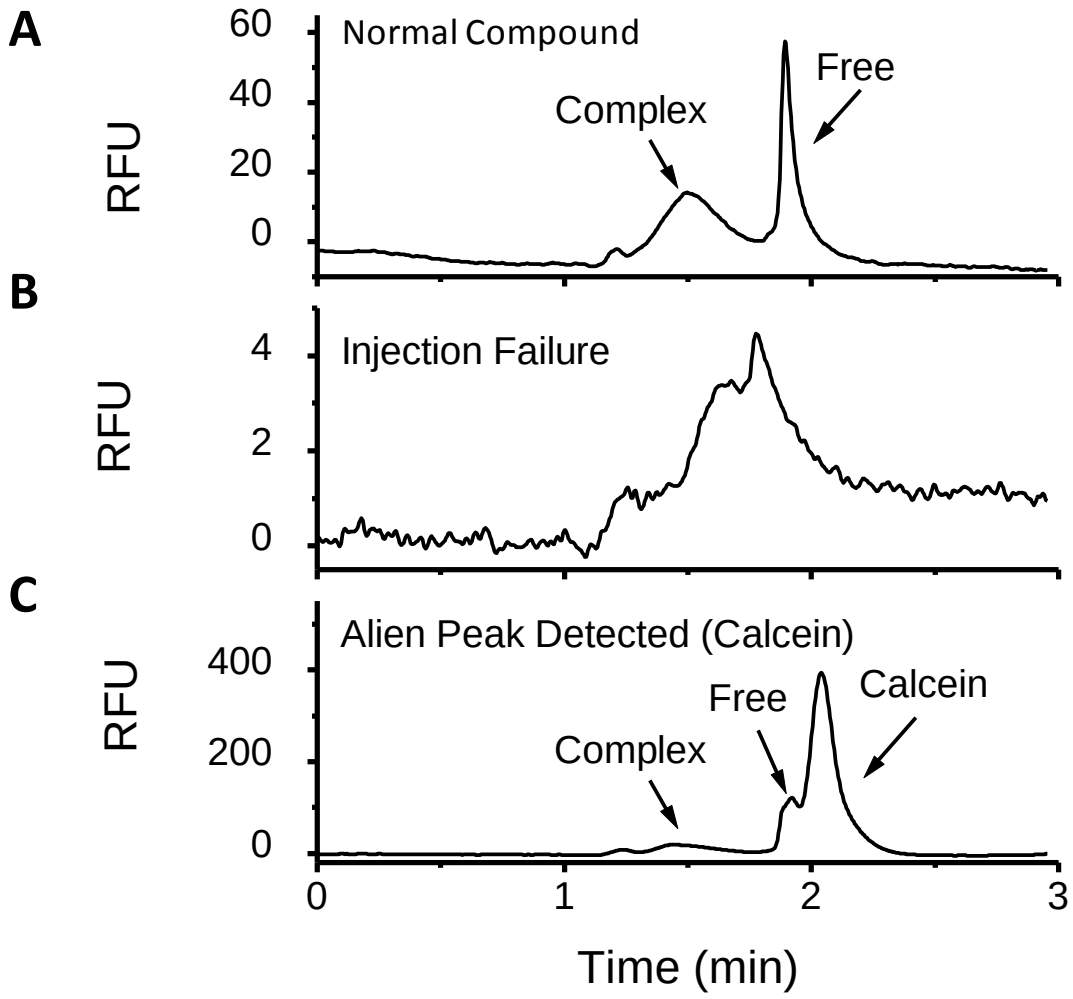

Figure 3-5. Comparison between the electropherograms of A. normal compound and false positives caused by B. injection failure and C. fluorescent compound.

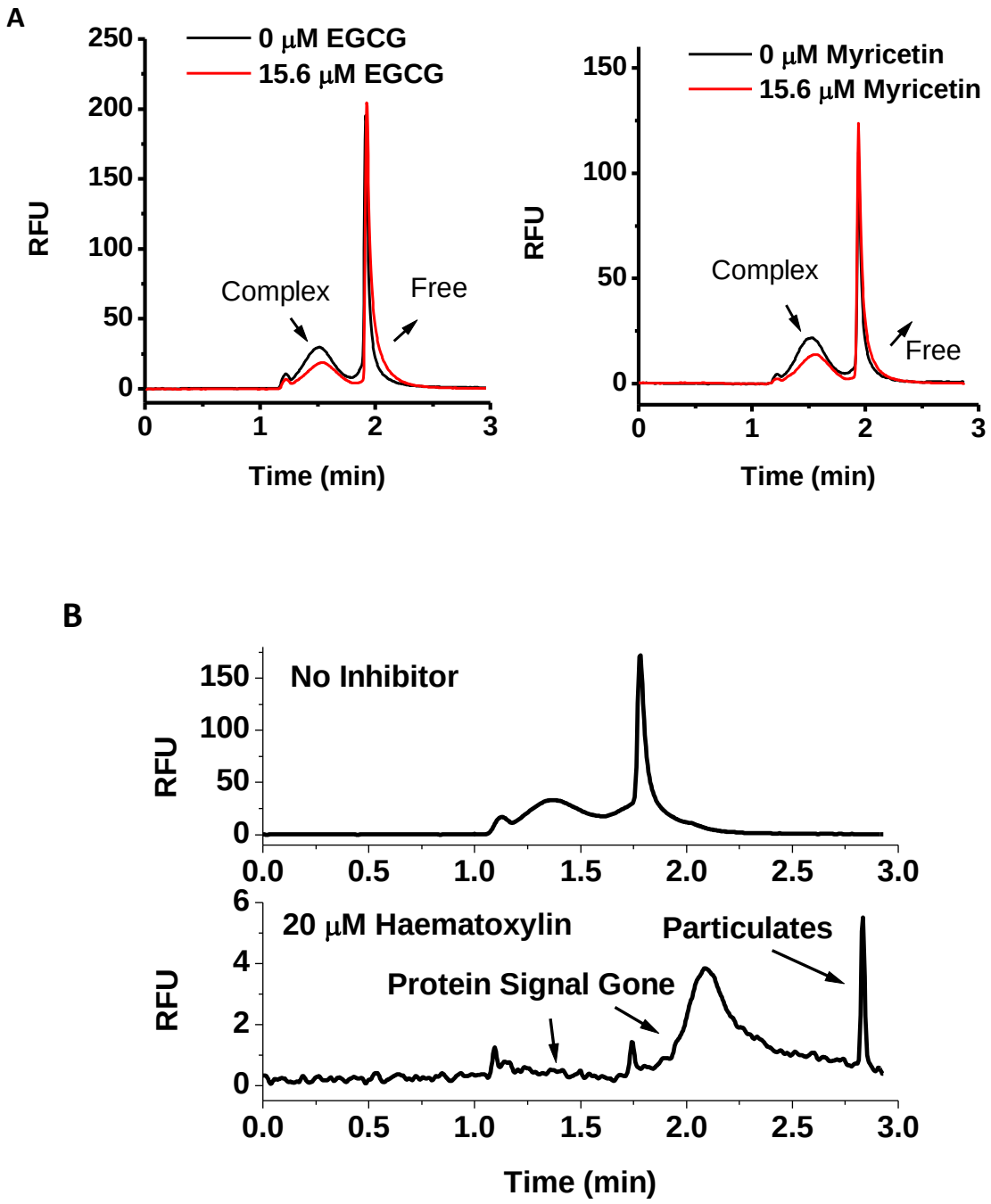

Figure 3-6. A. Examples of confirmed inhibitors showing inhibition by decrease in complex peak and increase in free peak. B. Protein aggreation aggents can be differentiated by examining the electropherogram. For haematoxylin, the proteins signal for both peaks are gone and sharp peaks correspond to the diffraction of insoluable particles were observed.

Dose response screen was performed on the selected compounds and confirmed hits were determined based on the fit of their dose response curves (DRC). CE confirmed 33 hits (69%), whereas FCPIA confirmed 59 hits (50%). Compounds were prioritized and repurchased from commercial sources based on activity in DRC and availability (14 compounds purchased for CE and 18 for FCPIA, with a 2 compound overlap). Upon repurchasing, compounds were retested in their original platforms usingDRC. In both platforms 8 compounds reconfirmed, and were then subjected to confirmation in the alternate platform. All repurchased compounds that reconfirmed in CE were also confirmed in FCPIA, however only 50% of the compounds that showed activity in FCPIA were considered hits in CE.

Compared to the FCPIA platform, CE clearly shows better specificity as demonstrated by low hitting rate and higher percentage of primary hits being confirmed by DRC and alternative methods. The specificity of CE rises from the fact that CE data is more information-rich. Instead of using absolute fluorescence intensity, CE detects two peaks and used relative peak area change as the selection criteria. Artifacts that are common to fluorescence based assays, such as fluorescence enhancing/quenching agents and protein aggregation inducing agents do not affect the CE assay as severely because: 1) CE has separation power which simplifies the protein matrix as the fluorescence signal is detected; 2) using peak area ratio corrects for factors that affect the two peaks equally; and 3) many artifacts can be teased out if alien peaks or abnormal peak shapes are observed. As shown in Figure 3-6 A, confirmed inhibitors cause complex peak to decrease and free peak to increase. However, protein aggregation inducing agent doesn't share the same character (Figure 3-6B). Another likely factor is the use of a single

modified protein (labeled Hsp70) rather than having both proteins modified for the FCPIA (one protein labeled and one immobilized).

Column lifetime. Unlike fluorescence based methods where discrete samples were analyzed through contactless readout, separation based methods involves continuously injecting samples onto the separation column where they are analyzed in a sequential manner. One question that can be anticipated with separation based screen is whether the separation columns can endure large number of samples. In our screen, we found the PFOTCS capillaries are stable for at least 500 injections without decline in performance. As shown in Figure 3-7A, over 500 injections were made on one column and the B/F ratios of control samples were still stable without signs of deterioration. Excellent agreement between columns was achieved as shown in Table 3-1.

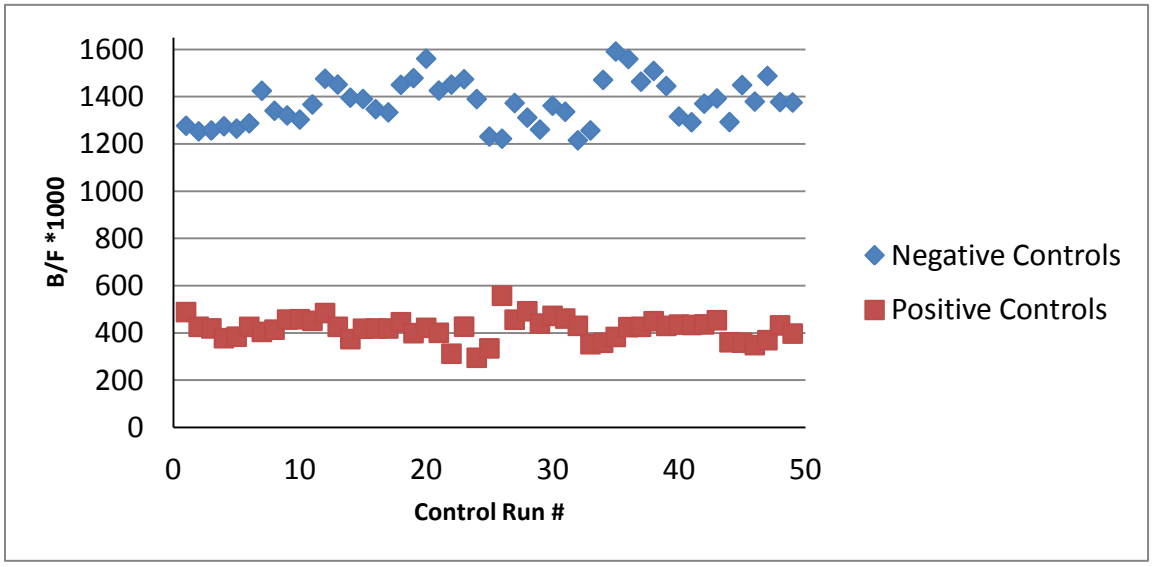

Figure 3-7. Long term stability of B/F ratios of a PFOTCS column over 500 assays run. Data of 24 negative control (blue diamond) and 24 positive control (red squares) are shown.

Parameters	RSDs
Peak area ratios (n=48) on a single column (Figure 3-7)	Positive controls: **6.9%** Negative controls: **11%**
Migration time on the same capillary (n=6)	Complex: **0.67%** Free: **0.43%**
Migration time on different capillaries (n=13)	**2.3%** (Rhodamine 110 runs when new capillaries were first put into use)

Table 3-1. RSDs in peak area ratios and migration times on a single capillary and between different capillaries.

Confirmed inhibitors from CE screen. Structures of the confirmed inhibitors were shown in Figure 3-8A and their dose response curves were shown in Figure 3-8B. Structurally, the majority of CE identified inhibitors has polyphenol type structures versus aromatic structures were prevalent with flow cytometry identified inhibitors. In-depth structure analysis cannot be performed because very limited conclusion can be drawn with a small number of inhibitors. With large scale screening encompassing a bigger variety of chemicals should better benefit such chemical biology studies and shed more light into drug development.

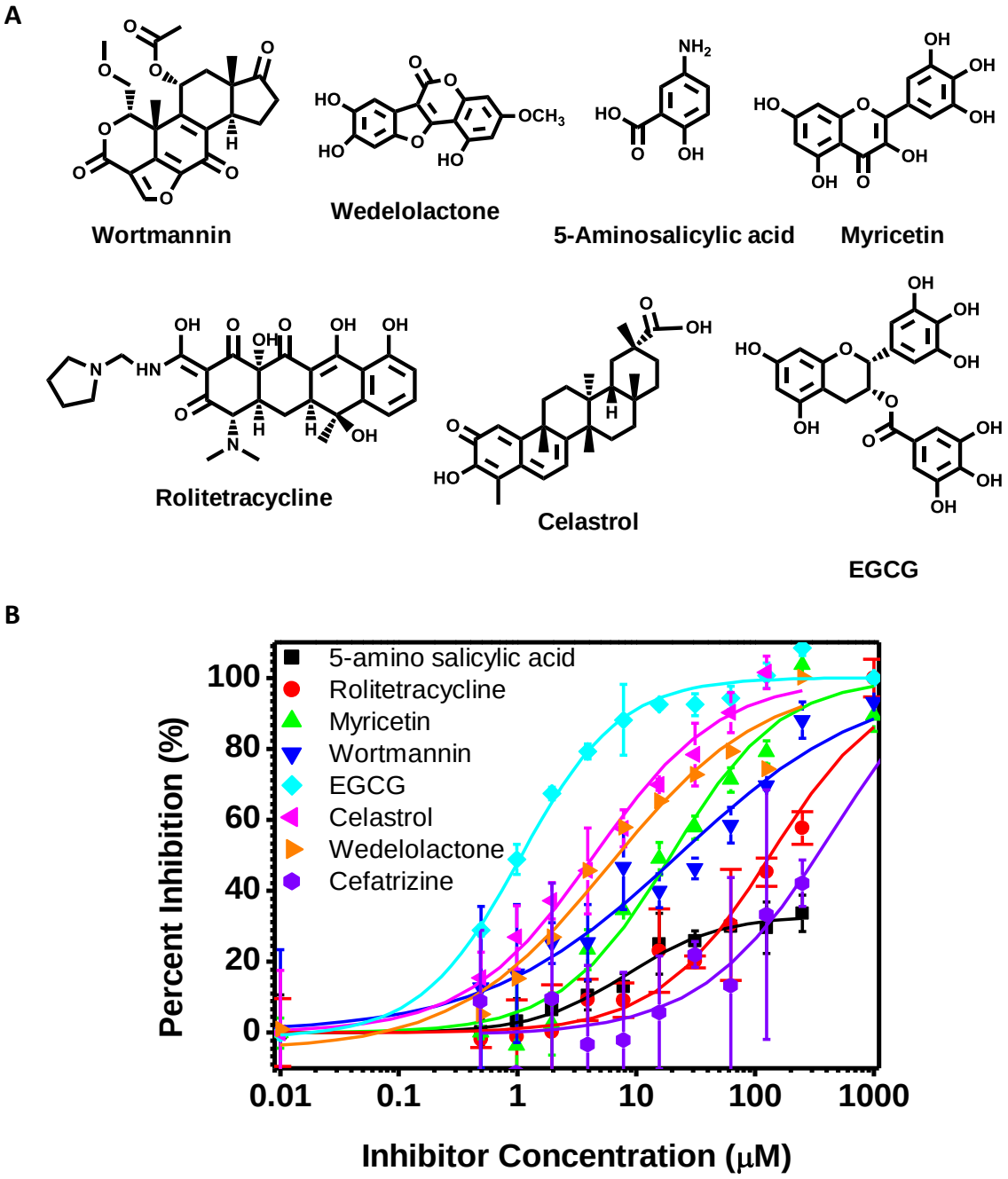

Figure 3-8. A. Chemical structures of 7 inhibitors confirmed by both CE and FCPIA. B. DRCs of the 7 inhibitors shown in Figure 3-7A.

Conclusions

As a separation technique, CE is widely used and highly advanced. However, as a high throughput screening platform for PPI, CE is still in its infancy. Our data suggests that a few aspects of this method remain to be improved. The data quality of CE results highly depends upon the quality of the separation capillary. We observed peak area ratio values drift as the derivatization wears off. This usually occurs after more than 500 injections. For a screen of a few thousand compounds, it is not a big issue. But for a full scale screen, more robust and corrosion resistive surface is highly desired. Fluorescence labeling gives best sensitivity. However, labeling related problems, such as multiple peaks and possible interference with the binding are all concerns that can be addressed by hyphenating CE separation to novel detection schemes. High data quality of CE comes at the price of relatively low throughput. Higher throughput requires faster and parallel separation, which is proven to be principally sound and practical[84]. An alternative approach to increasing throughput is use of microchip electrophoresis. Indeed, chip-based electrophoresis instruments are commercially available (Caliper) for HTS; however, these instruments are used for enzymatic assays. This work suggests that such instruments might be used for PPI assays if the method can be transferred to a chip format. And we believe with technological advances and demonstration with more PPIs, CE will become more accessible and amendable for routine PPI analysis and large scale high throughput screening projects in the near future.

CHAPTER 4
SAMPLING FROM NANOLITER PLUGS VIA ASYMMETRICAL SPLITTING OF SEGMENTED FLOW

Introduction

Precise and automated manipulation of small volumes is essential to miniaturized analytical techniques. Segmented flow microfluidics, where samples in the form of plugs are separated by an immiscible fluid within a channel or capillary[85], has emerged as an attractive approach to process arrays of samples with fL to nL volumes[86, 87]. This method has been applied in many areas including micro-scale chemical synthesis[88], in *vivo* chemical monitoring[53], reaction kinetics[89], protein crystallization[90], single cell assay[91] and high-throughput screening[55, 92]. In these applications, use of a second immiscible phase helps to compartmentalize samples so that identity and integrity of such small samples are preserved with minimal evaporation and chemical cross-talk. The format is also attractive because of potential for high-throughput. A number of unit operations, including mixing, extraction, and reagent addition, have been devised for processing samples in segmented flow[52]; however, more plug manipulation techniques are still needed to fully tap the potential of segmented flow microfluidics. In this work, we describe a method for removing samples or aliquots from arrays of plugs based on asymmetric splitting of segmented flow in a microfluidic device.

Although sampling is a necessary step in many analytical procedures, methods for

sampling from nanoliter plugs are limited. One method that has been described is to extract aqueous plugs from segmented flow to an aqueous stream, essentially converting segmented flow to single phase flow[54, 93, 94]. This conversion enables analysis by methods that are compatible with continuous flow, such as capillary electrophoresis; however, it also eliminates the advantages of segmented flow because after the oil is removed, the samples begin to disperse and dilute. Another approach for sampling makes use of a branch channel to peel daughter droplets off parent plugs flowing through the main fluid channel[95]. By adjusting the pressure at the fluid inlet, daughter droplets of 34-523 fL (10^{-15} L) volume can be removed from the parent plugs. Because this system was devised to study effect of confinement on reaction dynamics, many aspects of sampling were not explored such as collection of large numbers of plugs. This device was also not compatible with fluorinated oil due to high surface tension, which is a preferred carrier phase due to immiscibility with both aqueous and organic solvents. Sampling from plugs has also been achieved by pumping into a bifurcated channel to achieve symmetrical splitting[96]. This approach was used with a hierarchy of symmetrical splits to create an array of samples with $1/2^n$ volume where n was the number splits, from a single plug.

Extending the flow split approach to asymmetrical splitting so that arbitrary aliquots could be removed by pumping into channels with unequal flow resistances is complicated by the nature of segmented flow. Specifically, in segmented flow each plug creates flow resistance so that the total flow resistance in a channel is dependent not only on viscosity of the carrier phase and channel dimensions, but also on the number of plugs present in the channel[97, 98, 99] i.e., $\Delta P = \Delta P^{Poiseuille} + N\Delta P^{plug}$, where the pressure drop (ΔP) across a channel is the sum of the Poiseuille pressure drop of the carrier phase

($\Delta P^{Poiseuille}$) and the pressure drop across each of the N plugs (ΔP^{plug})[100]. Because each plug contributes pressure drop, flow resistance and splitting ratio changes as plugs are collected in the device.

A solution to this problem is presented here that was inspired by recent fundamental studies of segmented flow. Stable asymmetrical splitting of plugs has been reported by using a fluidic loop structure [57]. In this device, plugs are pumped into a loop that has unequal arm lengths to define a split ratio. Because the loop is closed, i.e. the arms reconnect downstream, unequal pressures do not build up downstream and stable splitting is obtained. This device is not applicable for sampling purposes because it recombines the split flow and therefore does not preserve the separation of split plugs. Other studies have shown that plugs flowing parallel to each other in interconnected channels can remain isolated by creating high interfacial tension within the contact region.[101, 102] In our system, we take advantage of the control and stability afforded by the loop design but, by fabricating posts inside the recombination region downstream of the split, create high interfacial tension that prevents split plugs from merging. This device allows sampling from plugs by asymmetrically splitting them and collecting the resulting splits into separate capillaries or channels. This splitting device adds to the segmented flow toolbox and should find applications where stable and variable sampling from plugs or asymmetrical splitting is needed.

Experimental Section

Chip Fabrication and surface derivatization. The microfluidic devices were

fabricated following standard soft lithography procedures in PDMS[103]. Briefly, SU-8 2075 photoresist (MicroChem Corp. Newton, MA) was spin-coated onto a 3" silicon wafer (purchased from University Wafer, Boston, MA) at 4000 rpm, pre-baked and exposed to UV radiation for 13.3 s (365- nm mercury line, 60 mJ/cm^2 power, Optical Associates, Inc.Milpitas, CA) through a dark field mask (Fine Line Imaging Co., Colorado Springs, CO) to crosslink the exposed features, and post-baked before employing SU-8 developer (MicroChem Corp. Newton, MA) to develop the remained SU-8 photoresist. The height of the master features was kept 60 μm across the whole microfluidic network. Channel width was 150 μm at the plug generation tee and narrowed down to 30 μm at the splitting area. The width of daughter plug receiving channels was 100 μm and plug separation posts were of 30 × 30 μm square cross-sections and spaced 30 μm apart from each other. After casting PDMS over the molds, the layer containing channels was removed and derivatizing reagent access holes were made by poking a blunt 18-gauge needle into the PDMS. After plasma bonding with a piece of unpatterned PDMS, the sealed device was placed on a hotplate (temperature set to 75 °C) for 10 min to enhance bonding. A 1 mL plastic syringe was used to deliver 3:100 (v:v) 1H, 1H, 2H, 2H-perfluorooctyltrichlorosilane solution in anhydrous hexadecane (both purchased from Sigma Aldrich, St. Louis, MO) into the channels through the punched access holes to flush the fluid channels. This step was repeated twice. Derivatized chips were then put on hotplate (temperature set to 75 °C) for 30 min to anneal derivatization. 100/160 and 50/150 silica capillaries (Polymicro Technologies, Phoenix, AZ), pre-silanized by 1H,1H,2H,2H-perfluorooctyltrichlorosilane, were inserted from the side of the chip into the micro-fabricated channels to construct fluid inlets and

outlets, respectively. To finish the fabrication, the devices were encased with PDMS in a plastic petri dish and baked at 80 °C in an oven overnight.

Plug splitting experiment. Aqueous plugs were generated by merging aqueous phase and oil phase at a tee junction fabricated upstream of the splitting channels[104]. Food dye diluted with water to1/3 of the original concentration was used as aqueous phase for visualization. For oil phase, 10:1 volume ratio Fluorinert FC-70 (purchased from 3M Corporate, St. Paul, MN) and surfactant 1H,1H,2H,2H-perfluoro-1-octanol (from Sigma Aldrich, St. Louis, MO) mixture was used. Flow rate was controlled by syringe pumps (Chemyx Inc., Stafford, TX) for both phases. Pictures showing splitting channels were taken by a digital camera (Stylus 1030 SW, Olympus Imaging America Inc., Center Valley, PA) through a Nikon inverted microscope (Eclipse TS100, Melville, NY).

Split ratio dependence upon plug input frequency. Plug input frequency was changed by varying the relative flow rate of oil and aqueous phase (1 μL/min total) at the plug generating tee upstream of the splitting area. Four different relative flow rates 0.5: 0.5, 0.7: 0.3, 0.9: 0.1 and 0.95: 0.05 (oil: aqueous) were used and the plug input frequency was about 2.5 Hz, 2.0 Hz, 1.0 Hz, and 0.5 Hz respectively with parent plug size of about 3.3 nL, 2.7 nL, 2.0 nL and 1.7 nL. Split ratios were determined by image analysis using ImageJ software.

Long term stability test and laser-induced fluorescence (LIF) detection. In the long term stability test, 1 μM fluorescein solution was used as the aqueous phase for

plug generation and splitting. LIF detection was performed with an epi-illumination apparatus[105]. Instrument control and data collection were performed using LabVIEW software written in house (National Instruments, Austin, TX). Data analysis and graphing was done by Origin 6.0 software.

Results and Discussion

Chip performance. A photograph of a microfluidic chip used for stable asymmetric splitting is shown in Figure 1A. The chip uses narrowed channels on the feed side of the loop to achieve splitting. Plugs break up at relatively high capillary number ($Ca = \eta\upsilon/\gamma$, where η, υ,and γ represent viscosity of the continuous phase, flow velocity and interfacial tension, respectively) and greater extension ($\varepsilon_0 = l_0/\pi w_0$, where l_0, w_0 are plug length and width respectively)[57]. Based on these considerations, a narrowed splitting tee (Figure 4-1B) is used to increase local linear flow rate and elongate plugs, so breakup of plugs is more efficient. By using different lengths of narrowed channel on each side of the loop (L_1 and L_2 in Figure 4-1A), asymmetric splitting is achieved as shown by the image in Figure 4-1A.

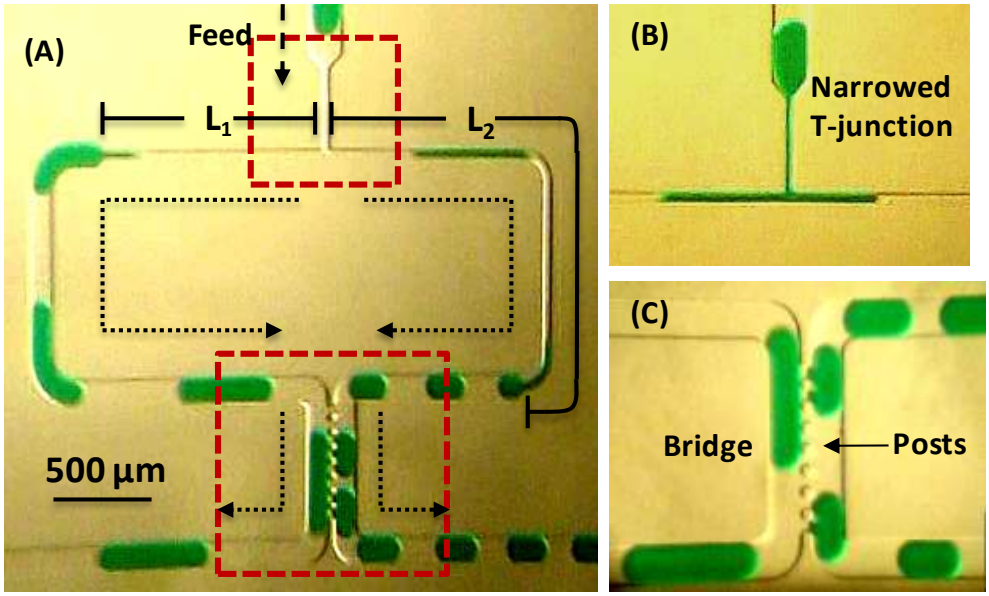

Figure 4-1. (A) Photomicrograph of microfluidic device for stable asymmetric splitting. Arrows indicate flow direction. This device has L2/L1 = 1.5 to define the split ratio. Flow rates for oil and aqueous phases are both 0.5 µL/min in generating the plugs upstream (at a tee, not shown). (B) Enlarged view of the narrowed splitting tee showing asymmetrical splitting of elongated plug. (C) Enlarged view of the pressure equalization bridge showing no coalescence between streams of plugs of different sizes.

To achieve stable a splitting ratio, the output channels of the splitting tee are "shorted" so that the pressure can equalize across the bridge (Figure 4-1C). As a result, the pressure drop caused by plugs that are collected in downstream outlet channels or tubing will not interfere with the splitting. To keep the split streams of plugs separate while being able to equalize the pressure, posts are built into the recombination channel to keep the plugs from merging and coalescing as they pass by the junction (Figure 4-2C). The total length of the bridge is made greater than the length of plugs on both sides to allow free oil flow around plugs to offset the pressure difference across the bridge;

otherwise, plugs undergo secondary splitting.

Controlling sampling ratio. A loop structure permits the split ratio to be controlled by varying the relative flow resistance of channels between the feed side and the reconnection point analogous to a parallel electrical circuit[57]. The volume ratio of the two daughter plugs produced on each side of the loop, V_1:V_2, is proportional to the ratio of volumetric flow rates, Q_1:Q_2, through each side of the loop. In rectangular fluid channels, $Q = \Delta P/\beta L$, where ΔP is the pressure drop, β is a function of channel height and width, and L is the length of the channel. Provided identical pressure drop across both arms of the loop, flow rate ratio should be inversely proportional to the ratio of channel length (in our device, the channel length ratio can be approximated as the length ratio of the narrowed channels because β is dominated by the narrow portion), that is V_1:V_2 should equal L_2:L_1.

To test the system for achieving different split ratios, devices with four length ratios in the splitting tee were fabricated (Figure 4-2). The length ratios (L_2:L_1) of the narrowed bifurcating channels were 1.5:1, 2.0:1, 3.9:1 and 5.6:1, which corresponded to the theoretical splitting ratios (V_1:V_2). Qualitatively, the observed split ratios increased with increasing length ratio as expected (shown in Figure 4-2); however, quantitatively we found that the actual split ratios differed from the expected value, especially with chips of larger split ratios. For example, the channel with a length ratio of 5.6:1 generated plugs with a volume ratio of 34:1. Volume ratios were estimated from the length of the plugs formed, which does not account for meniscus effects; however, this cannot account for the entire deviation.

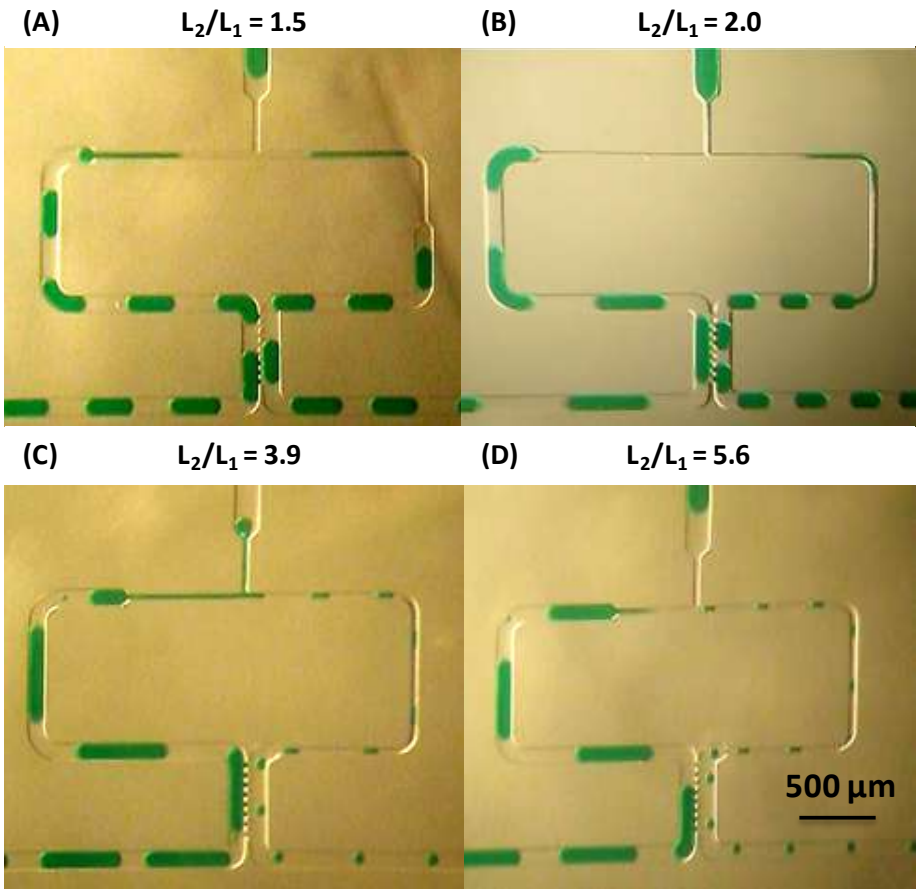

Figure 4-2. Photomicrographs showing microfluidic devices with different splitting ratios. Flow rates for oil and aqueous phases are both 0.5 µL/min for all devices. Length ratios of narrowed channels are given above each photograph.

The deviation is attributed to the presence of multiple plugs that coexist inside the loop structure, i.e. in the flow path upstream of the pressure equalization bridge, which cause additional pressure drop. Thus, the split ratio is not solely determined by the continuous phase and the split ratio; but, it tends to be higher than predicted because the channel (between the splitter and pressure equalization point) that collects smaller plugs has more plugs present and therefore creates a higher flow resistance in that channel.

Also, the capillary number for the side with longer channel and less flow rate tends to be lower, which makes pressure drop caused by a single plug even larger, which could further contribute to the deviation.

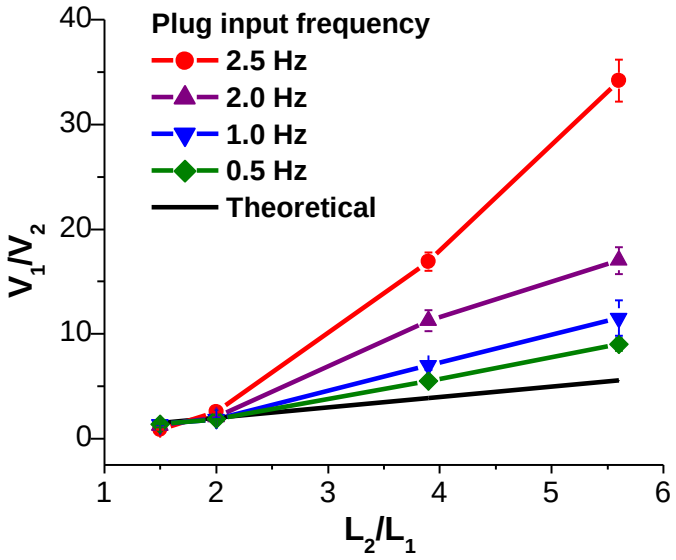

Figure 4-3. Effect of length ratio (L2/L1) on split ratio, i.e. the ratio of parent to daughter plug volume (V1/V2). Theoretical value is based on the assumption that the length ratio defines the split ratio. The experiment was performed with different plug generation frequencies, indicated on the graph, which in turn determined the number of plugs in the loop structure at one time. Chip design was that shown in Figure 2C. Each data point is the average of 3 plugs selected at random with 1 standard deviation used for the error bar.

If the deviation in split ratio is primarily caused by the presence of multiple plugs inside the loop structure, then the extent of this effect can be offset by lowering the frequency of plugs, i.e. by increasing the gap between them, so that fewer plugs are

present in the loop at one time creating less back pressure. As shown in Figure 3, as the plug frequency is decreased, the split ratio approaches that expected based on the relative channel lengths. When parent plug input frequency is lowered to 0.5 Hz, only the plug that is being split is present in the loop and the split ratio becomes close to the expected values. For the purpose of sampling, these results show that sampling ratio can be varied by both the loop structure and gap between plugs.

Long Term Stability. To evaluate stability in sampling ratio, we monitored the size of daughter plugs formed while splitting a series of plugs formed upstream. In this data analysis, we assume parent plugs are of regular size so that consistency in daughter plug size is indicative of splitting stability. We chose a chip design that produced 0.3 nL daughter plugs from 3.3 nL plugs when plugs were generated at 2.5 Hz for testing (Figure 4-2C). Fluorescence signal was monitored at the exit capillary for smaller daughter plug for more than 50 min (sample data from 5 replicates is shown in Figure 4-4A). To quantitatively evaluate split stability, plugs at 30 s interval were selected and peak widths were plotted against time showing no drift over this period (Figure 4-4B). The standard deviation of 6.3% in peak width indicates good long-term sampling stability and precision.

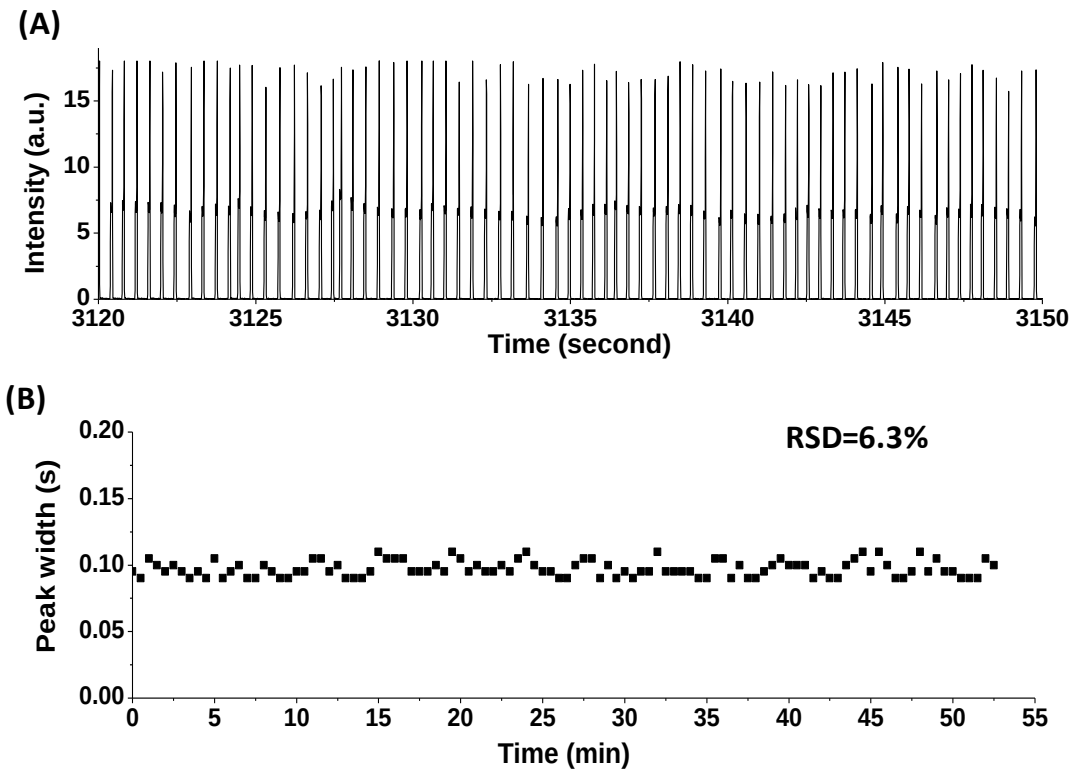

Figure 4-4. Stability of asymmetric splitting. (A) Fluorescence detection (in arbitrary units, a.u.) of series of daughter plugs detected downstream of the split. Data shown is portion of a 50 min experiment using device with design in Figure 2C. (B) Peak width of daughter plugs during a 50 min splitting experiment. A single plug was measured every 30 s.

In contrast, without the pressure equalization bridge (Figure 4-5), the plugs' split ratio rapidly changes preventing control of split ratio. These results illustrate that the pressure equalization bridge is effective at allowing stable asymmetric splitting and collection of resulting plugs.

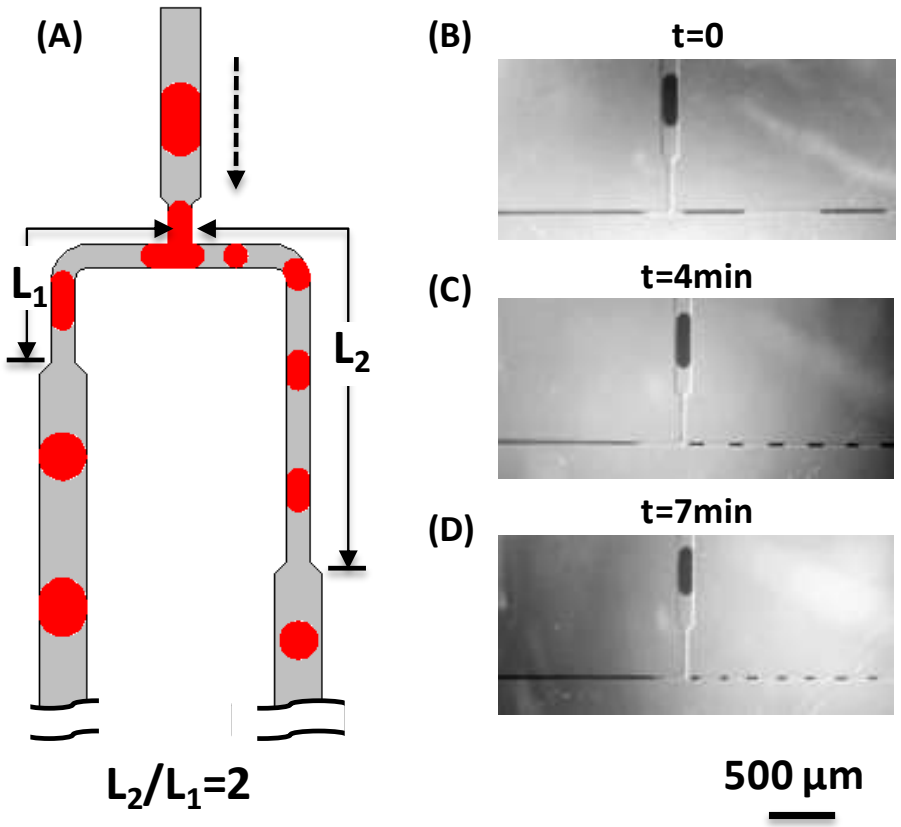

Figure 4-5. Unstable asymmetric splitting without a bridge. (A) Drawing of asymmetrical splitting tee used without a bridge to reequilibrate pressure after the split. The length ratio is controlled by adjusting both the narrowed region and the capillary length ratio of the side arms of the tee junction and the tubing receiving plugs. (B), (C) and (D) show the time evolution of splitting via the asymmetrical tee in a single splitting experiment, which indicates inconsistency in split ratio over time.

Conclusions

These results demonstrate that the design of Figure 1 allows 1.7 to 3.3 nL plugs to be split with fractions from 0.03 to 0.5. The system allows splitting of thousands of plugs with no deterioration over time. This is in contrast to simpler split designs (Figure 5) without a mechanism of re-equilibration of pressure which cannot maintain stable split ratios. The system also allows the resulting plugs, both parent and daughter, to be

collected into capillaries for storage or further manipulation. This is in contrast to other examples of stable, asymmetric split which were not explored for collection of fractions. The capability of sampling from plugs may be useful in a variety of chemical analysis procedures. For example, sample plugs collected from different sources, such as sampling probes[53], capillary separations [106, 107, 108], or multi-well plates[55, 92], could be split for analysis by different detectors or assays or to preserve part of a sample after analysis. Another application would be in high-throughput screening where an array of test compounds, stored as plugs, could be split such that only a fraction is used for a given screening assay allowing the remainder to be intact for another screen.

CHAPTER 5
CAPILLARY LIQUID CHROMATORGRAPHY FRACTION COLLECTION AND POST-COLUMN REACTION USING SEGMENTED FLOW MICROFLUIDICS

Introduction

Capillary Liquid Chromatography (cLC), compared to conventional scale HPLC, offers advantages such as reduced solvent consumption, better separation efficiency, and facile coupling to mass spectrometry[109, 110]. Despite these advantages, cLC was slow to be developed commercially. The advent of ESI-MS has moved cLC to a commonly used technique for proteomics[111]. Along with this application, capillary LC instrumentation has matured so that now commercial instruments are available that have adequate pumping, injection, and detection capability to realize many of the benefits of cLC[112 113]. While instrumentation has been improved, it is still difficult to collect fractions and perform post-column processing of samples from cLC. A practical obstacle is the difficulty in manipulating small volume samples. Capillary LC columns with inner diameter (ID) less than 300 um typically operate at < 1 μL/min flow rate resulting in nanoliter volume fractions, which is far smaller than what conventional fraction collection systems can handle. Lack of fraction collection limits the capabilities and workflow possible with cLC. It prevents use of slow secondary analytical techniques, like NMR, for identifying substances. It also restricts post-column sample manipulation such as digestion or labeling for detection.

Recently a novel approach to fraction collection from cLC, capillary electrophoresis, and microfluidic systems based on segmented flow has been reported[53, 107, 114, 115]. In this method, effluent from the column is collected as droplets bound by an immiscible oil. Using various microfluidic structures, regular droplets are formed from column effluent into picoliter to nanoliter volume. The advantage of this approach is that it is possible to store and manipulate low volume fractions reproducibly and at high-throughput. This work has shown several potential uses of fraction collection from microscale separations. One cLC application is off-line interface to ESI-MS which facilitates "peak parking" in which more time can be devoted to MS interrogation of particular peaks by slowing down the flow into the MS[115]. Another report demonstrated post-column digestion of proteins by adding enzymes to segmented flow fractions suggesting the potential of a novel top-down proteomic workflow at microscale[116]. Droplet fraction collection approach has been used for interfacing in 2-D separation at microscale[107]. A non-traditional use was creation of large concentration gradients from components[53].

In this report we extend the utility of this approach by developing post-column derivatization for fluorescence detection of proteins. Derivatization for fluorescence detection is desirable to enhance detection sensitivity, especially in microscale formats where UV-absorbance is often inadequate because of short pathlengths. Pre-column labeling is problematic for proteins because incomplete labeling of all targeted functional groups, for example amines, on a macromolecule results in multiple species leading to multiple or broadened peaks for a single protein. Post-column labeling is restricted to fluorogenic reagents, i.e. reagents must become fluorescent only after derivatization to

avoid a high background in detection. Post-column labels must also react quickly to prevent extra column band broadening. These twin requirements greatly restrict reagents that may be used for post-column derivatization of proteins. [117, 118] Here we demonstrate collection of separated proteins and subsequent post-column derivatization with the related fluoregenic reagent, NDA. In principle, the system can be adopted to other fluorogenic reactions with different excitation wavelengths and reaction kinetics. We also further evaluate conditions necessary for reproducible fraction collection. Technical difficulties such as protein adsorption and droplet data processing are also addressed.

Experimental

Chemicals and reagents. Chemicals and solvents were purchased from Sigma Aldrich (Saint Louis, MO) unless noted otherwise. 3-(4-Carboxybenzoyl) quinoline-2-Carboxaldehyde (CBQCA) and naphthalene-2,3-dicarboxaldehyde (NDA) were purchased from Invitrogen (Eugene, OR). HPLC grade water and methanol were both purchased from Burdick & Jackson (Muskegon, MI). Fused silica capillary was from Polymicro Technologies (Phoenix, AZ). Perfluorinated surfactant R_f-PEG, a perfluorinated linear alkane with hydrophilic tail group consisting of polyethylene glycol (PEG) repeats, was extracted from Zonyl-FSO100, which is a water suspension of a mixture of molecules that share the same structure $CF_3(CF_2)_m(CH_2CH_2O)_nH$, as described elsewhere[119]. Oil phases with additives used for segmenting flow were prepared fresh daily. All aqueous solutions were prepared with to 18 MΩ resistivity water purified using a Series 1090 E-pure system (Barnstead Thermolyne Cooperation, Dubuque, IA). Protein samples were dissolved in water with 3% methanol and 0.1% TFA as 1 mg/mL stock solution (except insulin which was dissolved in 10% HCl to better solubilize).

Capillary LC separation. Capillary LC columns were packed as described elsewhere [120]. Briefly, a frit was made by tapping nonporous silica (Micra Scientific, Inc., Northbrook, IL) into the outlet of a 75 μm inner diameter by 15 cm long fused silica capillary. The particles were briefly heated using a butane lighter to sinter them in place. The slurry used for packing consisted of 1 mg 3 μm C4 Prosphere particles with 300 Å pore size (purchased from Alltech, Deerfield, IL) suspended in 1 mL. The capillary LC column was packed to 5 cm column bed length at 500 psi using a custom-made pressure reservoir.

A Varian ProStar 210 (Varian, Palo Alto, CA) was used to pump mobile phase. Mobile phases were prepared daily, purged with helium and pass through 10 μm pore solvent filters (IDEX, Oak Harbor, WA) to remove particulates. Flow rate was 0.5 mL/min and split to achieve 300 nL/min through the column. Mobile phase A and B were water with 0.1% (v/v) trifluoroacetic acid (TFA) and methanol with 0.1% TFA, respectively. Injection was accomplished by disconnecting the column inlet from the pump and dipping it to a sample solution held in a pressure reservoir through a injection valve (Valco, Houston, TX). Gas pressure of 500 p.s.i for 20 s was applied yielding an injection volume of 50 nL. For separation, a linear gradient from 0% to 100% B was applied over 10 min. Then the system was held at 100% B for 5 min before re-equilibrating back to 100% A. A Spectra Series UV100 capillary UV detector from Thermo Scientific (Foster City, CA) was used to detect protein signal at 214 nm. The data was collected through NI USB-6008 data acquisition card (National Instrument, Austin, TX) and recorded by a home-written LabView program.

Droplet generation and fraction collection. Fractions from cLC were collected as segmented flow as shown in Figure 2A. A syringe pump (Fusion 400, Chemyx, Stafford, TX) was used to infuse perfluorodecalin with 1% PFO (v:v) and 0.5 mg/mL R_f-PEG at a flow rate of 0.3 μL/min into a PEEK Tee union (C360QTPK4, Valco, Houston, TX). The cLC effluent was pumped into another arm of the tee at 90 degrees to the oil input. This arrangement resulted in the continuous LC eluent being segmented into aqueous plugs separated by oil plugs. The resulting segmented stream flowed out the third arm of the tee into a 1.5 m length of 100 um inner diameter by 360 μm OD PFA tubing (Upchurch Scientific, Oak Harbor, OR) where they were stored for later analysis.

For some experiments, a flow injection system was used instead of the cLC to test the effect of oil phase content on droplet uniformity and stability. In this system, the cLC was replaced with a 6-port, 2-position valve (Valco, Houston, TX) with flow driven by a syringe pump (Fusion 400, Chemyx, Stafford, TX) at at 0.3 μL/min. The valve was used to switch between 50 μg/mL myoglobin in 0.1%TFA with 3% methanol and the solvent alone. The protein solution also contained diluted blue food color to allow visualization of this stream. A 20 cm long 20 mm inner diameter 360 mm outerdiameter fused silica capillary at the valve outlet was connected to the tee, replacing the column (Figure 2A), for flow segmentation. Resulting droplets were observed using a stereomicroscope (SMZ 745T, Nikon Instruments Inc., Melville, NY) equipped with a color CMOS camera (EO-1312C, Edmund Optics, Barrington, NJ. Resulting images were analyzed by Image J (US National Institutes of Health, Bethesda, MD).

Reagent addition and LIF detection. Reagent addition to droplet fractions was performed using a PDMS/capillary hybrid chip (Figure 3A) that was fabricated by soft lithography[121]. SU-8 2075 photoresist (Micro-Chem Corp. Newton, MA) was spin-coated onto a 3 inch silicon wafer (University Wafer, Boston, MA) at 4000 rpm. After pre-bake, the SU-8 coated silicon wafer was exposed to UV radiation for 13.3 s (365 nm mercury line, 60 mJ/cm^2 power, Optical Associates, Inc., Milpitas, CA) through a dark field mask (Fine Line Imaging Co., Colorado Springs, CO) to cross-link the exposed features in the desired microfluidic pattern. After exposure is the post-bake step and remaining photoresist treated with SU-8 developer (MicroChem Corp. Newton, MA). The resulting SU-8 features were 60 um high and 150 um, 60 um, and 200 μm wide at the droplet inlet, reagent addition, and droplet outlet respectively. PDMS was cast over the mold to create channels. Access holes were made by poking a blunt 18 gauge needle into the PDMS after removing from the mold. The PDMS with channels was sealed to a piece of unpatterned PDMS by plasma bonding followed by placing the combined device on a hot plate (temperature set to 75 °C) for 10 min. The surface of the channels were derivatized by filling the channels with 10:100 (v:v) H,1H,2H,2H-perfluorooctyltrichlorosilane solution in anhydrous via the punched access holes. The filled chip was placed on a hot plate (temperature set to 75 °C) for 30 min. A 100 μm ID by 160 μm OD silica capillary, pre-silanized by 1H, 1H, 2H, 2H-perfluorooctyltrichlorosilane, was inserted from the side of the chip into the microfabricated channel to construct a segmented flow inlet. The reagent inlet was made by inserting a piece of bare silica capillary that was 50 μm ID by 150 μm OD into the PDMS channel. The droplet outlet was made by inserting a piece of

Zeus PTFE 38 gauge (approximately 100 μm ID and 220 μm OD) tubing (Amazon, Seattle, WA), which was glued in place using 5 min epoxy.

To derivatize separated proteins, segmented flow fractions collected from the cLC column were pumped at 0.6 uL/min into the reagent addition chip while reagent was pumped at 0.3 μL/min using a syringe pump (Figure 3A). Derivatization reagent consisted of 1 mM NDA and 20 mM β−mercaptoethanol (BME) dissolved in 30% methanol and 70% 100 mM sodium tetraborate buffer at pH 9.3.

LIF detection[122, 123] was performed using an epi-illumination configuration based on a Zeiss Axiovert 35 M inverted microscope equipped with a 40x, 0.6 numerical aperture objective (Carl Zeiss, Inc., Thornwood, NY) and a Photon Technology International 814 photometer (Lawrenceville, NJ). The photometer was fitted with 490 ± 30 nm and 530 ± 30 nm band-pass filters for excitation and emission, respectively. The excitation source was 20 mW of 488 nm from an optically pumped semiconductor Sapphire laser (Coherent, Santa Clara, CA). The laser was focused onto the PFA tubing that is 100 mm in inner diameter and 360 mm in ourter diameter containing derivatized droplets. The droplets were pumped past the detection point at 0.9 μL/min for detection. The reaction time was controlled by the flow rate and tubing length from reagent addition to detection point. Instrument control and data collection were performed using LabVIEW software written in house (National Instruments, Austin, TX).

Pre-column derivatization using CBQCA reaction. CBQCA was used to derivatize protein samples following the directions of the Invitrogen manual. The reaction was quenched and acidified with 12 M HCl before injection.

Data processing. Oil is non-fluorescent, therefore, single point detection of segmented flow result in a trace with individual peaks that correspond to the signal of aqueous drops and valleys indicating the oil segments. Chromatograms were constructed from this data using Igor Pro 6.01 (Wavemetrics, Inc., Lake Oswego, OR). Each droplet was identified as an individual peak and peak center and peak amplitude information extracted using a built-in macro. Fluorescent signal amplitude was plotted against peak center value for chromatograms. Origin 6.0 and Cutter 7.0[63] were used to plot and process chromatograms.

Results and Discussion

Oil phase additive and droplet regularity. Capillary LC fractions were collected using a tee structure (Figure 2A) similar to other reports.[107, 114, 115, 124] This structure has been successfully used in many applications for generating reliable plugs; however, we found that when using perfluorodecalin as the oil, proteins in the segmented sample caused coalescence of plugs resulting in large and irregular droplets. This is illustrated by flow injection data for myoglobin in Figure 1A. These effects are detrimental to the separation because: 1) it reduces fraction collection frequency; 2) coalescence is variable, which makes downstream reagent injection and quantitation less reliable. We hypothesized that protein adsorption to the oil/droplet interface was causing this effect. Adsorption of proteins onto the aqueous/oil interface lowers the interfacial tension. With lower interfacial tension, droplets tend to be bigger[125, 126] and coalescence occurs more often. Protein concentration varies as a zone elutes from the column so that droplet segments generated at the center of the peak have higher protein concentrations

than those at the edges of the peak resulting in variable tendency to coalesce across a peak. Adding the fluorinated surfactant R_f-PEG to the oil phase to improved droplet regularity and stability (Figure 1B). In the fraction collection experiments described in below, PFO was also added. We found PFO alone does not help with the droplet generation. However, PFO does seem to improve the performance of reagent injector and is thus used in combination with R_f-PEG in the experiments that involve reagent addition.

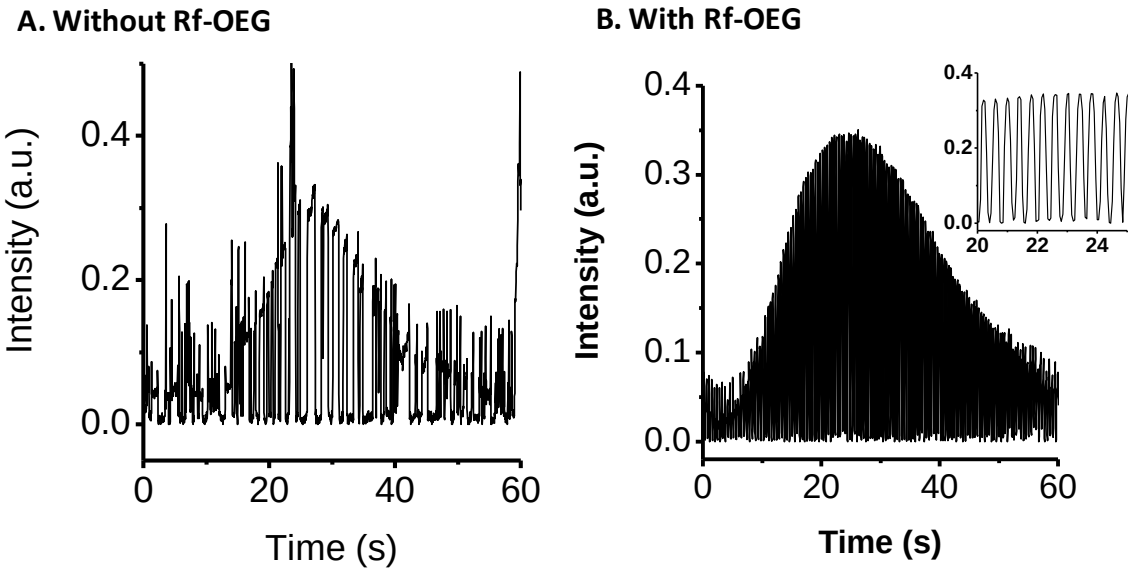

Figure 5-1. Oil phase surfactant's effect on droplet regularity: (A) is the droplet trace using pure perfluorodecalin as the carrier phase. (B) adding R_f-PEG as a oil phase additive, droplets that contain myoglobin at changing concentrationare smaller and the size distribution is tighter compared to without.

Separation and fraction collection. When collecting fractions, it is important that samples can be collected at a rate that does not broaden peaks. Typically, collection of 8 -10 fractions across a single peak is considered to be sufficient to not cause undue extra column broadening. Frequently, the number of fractions collected is minimized because of the difficulty of manipulating many fractions; however, the segmented flow

approach allows facile handling and manipulation of fractions so collecting large number of fractions is not cumbersome.

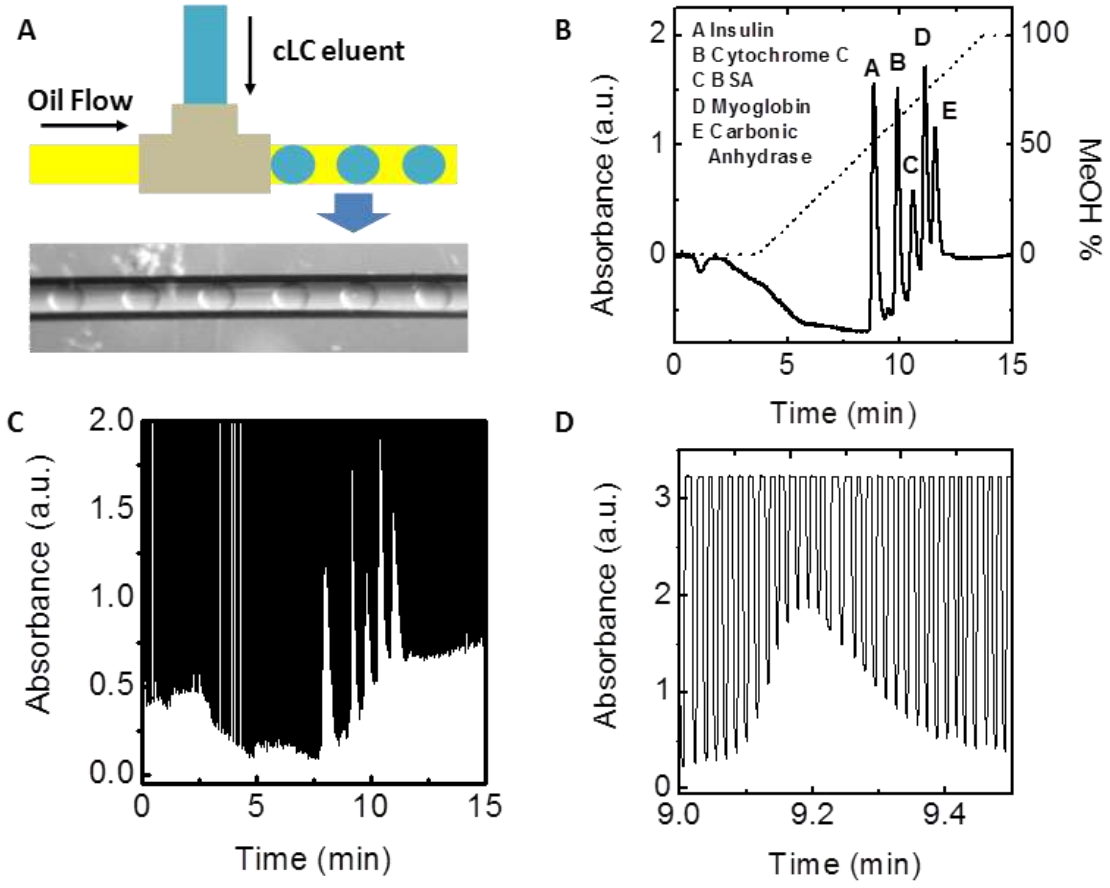

Figure 5-2. (A) Schematic drawing of the fraction collection using segmented flow microfluidics. Picture shows the fractions generated from capillary LC that are oil immersed droplets stored in a piece of PFA tuing. (B) Chromatogram of reversed phase capillary LC separation of 5 protein standards. (C) UV signal trace of the same separation but after fraction collection. Pefluorodecalin has abundant UV absorbance at 214 nm and maxed out the detector when it reaches the detection point. The valleys are the UV signal for the aqueous phase in this diagram. (D) Expanded view of insulin peak from Figure 2 (C) showing the fractionation of insulin peak into ~30 droplet fractions.

To illustrate these points, we compared separations of a test mixture of 5 proteins on-column and after fraction collection. Figure 2B is a chromatogram from separation of

a test mixture of proteins by reversed phase LC at 0.3 μL/min with on-column detection. Figure 2C illustrates a trace resulting from collecting the same separation in 5 nL fractions, corresponding to 1 Hz collection rate (see Fig. 2D) using the system in Figure 2A. The resulting fractions were pumped through the UV absorbance detector to generate the trace. As shown, resolution is preserved despite fraction collection. For example, resolution for insulin and cytochrome C before and after fraction collection were both 2.0. Figure 2D shows that ~30 fractions were collected across the insulin peak. Thus, it was possible to collect well over the minimal 8-10 fractions needed to preserve resolution in this sample chromatogram.

These data also show that fraction size does not change significantly despite the change in solvent due to gradient elution. Droplet size was 4.4 ± 0.4, 5.3 ± 0.5 and 5.7 ± 0.4 nL (n = 5 droplets) at 0%, 50% and 100% mobile phase B respectively. The slight increase in droplet size could be contributed to changes in viscosity with methanol content.

Reagent addition and fluorescence detection. For fluorescence detection, it is necessary to add derivatization reagent to collected fractions and allow time for reaction before detection. Adding reagent to preformed droplets has been demonstrated previously [86, 89, 90, 103]. A commonly used approach is to pump reagent continuously from a hydrophilic channel or capillary into a hydrophobic tee where sample plugs flow past. Reagent droplets that begin to form at the outlet of the hydrophilic channel merge with sample droplets (cLC fractions in this case) and rapidly mix due to recirculation effects in the droplets as they flow. This approach has been used for enzyme assays [127, 128, 129].

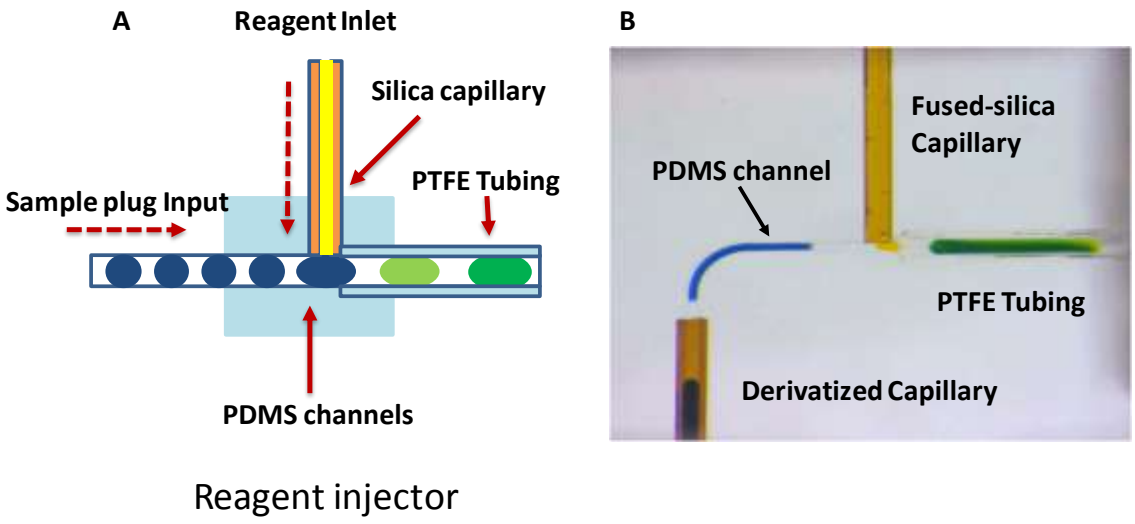

Figure 5-3. (A) Reagent addition chip design. (B) Bright field image of a functioning reagent addition chip. Blue plugs represent the pre-formed fractions. A drop of yellow reagent droplet is forming at the outlet of the reagent addition capillary which later merges with the incoming blue droplet and form a green droplet after the reagent addition step which inters the outlet that is made of a piece of PTFE tubing. Flow rates used here are identical to the fluorogenic reagent addition experiments.

We adapted this approach for our work using a PDMS/ capillary hybrid device (Figure 3A). In this device, PDMS is used as a mold to allow a fused silica capillary to act as a hydrophilic channel for delivering reagent. Teflon capillary collects fractions with reagents added as shown in Figure 3A. For this system, fluorogenic reagent is added to cLC plugs at half the flow rate of segmented flow.

Cross contamination may occur in these devices because a portion of a droplet passing the reagent inlet can be left behind and then combine with the following droplet. Such effects could lead to extra column band broadening in this application. Using narrow bore tubing in the reagent inlet helps keep the Peclet number and cross-contamination low[127]. Carry-over tests using food coloring confirmed the effectiveness of this design. Injection of yellow colored aqueous “reagent” into pre-formed dark blue fluid

segment results in green colored droplets. As shown in Figure 3B, the yellow reagent inlet is barely tainted by the previous blue droplet thus low contamination is carried to the next droplet flow by. The lack of extra column broadening or tailing in chromatograms is further evidence that cross-contamination is inconsequential with respect to cLC.

To test this system, we derivatized collected fractions with NDA/BME. NDA has been shown to be effective for post-column derivatization in CE separation[91] and offers nanomolar detection limit. From kinetic tests using a fluorescence plate reader, we found that fluorescence intensity of NDA/BME derivatives of BSA reached a maximum within 10 s. The fluorescence signal of the protein-NDA conjugate starts decreasing after 20 s which is consistent with results reported elsewhere[130]. Reaction time was controlled to be 15 s by placing the detector 15 s downstream of the reagent addition tee. Figure 4 shows the fluorescent signal trace of segmented flow coupled post-column derivatization with NDA reaction and on-line LIF detection. Oil segments are non-fluorescent and appear as the signal baseline. Aqueous drops are detected as individual peaks. Fluorescent signal of droplets increases with protein collected from the cLC separation so that the chromatogram can be reconstructed. Detection limit of BSA was around 2 μg/mL, which is about one magnitude improvement over UV absorbance detection. Further improvement of sensitivity requires is likely possible by using a laser that better matches the absorbance maximum of the derivatives (460 nm) and optimization of reaction conditions.

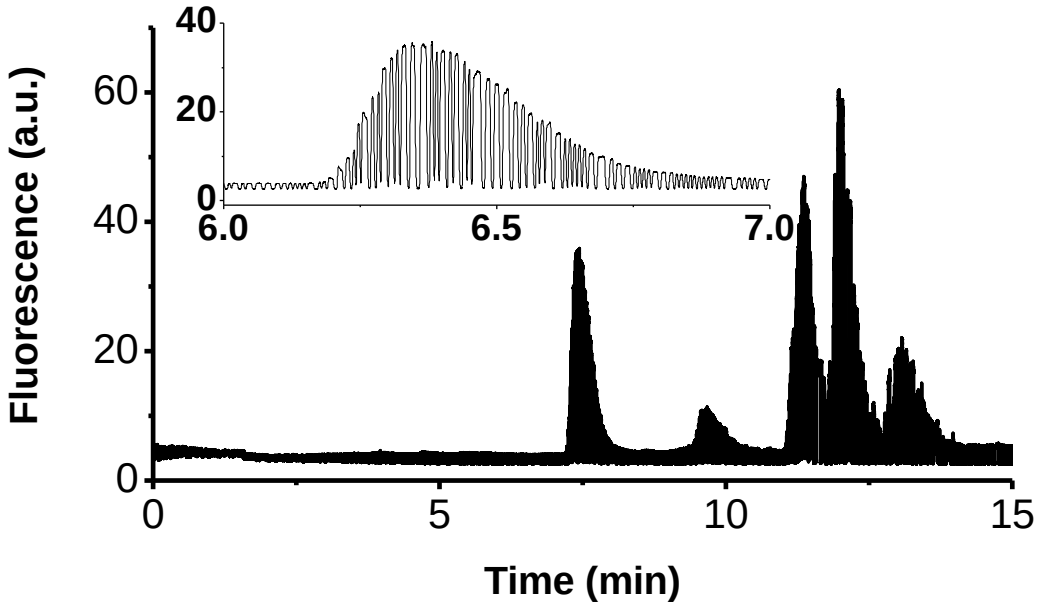

Figure 5-4. LIF signal trace of droplet fractions after NDA reagent is added.

An alternative to fraction collection for analysis is post-column derivatization in a continuous flow reactor[131]. In continuous flow post-column reactors, it is important to keep the reaction fast and mixing efficient so that not much resolution will be sacrificed. Segmented flow eases this requirement because diffusion is limited to within each droplet and once the fractions are generated, resolution does not change over time. Therefore, in principle even reactions with relatively slow reaction kinetics, such as nano-orange, CBQCA, and FQ could be used post-column. Reaction time can be controlled by varying the length between the reagent addition point and the detection window. Off-line incubation[132] can be used if the reaction time is on the order of hours. Also, with derivatization with segmented flow does not require an on-line system, so collected

proteins can be stored and then derivatized later. For example, in these experiments proteins were typically derivatized and detected 1-2 h after the fractions were collected.

Comparison to pre-column derivatization. Compared to post-column derivatization, pre-column deriviatzation yields a more complex chromatogram as illustrated in Figure 5 which compares chromatograms for 5 protein standards detected by UV-absorbance, by UV after pre-column derivatization with CBQCA, and by LIF after post-column derivatization with NDA (reconstructed as described in Experimental section). With CBQCA pre-column labeling, extra and overapping peaks are found (including a large deadtime peak), likely due to excess CBQCA and multiple labeling of proteins[133] making peak assignment and quantitation difficult. On the other hand, the post-column approach circumvents the "multiple peak problem" by decoupling separation and labeling reaction and using the fluorogenic reaction simply as an indicator of proteins' presence.

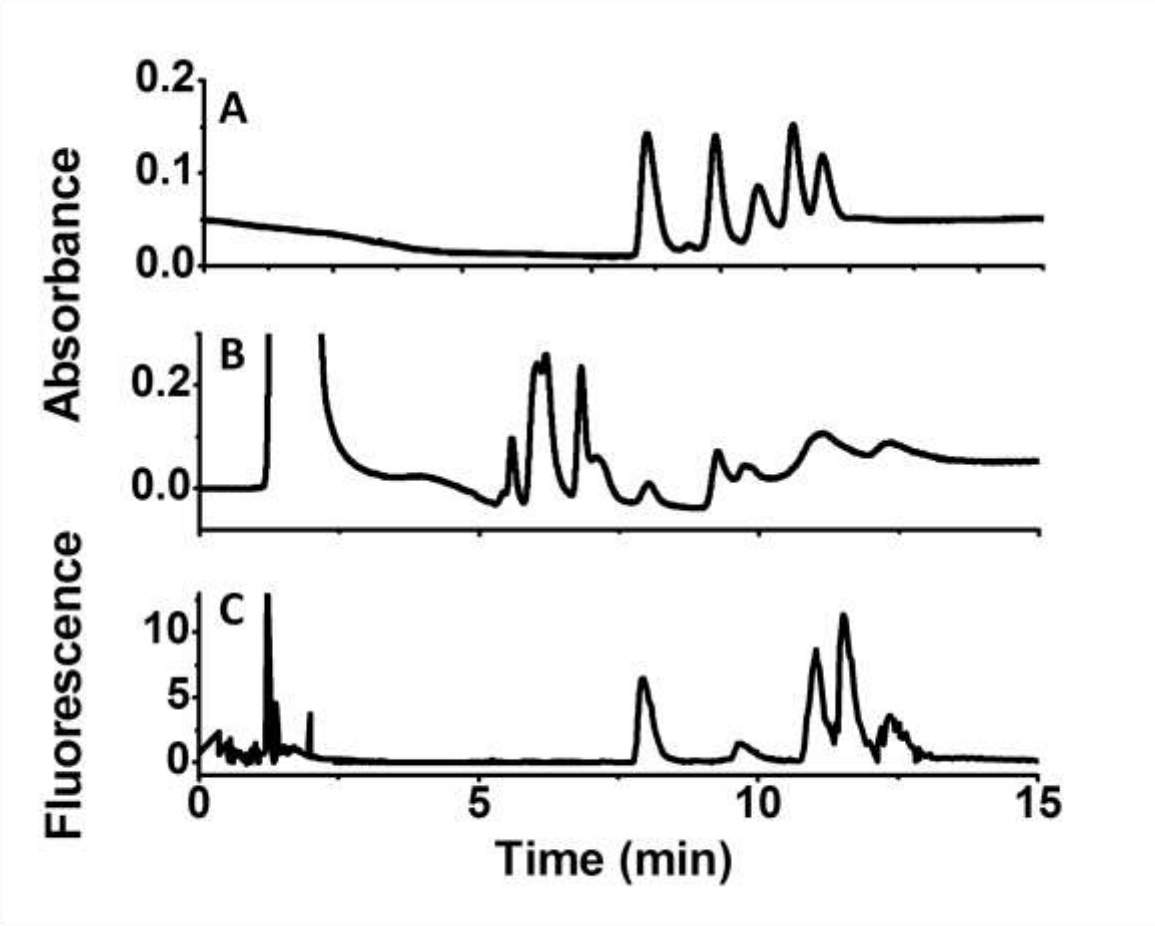

Figure 5-5. (A) UV chromatogram of 5 protein standards. (B) UV chromatogram of the same five proteins that are CBQCA pre-column labeled. (C) LIF chromatogram reconstructed from Figure 4(A).

In implementing a post-column reactor, attention is usually focused on reducing extra-column band broadening due to dispersion and insufficient mixing. Segmented flow, however, provides an alternative to the traditional post-column reactor solutions. Operating at a high enough sampling frequency, segmented flow allows resolution to be maintained throughout post column fraction manipulations such as fraction collection and post-column reaction. Thus, the resolution for insulin and cytochrome C peak from both on-line and off-line detection is 2.0 despite the storage and derivatization associated with

off-line detection. The fluorescence trace also does not have drift associated with the gradient, as expected. Figure 5C also shows that relative sensitivities of LIF detection of proteins are different from the UV detection. At same protein concentrations, the NDA reaction appears to be less sensitive for cytochrome c and carbonic anhydrase.

Conclusions

In this work, we demonstrate that segmented flow microfluidics can be used to collect fraction and perform post-column reaction for capillary LC separation. Taking advantage of the capability of manipulating small volumes, we were able to show that in the mirofluidic format, we can do the fraction collection at high enough frequency so that chromatographic information is preserved. One potential application of this study is the quantitation of low abundance proteins, which is hard with other detection schemes. Fraction collection offers much flexibility and versatility in post column sample processing. Aside from the LIF detection that we demonstrated, we believe this approach will enable more applications in capillary based separation techniques, for example, multiplexed detection and multi-dimensional separation. Here, we used reversed phase LC (figure) separation as a model system. However, the fraction collection and post-column reaction schemes described here should be easily adapted to other chromatography modes such as size exclusion and ion-exchange chromatography.

CHAPTER 6
FUTURE DIRECTIONS

CE is an efficient and highly developed analytical method. In this work, we demonstrate that CE is indeed a powerful tool for PPI analysis. It offers many unique advantages as a screening technology for PPI inhibitors. However, as a high throughput screening platform for PPI, CE is still in its infancy. For large scale high throughput screening, more work remains to be done: 1) Improve the throughput of CE assays via ultra fast separation and parallelization; 2) Full scale screening that allows comprehensive assessment of CE's strength and limitations

Fast CE Separation

With current setting based on commercial CE instrumentation, the Hsp70-Bag3 assay has a throughput of 6.5 min per sample or 220 assays per day. One way to improve the throughput would be to speed up the separation. In fact, fast CE is not only principally sound, but also practically feasible[74]. With sharp injection band and high electric field, separation time can be well within a few seconds while achieving high separation efficiency as indicated in the equation below:

$$R_s = (\mu_1 - \mu_2)\sqrt{\frac{V}{D(\mu_{avg}+\mu_{eof})}} \qquad \text{(Eq. 6-1)}$$

where R_s is the resolution of molecule 1 and 2, μ_i is the electrophoretic mobility of molecules, μ_{avg} is the average electrophoretic mobility, μ_{eof} is the mobility contribution from EOF, D is the diffusion coefficient and V is the voltage drop across the separation length. From this equation, it is clear higher voltage and faster EOF should are very straightforward ways to speed up CE.

Fast CE separation has been demonstrated both in the capillary and the micro-chip format. In either case, small cross-section is the key in keeping the current low when voltage is high. So far all successful examples are demonstrated with bare silica capillary or un-derivatized glass chips that utilize strong EOF and electrokinetic injection. Electrokinetic injection, although very convenient to use, greatly limits fast CE in applications that require surface derivatized capillary and suppressed EOF. To overcome the dependency of strong EOF, it is necessary to add hydrodynamic injection capabilities to the existing fast CE setups for PPI analysis.

Another approach is to add the vacuum injection to the flow-gated CE system. Flow gate is essentially a cross shaped union that is connected to the inlet of the separation capillary (Figure 6-1A). Sample is introduced as continuous flow that comes in from the opposing side of the cross via another piece of tubing with a small gap (100 μm or less) between the sample introduction tubing and the separation capillary. When injection is not performed, the sample flow is directed away towards the waste by an orthogonal "gating flow", which is basically separation buffer that flows at high flow rate (100 times higher than the sample flow). During separation, the gating flow will be stopped for a brief period of time to allow sample to build up in the gap between the

sample outlet and the separation capillary inlet, followed by electrokinetic injection. After injection, the sample zone will be cleared by restarting the gating flow to flush away the residual samples in the flow gate. Then high voltage can be applied to start the separation.

Initially developed for Capillary LC-CZE 2D separation, flow-gated injection is a very useful injection scheme for CE that allows continuous sample introduction and efficient injection. To acquire the vacuum injection capability, an easy modification can be made as shown in Figure 6-1B. Traditionally, the buffer reservoir at the outlet of the separation capillary only provides the electrical contact to the high voltage power supply. In the modified system, an air-tight chamber will be used instead. It not only provides electrical contact, but also allows vacuum to be connected to draw sample during injection and separation (optional) steps. The on and off of the vacuum source can be controlled by an electronicallly actuated valve. The injection volume is controlled by both the vacuum level and the injection time.

Combining the injection system described above with small bore surface derivatized capillary (20 μm and below) and short length (less than 10 cm), this approach will enhances the separation speed substantially.

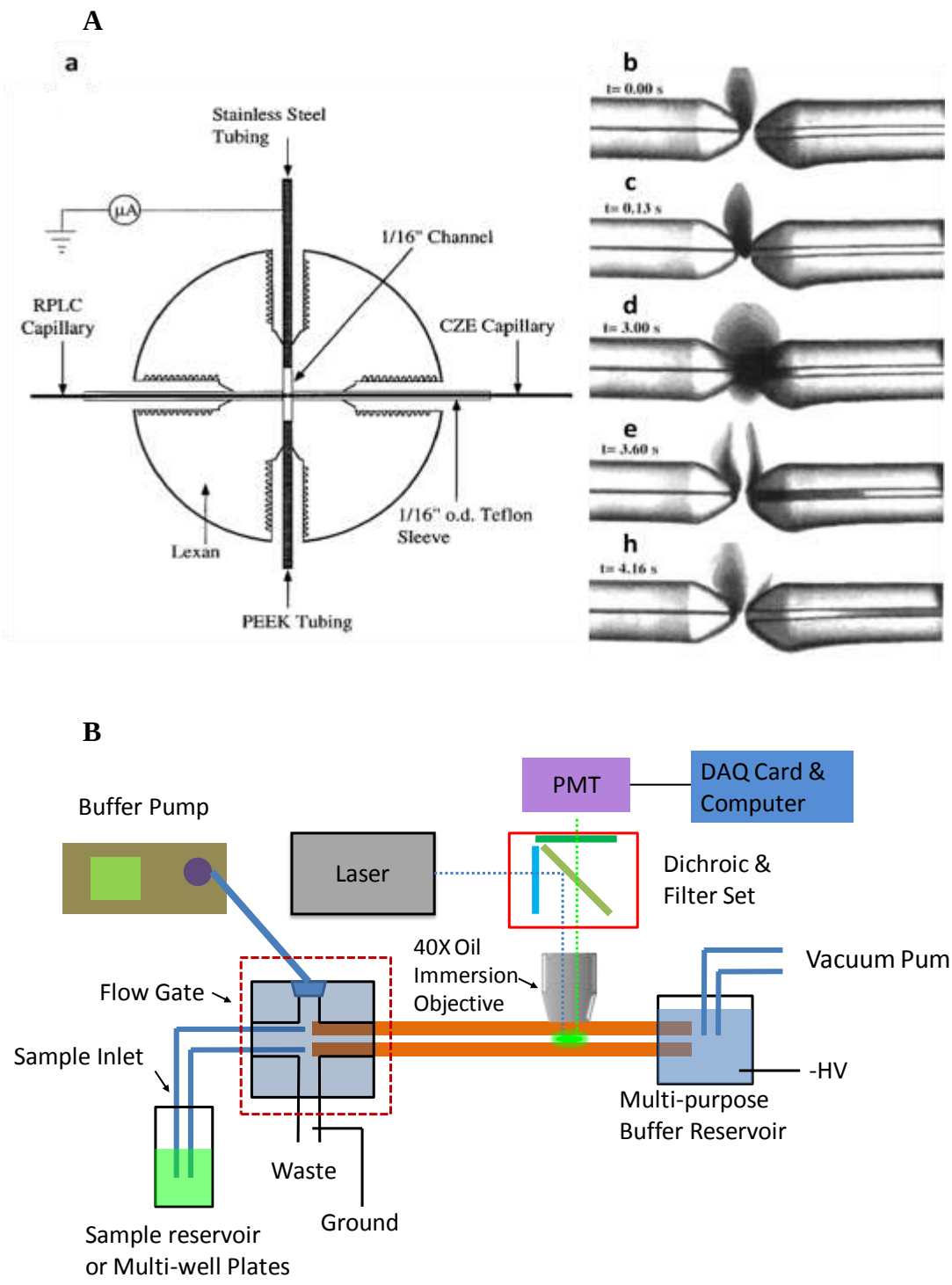

Figure 6-1. A Mechanism of flow-gated CE injection[134]. B. Instrumental design of adding vacuum injection capabilities to flow-gated CE.

One unique advantage of the flow-gated injection is the continuous flow sample introduction. This feature allows automated and high throughput sample introduction from micro-titer plates. Commercial CE instruments exclusively use a moving stage loaded with buffer that moves at every rinsing, injection and separation step. The mechanical movement not only takes time, but also increases the probability of instrument failure. Flow gated injection solves this problem by decoupling the sample introduction and CE separation, which should enhance system reliability in addition to sample throughput.

Droplet Microfluidics and Chip Based CE

CE consumes only a few nano-liter volume samples or lower, which could potentially lead to significant reagent saving in large scale HTS. However, commercial instruments typically require at least 10 μL sample volume to initiate the analysis. Segmented flow coupled micro-chip CE can be a promising alternative to realize the full miniaturization potential of CE. In this approach, library compounds stored in a multi-well plate can be reformatted into oil segmented fluid plugs stored in a piece of tubing (Figure 6-2A). After sampling and reagent addition, the segmented flow content will be extracted into a continuous aqueous phase and analyzed by CE-LIF via devices depicted in Figure 6-2 B and 6-2 C.

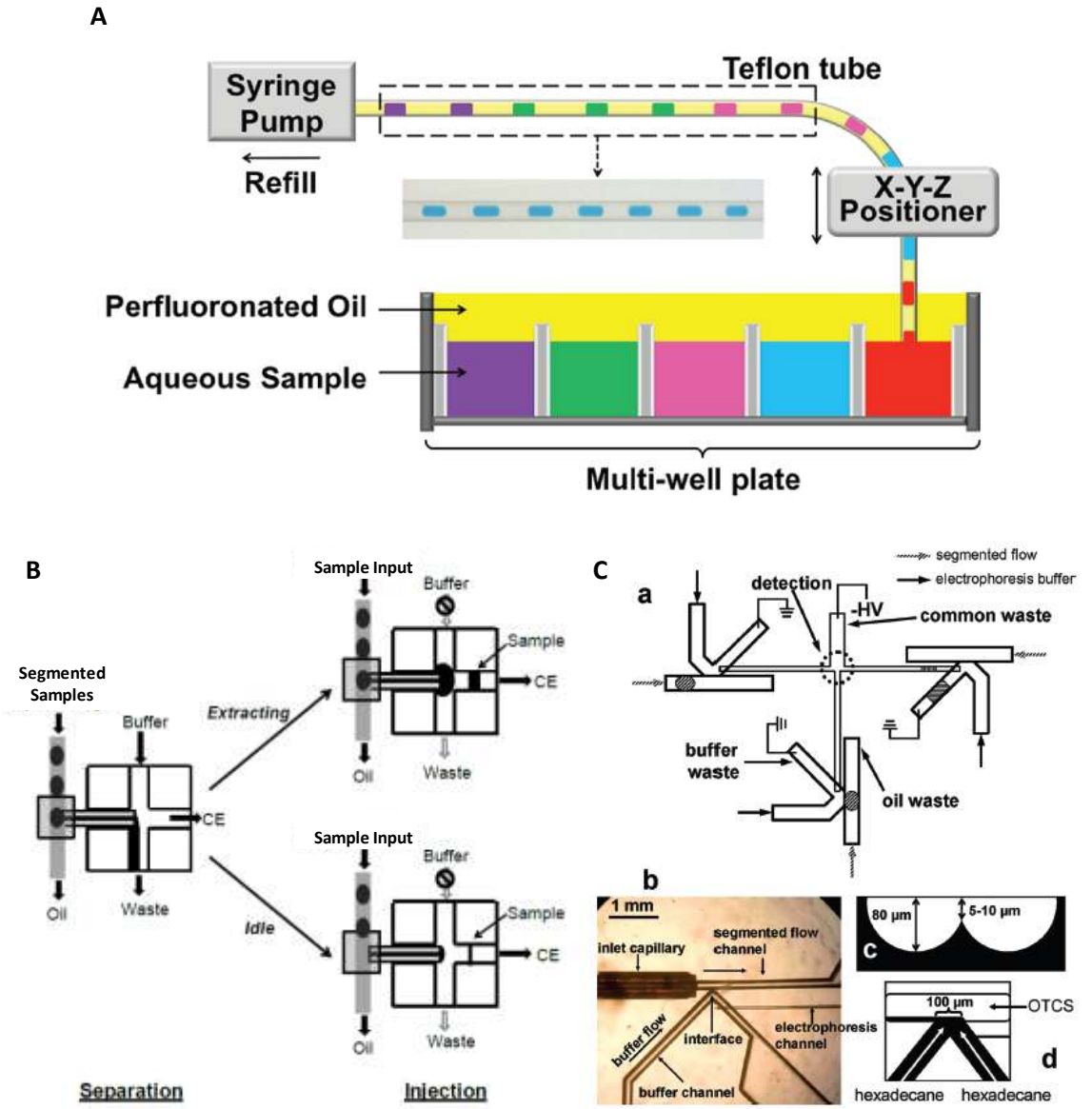

Figure 6-2. (A) Samples stored in multi-well plates can be re-formatted into oil-segmented fluid plugs using a syringe pump to draw aqueous samples and fluorinated oils as alternating fluid plugs in a piece of Teflon tubing. These sample plugs can be further manipulated and analyzed by CE.[129] (B) Coupling segmented flow to a traditional flow-gated CE setup[53]; C. microfluidic devices can be fabricated to extract and analyze segmented flow samples with on-chip CE-LIF[77].

Preliminary results suggest that the schemes shown in Figure 6-2B and 2C are able to increase the throughput of CE assays to over 10,000 assays per day, meeting the requirement of HTS. Future work in this area will involve development of surface modification techniques that is compatible with the micro-chip fabrication process.

Label Free Detection

The assay described herein used fluorescently labeled protein and LIF detection. LIF has best sensitivity and simplifies the data interpretation. One concern with this fluorescence detection though is that labeling may interfere with the binding if they happen to be at the protein binding site or change protein's allosteric property. The assay can be fully validated if the labeling site is carefully identified and affinity studies suggest the protein behave the same as without the fluorescent tag. Still, label free detection will make CE more generic to PPI targets and simplify the method development

Two "label free" detection schemes are considered here. The first approach is post-column derivatization coupled to LIF detection. As mentioned in Chapter 5, in the post-column derivatziation mode, native proteins are separated as they are and labeling and fluorescence detection happens after separation. Sensitive detection can be achieved without labeling proteins in the first place. Coupling CE to post-column derivatzation and LIF detection has been demonstrated previously and Figure 6-3 A illustrates one of the many configurations of CE coupled to post-column derivatization. The drawback is that the detection step provides very limited selectivity of analytes been separated. Unlike the pre-column derivatization mode, all species that form fluorescent products with the

fluorogenic reagents will be detected. It can be expected that the post-column mode will place higher requirements on protein sample purity and separation.

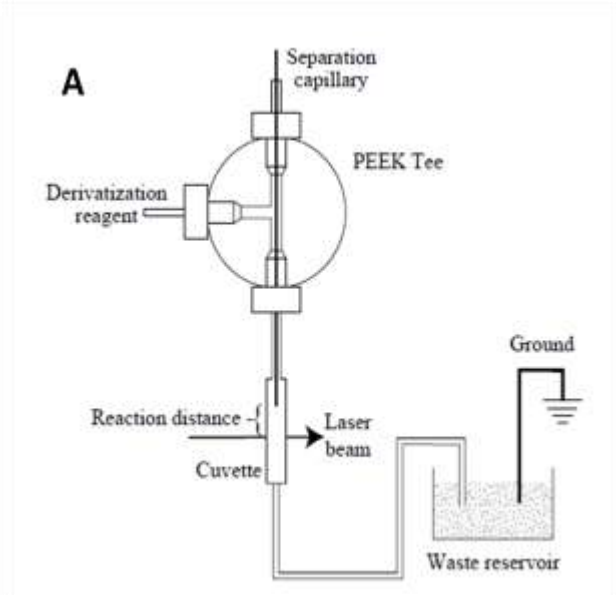

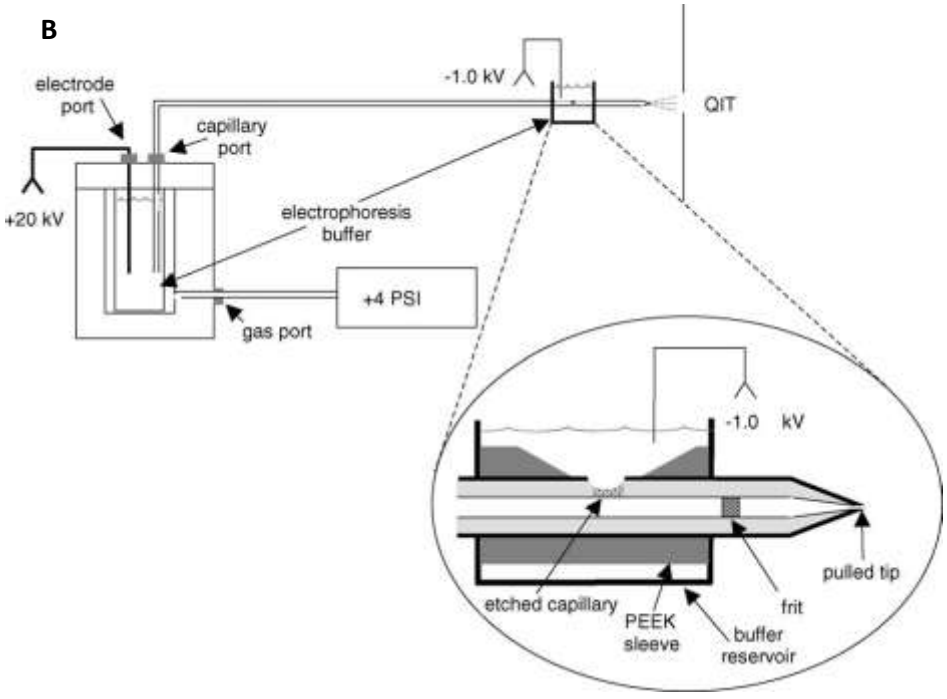

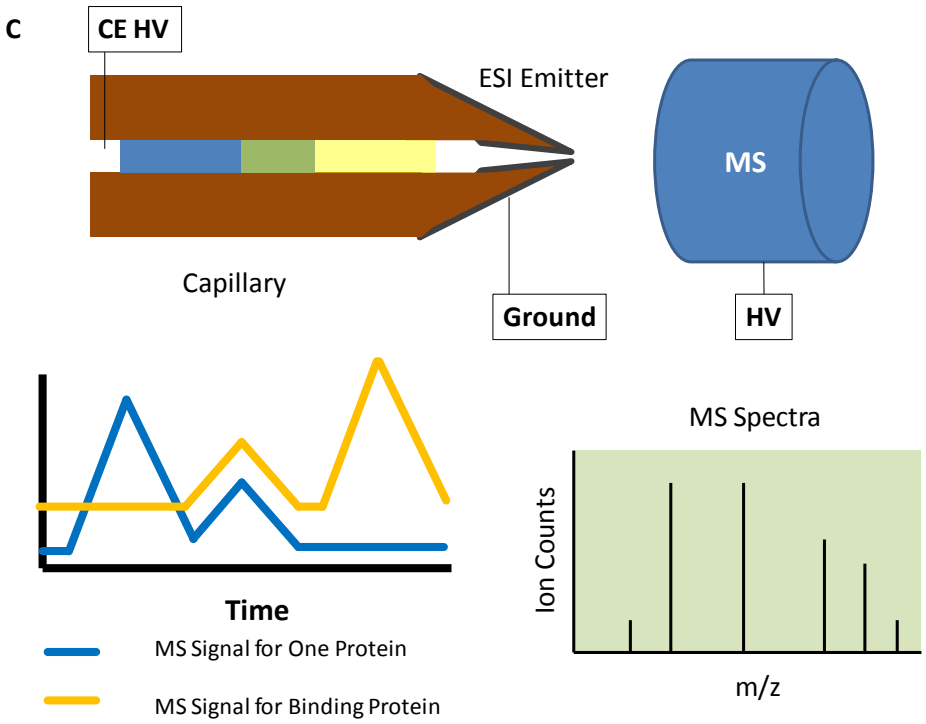

Figure 6-3. A. Post-column derivatization and LIF detection setup for CE separation of intact proteins.[135] (B) A sheath flow CE-ESI-MS system[136]. C. MS detection of APCE separation of PPIs.

Another promising alternative is Mass Spectrometry detection. With soft ionization techniques such as ElectroSpray Ionization (ESI) and Matrix Assisted Laser Desorption Ionization (MALDI), liquid phase biomolecules such as proteins can be converted into charged gas phase ions that are analyzed by various mass analyzers to obtain molecular weight and some quantitative information. Coupled to separations such as LC and CE and used as a detector, MS not only serves as a universal and sensitive detector, but also adds much specificity to the detection scheme due to the high resolution.

CE-MS has also been demonstrated with a variety of different analytes including intact proteins. By coupling MS detection to affinity CE studies, the labeling problem can be overcome without compromising the selectivity. Simultaneous monitoring of different

analytes also allows additional information and confidence in detecting binding events (Figure 6-3C). Challenges of top down proteomics are also the major concerns with this approach. MS, by and large still has limited dynamic range and inadequate resolving power for intact proteins. Only the most state of the art MS hardware has the promise of tackling the difficulties of detecting intact proteins.

APPENDIX A

LIST OF 18 COMPOUNDS TESTED IN CE SECONDARY ASSAY

Compound Number	Compound Name
1	Homidium Bromide
2	Methylergonovine maleate
3	Levodopa
4	Laudanosoline
5	5-Aminosalicyclic acid
6	Methyldopa
7	Tanshione IIA
8	Oxytetracycline
9	NCl16221
10	FK866
11	Pyrvinium pamoate
12	Carminic acid
13	Captopril
14	EGCG
15	Cortisone
16	Meclocycline sulfosalicylate
17	Purpurogallin
18	Hematoxylin

APPENDIX B

LIST OF COMPOUND #9 AND ITS STRUCTUAL ANALOGUES

Compound Number	Compound Name
9	Bis-benzoic acid,2,2'-[(9,10-dihydro-9,10-dioxo-1,5-anthracenediyl)diimino]
9A	Anthraquinone-2 6-disulfonic acid
9B	9B: Anthranrufin
9C	9C: R494291
9D	9D: JFD00244
9E	9E: 2,2′-Iminodibenzoic acid
9F	9F: 1-(Methylamino)anthraquinone
9G	9G: 2,5-diaminoterephthalic acid
9H	9H: 1-[(2-Hydroxyethyl)amino]-9,10-dioxo-9,10-dihydro-2-anthracenecarboxylic acid

REFERENCES

1. J. A. Wells, C. L. McClendon, *Nature* **2007**, *450*. 1001-1009

2. N. H. H. Heegaard, S. Nilsson, N. A. Guzman, *Journal of Chromatography B: Biomedical Sciences and Applications* **1998**, *715*. 29-54

3. G. M. Whitesides, *Nature* **2006**, *442*. 368-373

4. L. Michaelis, *Biochemische Zeitschrift* **1909**. 81-86

5. J. W. Jorgenson, K. D. Lukacs, *Analytical Chemistry* **1981**, *53*. 1298-1302

6. Y. Cheng, N. Dovichi, *Science* **1988**, *242*. 562-564

7. J. P. Landers, *CRC Press, Inc.* **1997**.

8. Y. H. Chu, L. Z. Avila, J. M. Gao, G. M. Whitesides, *Accounts of Chemical Research* **1995**, *28*. 461-468

9. K. Shimura, B. L. Karger, *Analytical Chemistry* **1994**, *66*. 9-15

10. N. M. Schultz, R. T. Kennedy, *Analytical Chemistry* **1993**, *65*. 3161-3165

11. N. M. Schultz, L. Huang, R. T. Kennedy, *Analytical Chemistry* **1995**, *67*. 924-929

12. P. L. Yang, R. J. Whelan, E. E. Jameson, J. H. Kurzer, L. S. Argetsinger, C. Carter-Su, A. Kabir, A. Malik, R. T. Kennedy, *Analytical Chemistry* **2005**, *77*. 2482-2489

13. P. L. Yang, R. J. Whelan, Y. W. Mao, A. W. M. Lee, C. Carter-Su, R. T. Kennedy, *Analytical Chemistry* **2007**, *79*. 1690-1695

14. F. A. Gomez, L. Z. Avila, Y.-H. Chu, G. M. Whitesides, *Analytical Chemistry* **1994**, *66*. 1785-1791

15. M. Berezovski, A. Drabovich, S. M. Krylova, M. Musheev, V. Okhonin, A. Petrov, S. N. Krylov, *Journal of the American Chemical Society* **2005**, *127*. 3165-3171

16. N. H. H. Heegaard, *Journal of Chromatography A* **1994**, *680*. 405-412

17. N. H. H. Heegaard, R. T. Kennedy, *Electrophoresis* **1999**, *20*. 3122-3133

18. C. Schou, N. H. H. Heegaard, *Electrophoresis* **2006**, *27*. 44-59

19. J. F. Rual, K. Venkatesan, T. Hao, T. Hirozane-Kishikawa, A. Dricot, N. Li, G. F. Berriz, F. D. Gibbons, M. Dreze, N. Ayivi-Guedehoussou, N. Klitgord, C. Simon, M. Boxem, S. Milstein, J. Rosenberg, D. S. Goldberg, L. V. Zhang, S. L. Wong, G. Franklin, S. M. Li, J. S. Albala, J. H. Lim, C. Fraughton, E. Llamosas, S. Cevik, C. Bex, P. Lamesch, R. S. Sikorski, J. Vandenhaute, H. Y. Zoghbi, A. Smolyar, S. Bosak, R. Sequerra, L. Doucette-Stamm, M. E. Cusick, D. E. Hill, F. P. Roth, M. Vidal, *Nature* **2005**, *437*. 1173-1178

20. T. Berg, *Current Opinion in Drug Discovery & Development* **2008**, *11*. 666-674

21. A. J. Wilson, *Chemical Society Reviews* **2009**, *38*. 3289-3300

22. M. R. Arkin, A. Whitty, *Curr Opin Chem Biol* **2009**, *13*. 284-90

23. E. M. Phizicky, S. Fields, *Microbiological Reviews* **1995**, *59*. 94-123

24. J. Lebowitz, M. S. Lewis, P. Schuck, *Protein Science* **2002**, *11*. 2067-2079

25. P. Schuck, *Analytical Biochemistry* **2003**, *320*. 104-124

26. F. Krause, *ELECTROPHORESIS* **2006**, *27*. 2759-2781

27. F. J. Stevens, *Biochemistry* **1986**, *25*. 981-993

28. H. Ehring, *Analytical Biochemistry* **1999**, *267*. 252-259

29. A. N. Hoofnagle, K. A. Resing, N. G. Ahn, *Annual Review of Biophysics and Biomolecular Structure* **2003**, *32*. 1-25

30. D. R. Müller, P. Schindler, H. Towbin, U. Wirth, H. Voshol, S. Hoving, M. O. Steinmetz, *Analytical Chemistry* **2001**, *73*. 1927-1934

31. B. T. Ruotolo, S. J. Hyung, P. M. Robinson, K. Giles, R. H. Bateman, C. V. Robinson, *Angewandte Chemie-International Edition* **2007**, *46*. 8001-8004

32. B. T. Ruotolo, J. L. P. Benesch, A. M. Sandercock, S. J. Hyung, C. V. Robinson, *Nature Protocols* **2008**, *3*. 1139-1152

33. H. Takahashi, T. Nakanishi, K. Kami, Y. Arata, I. Shimada, *Nature Structural Biology* **2000**, *7*. 220-223

34. T. Heyduk, Y. Ma, H. Tang, R. H. Ebright, in *Methods in Enzymology*, ed. A. Sankar. Academic Press, 1996, vol. Volume 274, pp 492-503.

35. K. Truong, M. Ikura, *Current Opinion in Structural Biology* **2001**, *11*. 573-578

36. Y. Hou, D. E. McGuinness, A. J. Prongay, B. Feld, P. Ingravallo, R. A. Ogert, C. A. Lunn, J. A. Howe, *Journal of Biomolecular Screening* **2008**, *13*. 406-414

37. D. L. Roman, J. N. Talbot, R. A. Roof, R. K. Sunahara, J. R. Traynor, R. R. Neubig, *Molecular Pharmacology* **2007**, *71*. 169-175

38. R. Karlsson, A. Falt, *Journal of Immunological Methods* **1997**, *200*. 121-133

39. M. M. Pierce, C. S. Raman, B. T. Nall, *Methods-a Companion to Methods in Enzymology* **1999**, *19*. 213-221

40. B. Kobe, G. Guncar, R. Buchholz, T. Huber, B. Maco, N. Cowieson, J. L. Martin, M. Marfori, J. K. Forwood, *Biochemical Society Transactions* **2008**, *36*. 1438-1441

41. E. Dicapua, A. Engel, A. Stasiak, T. Koller, *Journal of Molecular Biology* **1982**, *157*. 87-103

42. J. Inglese, R. L. Johnson, A. Simeonov, M. Xia, W. Zheng, C. P. Austin, D. S. Auld, *Nat Chem Biol* **2007**, *3*. 466-479

43. R. G. Nielsen, E. C. Rickard, P. F. Santa, D. A. Sharknas, G. S. Sittampalam, *Journal of Chromatography* **1991**, *539*. 177-185

44. R. Lausch, O. W. Reif, P. Riechel, T. Scheper, *Electrophoresis* **1995**, *16*. 636-641

45. H. Stutz, *Electrophoresis* **2009**, *30*. 2032-2061

46. C. A. Lucy, A. M. MacDonald, M. D. Gulcev, *Journal of Chromatography A* **2008**, *1184*. 81-105

47. I. Rodriguez, S. F. Y. Li, *Analytica Chimica Acta* **1999**, *383*. 1-26

48. J. Horvath, V. Dolnik, *Electrophoresis* **2001**, *22*. 644-655

49. M. P. Mayer, B. Bukau, *Cellular and Molecular Life Sciences* **2005**, *62*. 670-684

50. V. A. Assimon, A. T. Gillies, J. N. Rauch, J. E. Gestwicki, *Curr Pharm Des* **2013**, *19*. 404-17

51. M. Gamerdinger, S. Carra, C. Behl, *J Mol Med* **2011**, *89*. 1175-1182

52. S. Y. Teh, R. Lin, L. H. Hung, A. P. Lee, *Lab on a Chip* **2009**, *9*. 3604-3604

53. M. Wang, G. T. Roman, K. Schultz, C. Jennings, R. T. Kennedy, *Analytical Chemistry* **2008**, *80*. 5607-5615

54. G. T. Roman, M. Wang, K. N. Shultz, C. Jennings, R. T. Kennedy, *Analytical Chemistry* **2008**, *80*. 8231-8238

55. J. Pei, Q. Li, R. T. Kennedy, *Journal of the American Society for Mass Spectrometry 21*. 1107-1113

56. H. Song, D. L. Chen, R. F. Ismagilov, *Angewandte Chemie-International Edition* **2006**, *45*. 7336-7356

57. D. R. Link, S. L. Anna, D. A. Weitz, H. A. Stone, *Physical Review Letters* **2004**, *92*. 4

58. C. G. Evans, L. Chang, J. E. Gestwicki, *Journal of Medicinal Chemistry* **2010**, *53*. 4585-4602

59. G. Chiappetta, M. Ammirante, A. Basile, A. Rosati, M. Festa, M. Monaco, E. Vuttariello, R. Pasquinelli, C. Arra, M. Zerilli, M. Todaro, G. Stassi, L. Pezzullo, A. Gentilella, A. Tosco, M. Pascale, L. Marzullo, M. A. Belisario, M. C. Turco, A. Leone, *J Clin Endocrinol Metab* **2007**, *92*. 1159-63

60. P. Liu, B. Xu, J. Li, H. Lu, *FEBS Lett* **2009**, *583*. 401-6

61. M. Festa, L. Del Valle, K. Khalili, R. Franco, G. Scognamiglio, V. Graziano, V. De Laurenzi, M. C. Turco, A. Rosati, *Am J Pathol* **2011**, *178*. 2504-12

62. R. T. Kennedy, I. German, J. E. Thompson, S. R. Witowski, *Chemical Reviews* **1999**, *99*. 3081-+

63. J. G. Shackman, C. J. Watson, R. T. Kennedy, *Journal of Chromatography A* **2004**, *1040*. 273-282

64. J. K. Towns, F. E. Regnier, *Analytical Chemistry* **1991**, *63*. 1126-1132

65. J. F. Rual, K. Venkatesan, T. Hao, T. Hirozane-Kishikawa, A. Dricot, N. Li, G. F. Berriz, F. D. Gibbons, M. Dreze, N. Ayivi-Guedehoussou, N. Klitgord, C. Simon, M. Boxem, S. Milstein, J. Rosenberg, D. S. Goldberg, L. V. Zhang, S. L. Wong, G. Franklin, S. Li, J. S. Albala, J. Lim, C. Fraughton, E. Llamosas, S. Cevik, C. Bex, P. Lamesch, R. S. Sikorski, J. Vandenhaute, H. Y. Zoghbi, A. Smolyar, S. Bosak, R. Sequerra, L. Doucette-Stamm, M. E. Cusick, D. E. Hill, F. P. Roth, M. Vidal, *Nature* **2005**, *437*. 1173-8

66. U. Stelzl, U. Worm, M. Lalowski, C. Haenig, F. H. Brembeck, H. Goehler, M. Stroedicke, M. Zenkner, A. Schoenherr, S. Koeppen, J. Timm, S. Mintzlaff, C. Abraham,

N. Bock, S. Kietzmann, A. Goedde, E. Toksoz, A. Droege, S. Krobitsch, B. Korn, W. Birchmeier, H. Lehrach, E. E. Wanker, *Cell* **2005**, *122*. 957-68

67. D. A. Bonsor, E. J. Sundberg, *Biochemistry* **2011**, *50*. 2394-402

68. M. Vidal, M. E. Cusick, A. L. Barabasi, *Cell* **2011**, *144*. 986-98

69. E. T. Powers, R. I. Morimoto, A. Dillin, J. W. Kelly, W. E. Balch, *Annual review of biochemistry* **2009**, *78*. 959-91

70. A. D. Thompson, A. Dugan, J. E. Gestwicki, A. K. Mapp, *ACS chemical biology* **2012**, *7*. 1311-20

71. L. N. Makley, J. E. Gestwicki, *Chemical biology & drug design* **2013**, *81*. 22-32

72. M. C. Smith, J. E. Gestwicki, *Expert reviews in molecular medicine* **2012**, *14*. e16

73. J. A. Wells, C. L. McClendon, *Nature* **2007**, *450*. 1001-9

74. I. German, D. D. Buchanan, R. T. Kennedy, *Analytical Chemistry* **1998**, *70*. 4540-4545

75. P. C. Simpson, D. Roach, A. T. Woolley, T. Thorsen, R. Johnston, G. F. Sensabaugh, R. A. Mathies, *Proceedings of the National Academy of Sciences of the United States of America* **1998**, *95*. 2256-2261

76. Y. He, E. S. Yeung, *Electrophoresis* **2003**, *24*. 101-108

77. J. Pei, J. Nie, R. T. Kennedy, *Analytical Chemistry* **2010**, *82*. 9261-9267

78. L. Chang, A. D. Thompson, P. Ung, H. A. Carlson, J. E. Gestwicki, *The Journal of biological chemistry* **2010**, *285*. 21282-91

79. L. Chang, E. B. Bertelsen, S. Wisen, E. M. Larsen, E. R. Zuiderweg, J. E. Gestwicki, *Analytical biochemistry* **2008**, *372*. 167-76

80. A. A. Shemetov, N. B. Gusev, *Archives of biochemistry and biophysics* **2011**, *513*. 1-9

81. L. L. Blazer, D. L. Roman, M. R. Muxlow, R. R. Neubig, *Current protocols in cytometry / editorial board, J. Paul Robinson, managing editor ... [et al.]* **2010**, *Chapter 13*. Unit 13 11 1-15

82. L. Tao, R. T. Kennedy, *Electrophoresis* **1997**, *18*. 112-117

83. J. H. Zhang, T. D. Y. Chung, K. R. Oldenburg, *Journal of Biomolecular Screening* **1999**, *4*. 67-73

84. R. T. Kennedy, I. German, J. E. Thompson, S. R. Witowski, *Chemical Reviews* **1999**, *99*. 3081-3132

85. W. B. Furman, *Continuous Flow Analysis Theory and Practice*. MARCEL DEKKER, INC: New York, 1976.

86. H. Song, J. D. Tice, R. F. Ismagilov, *Angewandte Chemie-International Edition* **2003**, *42*. 768-772

87. D. T. Chiu, R. M. Lorenz, G. D. M. Jeffries, *Anal. Chem.* **2009**, *81*. 5111-5118

88. I. Shestopalov, J. D. Tice, R. F. Ismagilov, *Lab on a Chip* **2004**, *4*. 316-321

89. H. Song, R. F. Ismagilov, *J. Am. Chem. Soc.* **2003**, *125*. 14613-14619

90. B. Zheng, L. S. Roach, R. F. Ismagilov, *J. Am. Chem. Soc.* **2003**, *125*. 11170-11171

91. M. Y. He, J. S. Edgar, G. D. M. Jeffries, R. M. Lorenz, J. P. Shelby, D. T. Chiu, *Analytical Chemistry* **2005**, *77*. 1539-1544

92. D. L. L. Chen, R. F. Ismagilov, *Curr. Opin. Chem. Biol.* **2006**, *10*. 226-231

93. R. T. Kelly, J. S. Page, I. Marginean, K. Q. Tang, R. D. Smith, *Angewandte Chemie-International Edition* **2009**, *48*. 6832-6835

94. L. M. Fidalgo, G. Whyte, B. T. Ruotolo, J. L. P. Benesch, F. Stengel, C. Abell, C. V. Robinson, W. T. S. Huck, *Angewandte Chemie-International Edition* **2009**, *48*. 3665-3668

95. Y. Liu, S. Y. Jung, C. P. Collier, *Anal. Chem.* **2009**, *81*. 4922-4928

96. D. N. Adamson, D. Mustafi, J. X. J. Zhang, B. Zheng, R. F. Ismagilov, *Lab on a Chip* **2006**, *6*. 1178-1186

97. M. J. Fuerstman, P. Garstecki, G. M. Whitesides, *Science* **2007**, *315*. 828-832

98. M. J. Fuerstman, A. Lai, M. E. Thurlow, S. S. Shevkoplyas, H. A. Stone, G. M. Whitesides, *Lab on a Chip* **2007**, *7*. 1479-1489

99. B. J. Smith, D. P. Gaver, *Lab on a Chip 10*. 303-312

100. J. Ratulowski, H. C. Chang, *Physics of Fluids a-Fluid Dynamics* **1989**, *1*. 1642-1655

101. M. Prakash, N. Gershenfeld, *Science* **2007**, *315*. 832-835

102. G. Cristobal, J. P. Benoit, M. Joanicot, A. Ajdari, *Appl. Phys. Lett.* **2006**, *89*.

103. J. C. McDonald, G. M. Whitesides, *Acc. Chem. Res.* **2002**, *35*. 491-499

104. T. Thorsen, R. W. Roberts, F. H. Arnold, S. R. Quake, *Physical Review Letters* **2001**, *86*. 4163-4166

105. K. R. Reid, R. T. Kennedy, *Anal. Chem.* **2009**, *81*. 6837-6842

106. J. S. Edgar, G. Milne, Y. Q. Zhao, C. P. Pabbati, D. S. W. Lim, D. T. Chiu, *Angewandte Chemie-International Edition* **2009**, *48*. 2719-2722

107. X. Z. Niu, B. Zhang, R. T. Marszalek, O. Ces, J. B. Edel, D. R. Klug, A. J. Demello, *Chemical Communications* **2009**. 6159-6161

108. Q. Li, J. Pei, P. Song, R. T. Kennedy, *Analytical Chemistry 82*. 5260-5267

109. J. P. C. Vissers, *Journal of Chromatography A* **1999**, *856*. 117-143

110. J. Hernández-Borges, Z. Aturki, A. Rocco, S. Fanali, *Journal of Separation Science* **2007**, *30*. 1589-1610

111. Y. Ishihama, *Journal of Chromatography A* **2005**, *1067*. 73-83

112. E. Rapp, U. Tallarek, *Journal of Separation Science* **2003**, *26*. 453-470

113. H. F. Zou, X. D. Huang, M. L. Ye, Q. Z. Luo, *Journal of Chromatography A* **2002**, *954*. 5-32

114. J. S. Edgar, G. Milne, Y. Zhao, C. P. Pabbati, D. S. W. Lim, D. T. Chiu, *Angewandte Chemie-International Edition* **2009**, *48*. 2719-2722

115. Q. Li, J. Pei, P. Song, R. T. Kennedy, *Analytical Chemistry* **2010**, *82*. 5260-5267

116. J. Ji, L. Nie, L. Qiao, Y. X. Li, L. P. Guo, B. H. Liu, P. Y. Yang, H. H. Girault, *Lab on a Chip* **2012**, *12*. 2625-2629

117. B. Nickerson, J. W. Jorgenson, *Journal of Chromatography A* **1989**, *480*. 157-168

118. T. T. Lee, E. S. Yeung, *Journal of Chromatography* **1992**, *595*. 319-325

119. L. S. Roach, H. Song, R. F. Ismagilov, *Analytical Chemistry* **2004**, *77*. 785-796

120. R. T. Kennedy, J. W. Jorgenson, *Analytical Chemistry* **1989**, *61*. 1128-1135

121. G. M. Whitesides, E. Ostuni, S. Takayama, X. Y. Jiang, D. E. Ingber, *Annual Review of Biomedical Engineering* **2001**, *3*. 335-373

122. M. W. Lada, T. W. Vickroy, R. T. Kennedy, *Analytical Chemistry* **1997**, *69*. 4560-4565

123. L. Hernandez, J. Escalona, N. Joshi, N. Guzman, *Journal of Chromatography* **1991**, *559*. 183-196

124. J. S. Edgar, G. Milne, Y. Zhao, C. P. Pabbati, D. S. W. Lim, D. T. Chiu, *Angewandte Chemie* **2009**, *121*. 2757-2760

125. V. Cristini, Y. C. Tan, *Lab on a Chip* **2004**, *4*. 257-264

126. K. Wang, Y. C. Lu, J. H. Xu, G. S. Luo, *Langmuir* **2009**, *25*. 2153-2158

127. H. Song, H. W. Li, M. S. Munson, T. G. Van Ha, R. F. Ismagilov, *Analytical Chemistry* **2006**, *78*. 4839-4849

128. T. R. Slaney, J. Nie, N. D. Hershey, P. K. Thwar, J. Linderman, M. A. Burns, R. T. Kennedy, *Analytical Chemistry* **2011**, *83*. 5207-5213

129. S. W. Sun, T. R. Slaney, R. T. Kennedy, *Analytical Chemistry* **2012**, *84*. 5794-5800

130. K. L. Kostel, S. M. Lunte, *Journal of Chromatography B: Biomedical Sciences and Applications* **1997**, *695*. 27-38

131. R. S. Deelder, M. G. F. Kroll, A. J. B. Beeren, J. H. M. Van Den Berg, *Journal of Chromatography A* **1978**, *149*. 669-682

132. M. Wang, T. Slaney, O. Mabrouk, R. T. Kennedy, *Journal of Neuroscience Methods* **2010**, *190*. 39-48

133. H. A. Bardelmeijer, J. C. M. Waterval, H. Lingeman, R. van't Hof, A. Bult, W. J. M. Underberg, *Electrophoresis* **1997**, *18*. 2214-2227

134. T. F. Hooker, J. W. Jorgenson, *Analytical Chemistry* **1997**, *69*. 4134-4142

135. M. Ye, S. Hu, W. W. C. Quigley, N. J. Dovichi, *Journal of Chromatography A* **2004**, *1022*. 201-206

136. J. L. Edwards, C. N. Chisolm, J. G. Shackman, R. T. Kennedy, *Journal of Chromatography A* **2006**, *1106*. 80-88